Space Science Reviews (2024) 220:49
https://doi.org/10.1007/s11214-024-01069-y

Exploring the Composition of Europa with the Upcoming Europa Clipper Mission

T.M. Becker[1,2] · M.Y. Zolotov[3] · M.S. Gudipati[4] · J.M. Soderblom[5] · M.A. McGrath[6] · B.L. Henderson[4] · M.M. Hedman[7] · M. Choukroun[4] · R.N. Clark[8] · C. Chivers[9] · N.S. Wolfenbarger[10] · C.R. Glein[1] · J.C. Castillo-Rogez[4] · O. Mousis[11] · K.M. Scanlan[10] · S. Diniega[4] · F.P. Seelos[12] · W. Goode[13] · F. Postberg[14] · C. Grima[10] · H.-W. Hsu[13] · L. Roth[15] · S.K. Trumbo[16] · K.E. Miller[1] · K. Chan[10] · C. Paranicas[12] · S.M. Brooks[4] · K.M. Soderlund[10] · W.B. McKinnon[17] · C.A. Hibbitts[12] · H.T. Smith[12] · P.M. Molyneux[1] · G.R. Gladstone[1,2] · M.L. Cable[4] · Z.E. Ulibarri[13] · B.D. Teolis[1] · M. Horanyi[13] · X. Jia[18] · E.J. Leonard[4] · K.P. Hand[4] · S.D. Vance[4] · S.M. Howell[4] · L.C. Quick[19] · I. Mishra[16] · A.M. Rymer[12] · C. Briois[20] · D.L. Blaney[4] · U. Raut[1,2] · J.H. Waite[1] · K.D. Retherford[1,2] · E. Shock[3] · P. Withers[21] · J.H. Westlake[12] · I. Jun[4] · K.E. Mandt[19] · B.J. Buratti[4] · H. Korth[12] · R.T. Pappalardo[4] · the Europa Clipper Composition Working Group

Received: 10 February 2023 / Accepted: 16 April 2024 / Published online: 19 June 2024
© The Author(s) 2024

Abstract
Jupiter's icy moon, Europa, harbors a subsurface liquid water ocean; the prospect of this ocean being habitable motivates further exploration of the moon with the upcoming NASA Europa Clipper mission. Key among the mission goals is a comprehensive assessment of the moon's composition, which is essential for assessing Europa's habitability. Through powerful remote sensing and *in situ* investigations, the Europa Clipper mission will explore the composition of Europa's surface and subsurface, its tenuous atmosphere, and the local space environment surrounding the moon. Clues on the interior composition of Europa will be gathered through these assessments, especially in regions that may expose subsurface materials, including compelling geologic landforms or locations indicative of recent or current activity such as potential plumes. The planned reconnaissance of the icy world will constrain models that simulate the ongoing external and internal processes that act to alter its composition. This paper presents the composition-themed goals for the Europa Clipper mission, the synergistic, composition-focused investigations that will be conducted, and how the anticipated scientific return will advance our understanding of the origin, evolution, and current state of Europa.

Keywords Europa · Clipper · Mission · Composition

Europa Clipper: A Mission to Explore Ocean World Habitability
Edited by Haje Korth, Bonnie J. Buratti and David Senske

Extended author information available on the last page of the article

1 Introduction

NASA's Europa Clipper mission will conduct a detailed reconnaissance of Jupiter's icy moon Europa with the primary goal of assessing its habitability (Pappalardo et al. 2024; Vance et al. 2023, both this collection). Through a series of close flybys, the flight system will acquire remote sensing and *in situ* data to investigate the (1) composition, (2) geological features, and (3) interior of the moon, and (4) to search for current and recent activity. The mission's Composition Working Group is charged with providing a high-level, cross-instrument and cross-discipline, composition-driven science perspective to meet the Europa Clipper mission objective to assess the habitability of Europa's ocean through its composition and chemistry. This paper presents the planned compositional studies of Europa's local space environment, atmosphere, surface, and subsurface that will be used to elucidate ongoing processing of the moon and complete the full examination of whether the conditions on Europa are, or have ever been, suitable for life.

1.1 Understanding Europa Through Its Composition

The detailed study of Europa's composition is one of the three foundational areas of investigation of the Europa Clipper mission, along with studies of the moon's interior (Roberts et al. 2023, this collection) and geology (Daubar et al. 2024, this collection). Although the moon's external envelope is primarily composed of water ice, observations continue to reveal complex compositions and non-water ice materials in the atmosphere, on the surface, and by inference, within the ice shell and ocean (e.g., Carlson et al. 2009). Some visible surface colorings are associated with physical features (Fig. 1) such as linea and chaos regions, suggesting geologic processes that are exposing endogenic materials. Other, more widespread materials could be exogenic, emplaced on Europa's surface from micrometeoroid impacts, including those derived from other Jovian satellites, and from material ejected by Jupiter's volcanically active moon, Io. Embedded within Jupiter's extreme radiation environment, Europa's surface materials are subjected to intense radiolytic processing that further changes their composition and possibly affects spectral properties (e.g., color) of endogenic and exogenic compounds on the surface (e.g., Johnson and McCord 1971; Carlson et al. 1999b).

Europa's sputter-induced atmosphere and local space environment (Fig. 2) are reflections of the atoms, molecules, and ice/dust grains that have been lofted from the surface and further altered through irradiation (e.g., McGrath et al. 2009; Johnson et al. 2019). For consistency in terminology in this work, atoms and molecules are considered to be neutral by default, distinct from positively- or negatively-charged ions. Here these atoms, molecules, and ions (e.g., O^+, H^+, OH^-, S^+) are referred to as 'particles.' The term 'particle' is also often used to describe macroscopic material (larger than a few nanometers). Throughout the paper, these larger particles, like those that can be collected by the dust analyzing investigation on Europa Clipper, are distinguished by describing them as ice or dust 'grains.' Analyses of the particles and ice/dust grains will be used to understand not only the makeup of, and the interaction between, the atmosphere, surface, and subsurface, but also the volatile transport and the structure of the atmosphere.

Identifying the sources and sinks of non-icy constituents on Europa improves our understanding of the bulk composition and structure of the moon and its thermal, physical, chemical, and geological evolution. Throughout this work, "non-ice" materials are defined to be anything that is not H_2O ice, and thus includes salts, silicates, organic matter, and gas hydrates. Characterizing the presence and distribution of organic and/or carbon-bearing inorganic materials, and the composition of any salts provide strong compositional constraints on the habitability of Europa.

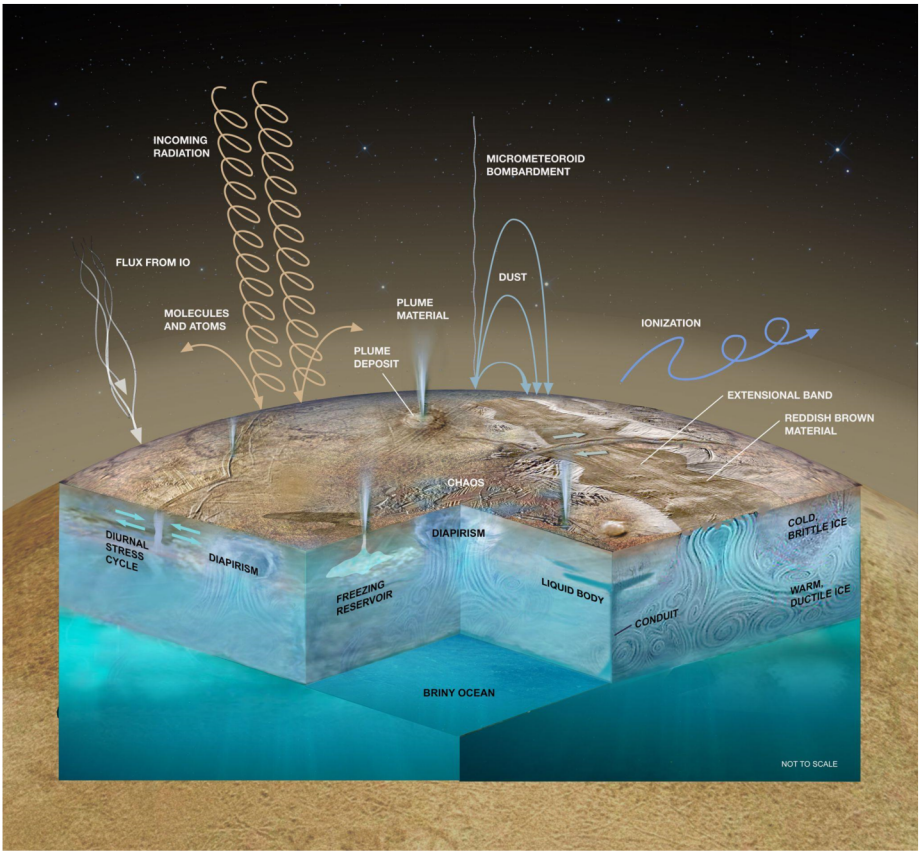

Fig. 1 Artistic concept showing a variety of known and hypothesized processes that affect the composition of Europa's tenuous atmosphere, its surface, and its upper interior in the last 10^8 years. Processes within Europa's ocean and ice shell may bring oceanic material to the surface, and some surface material may be delivered beneath the surface through geologic events. The surface composition is altered through exposure to radiation by Jupiter's magnetic field and from incoming material from space, particularly material spewed from Io's volcanoes. Volatiles and ice/dust grains are sputtered from the surface into the thin atmosphere by irradiation and micrometeoroid bombardment. Some of that material returns to the surface, while some of the molecules and atoms escape and may form a neutral cloud or even torus around Jupiter. The compositional investigations conducted by the Europa Clipper mission will identify and characterize the distribution of materials on the moon, constraining past and ongoing processes and exchanges of materials, and ultimately provide key information about the habitability of Europa

1.2 Previous Exploration of Europa's Composition

Motivation for a dedicated Europa mission was cultivated by the captivating images and spectra of the moon that were acquired over the past several decades, particularly those from spacecraft flybys that include Pioneer 10, Pioneer 11, Voyager 1, Voyager 2, Cassini, New Horizons, and Juno, as well as Earth-based studies, including data collected by the Hubble Space Telescope (HST) and more recently the James Webb Space Telescope (JWST). The wealth of relatively high-resolution data obtained during multiple Europa passes by the Galileo spacecraft (see Pappalardo et al. 2009) include magnetic field measurements from that led to the inference of a salt-bearing liquid water ocean beneath Europa's ice

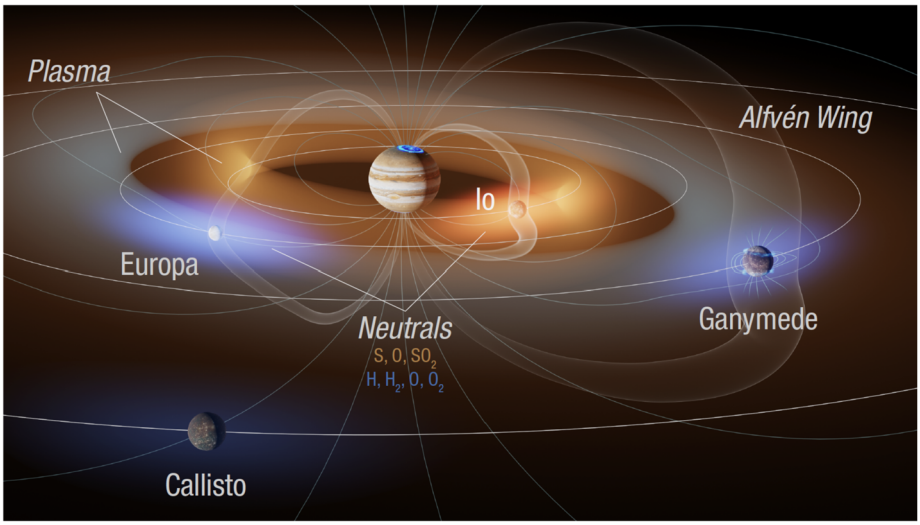

Fig. 2 An artistic view of the space environment around Jupiter. Io's neutral cloud and plasma torus (orange) are primarily produced from material ejected by Io's volcanoes. Similar neutral clouds and a neutral and/or plasma torus may exist around Europa (blue), created by particles sputtered from the surface and the atmosphere that escape Europa's Hill sphere. Image credit: Szalay et al. (2022)

shell (Kivelson et al. 2000) and imaging that revealed alluring geologic scrapes and scars on the surface that suggest past, or possibly present, ocean-to-surface connections (Greeley et al. 1998). More recent ground-based and near-Earth space-based observations ranging in wavelengths from the far-ultraviolet (FUV) to sub-millimeter wavelengths have since been conducted to develop compositional surface maps, identify key constituents of the atmosphere and surface non-ice compounds, understand Europa's surrounding environment, and search for and characterize potential plumes (e.g., Roth et al. 2014b,a; Becker et al. 2018, 2022; Jia et al. 2018; Trumbo et al. 2019a, 2022; Villanueva et al. 2023; Trumbo and Brown 2023). Laboratory, field, and modeling efforts provide critical insights for interpreting these observations, for exploring the exchange of materials between the atmosphere, surface, and interior, and for identifying additional mechanisms for the processing and alteration of surface and atmospheric materials, with the goal of understanding the formation, evolution, and current processes occurring on the moon.

1.3 Composition and Habitability

Compositional measurements provide key data for constraining the habitability of Europa. The characteristics of the physical and chemical environments in icy, oceanic and subocean niches, and possible metabolic reactions of putative organisms, could be constrained through compositional measurements of the surface, atmosphere, and any possible plume material (Vance et al. 2023, this collection). Speciation of the subsurface salts emplaced on the surface or of sputtered ice/dust grains will be used to constrain acidity (pH), salinity, and the oxidation state of the oceanic water, current and previous water-rock interactions, and brine chemistry within the ice shell. Oxidized (sulfate- and/or carbonate-rich) and reduced (sulfide- and/or organic-rich) oceanic compositions will be distinguished through compositional measurements of the surface and atmosphere if there is sufficient exchange of materials. The concentration and occurrence of surface radiolytic products are important for

evaluating fluxes of oxidants (e.g., O_2, H_2O_2, Cl-O species) and acids (e.g., H_2SO_4, HCl) to the subsurface and their effects on habitability. Additionally, concentrations of inorganic and organic species in possible atmospheric plumes or recent plume deposits elucidate the chemical disequilibria that may provide metabolic energy for organisms that do not require light as an energy source. The compilation of the collected compositional data will be used to constrain the origin and history of the water envelope and corresponding changes in the environments with implications for survivability, adaptation, extinction, and evolution of living species, if they are or were present.

1.4 The Europa Clipper Mission's Composition Goals

To achieve the Europa Clipper mission goal to assess the habitability of the satellite, the composition-focused objective is to *understand the habitability of Europa's ocean through composition and chemistry*. The mission success criterion is to *identify the composition and sources of key non-ice constituents on the surface and in the atmosphere, including any carbon-containing compounds*. This objective will be met through the completion of three Level-1 science requirements pertaining specifically to the atmospheric and space environment composition, the global surface composition, and the surface composition associated with specific landforms at spatial resolutions surpassing 300 m/pixel. One additional Level-1 science requirement shared across the thematic working groups is to search for and characterize any recent or current activity on Europa. The composition-related Level-1 science requirements, a summary of their implementation (Level-2 science requirements), and the primary investigations that will achieve these requirements are listed in Table 1.

The comprehensive payload consists of ten science instruments and an engineering radiation monitor that will also be used for science applications: The Mapping Imaging Spectrometer for Europa (MISE); the Europa Imaging System (EIS) Narrow Angle Camera (NAC) and Wide Angle Camera (NAC); the Europa THermal EMission Imaging System (E-THEMIS); the Europa Ultraviolet Spectrograph (Europa-UVS); the Radar for Europa Assessment and Sounding: Ocean to Near-surface (REASON); the Europa Clipper Magnetometer (ECM); the Plasma Instrument for Magnetic Sounding (PIMS); the MAss SPectrometer for Planetary EXploration/Europa (MASPEX); the SUrface Dust Analyzer (SUDA); and the Radiation Monitor (RadMon). In addition, there is a Gravity and Radio Science (G/RS) investigation. The remote-sensing instruments' fields of view (FOVs) overlap and can operate simultaneously to acquire complementary datasets at identical observational geometries.

The description of each of these investigations, including details about their operation and planned science activities, can be found in companion papers in this topical collection (Blankenship et al. 2024; Blaney et al. 2024; Westlake et al. 2023; Turtle et al. 2024; Christensen et al. 2024; Waite et al. 2024; Kempf et al. 2024; Retherford et al. 2024; Kivelson et al. 2023; Mazarico et al. 2023; Meitzler et al. 2023). Table 2 provides an overview of the composition-related capabilities and planned measurements for each investigation. As described in the following sections, the data collected during these science investigations will be used both independently and synergistically to study the composition of Europa's surface (Sect. 2), subsurface and deeper interior (Sect. 3), atmosphere and local space environment (Sect. 4), and putative plumes (Sect. 5). These observations constrain past and ongoing processes (Sect. 6), and provide a broad context, including the habitability of Europa (Sect. 7).

Table 1 The composition-related science requirements of the Europa Clipper mission

Composition-related baseline Level-1 science requirement	Level-2 science requirement	Primary investigations
Global Composition: Create a compositional map at $\leq$10 km spatial scale covering $\geq$60% of the surface, sufficient to identify non-ice materials, especially organic compounds.	Determine the global-scale composition and chemistry of Europa; identify units, large-scale variability, exogenic compositional signatures, and evidence of possible large-scale heterogeneity in the ocean by obtaining global-scale infrared imaging spectroscopy of sufficient quality to measure absorption features due to hydrated salts and organics.	MISE
	Map compositionally diagnostic properties in the *in situ* volatile and (ice/dust) grain datasets to determine the surface composition and chemistry, including the identification of any hydrated minerals and organic compounds, and seek indicators of ocean geochemical processes relevant to habitability.	MASPEX, SUDA
Landform Composition: Characterize the composition of $\geq$0.3% of the surface, globally distributed at $\leq$300 m spatial scale, sufficient to identify non-ice materials, especially organic compounds.	Determine the regional-scale surface composition and chemistry, identify exogenic compositional signatures, and understand the chemical pathways between the ocean and surface and implications for the habitability of the ocean through regional scale infrared imaging spectroscopy of sufficient quality to measure absorption features due to hydrated salts and organic compounds.	MISE
Atmospheric Composition: Characterize the composition and sources of volatiles, particulates, and plasma, sufficient to identify the signatures of non-ice materials, including organic compounds, in at least one of the above forms, in globally distributed regions of the atmosphere and local space environment.	Identify the global distribution of major volatiles in the atmosphere and local space environment and resolve key organic compounds, their sources, and their relative abundances where volume mixing ratios are $>1.67 \times 10^{-4}$.	MASPEX
	Characterize the composition of near surface exospheric ice/dust grains, including any organic compounds if present, and distinguish between exogenic and endogenic sources of material across globally-distributed regions and in unique geographical locations.	SUDA
	Map the vertical structure and composition of the atmosphere in regions that are globally distributed and sampled on timescales commensurate with the Europa-Jupiter half-synodic period.	Europa-UVS
	Measure the energy per charge characteristics of the Europa ionosphere, possible plume ionosphere, and the magnetosphere to characterize their compositions and plasma sources.	PIMS
Current Activity: Search for and characterize any current activity, notably plumes or thermal anomalies, in regions that are globally distributed.	Search for and characterize the vapor composition of any plumes >30 km in height.	Europa-UVS
	Map daytime and nighttime temperatures to characterize the thermal state of the ice shell and identify heat flow anomalies, regolith depth, and block abundance.	E-THEMIS
	Identify and characterize potential recent and/or ongoing activity in any encountered plumes <110 km in altitude; determine composition including organic compounds if present, number density, and size distribution of any plume ice/dust grains to identify and constrain the plume's source mechanism and salinity of the source.	SUDA

Table 1 (*Continued*)

Composition-related baseline Level-1 science requirement	Level-2 science requirement	Primary investigations
	Measure the composition of volatiles at <110 km spatial scale to characterize any active geological features and determine the relative fluxes of endogenous particles and gases in any encountered plume material in order to constrain ocean geochemical properties relevant to habitability.	MASPEX
	Characterize albedo and color variations of globally-distributed regions at <500-m pixel scale to search for recent activity by documenting any surface changes between repeat images and identifying signatures of fresh materials.	EIS

2 The Surface Composition of Europa

The current knowledge about the surface composition of Europa is derived primarily from spectroscopic remote sensing observations by ground-based telescopes, the HST, and the Galileo, Cassini, and New Horizons spacecraft, and through the comparison of these measured spectral signatures with those from laboratory analog materials. While these numerous campaigns have confirmed the surface is dominated by H_2O ice, it has also resulted in the detection of non-ice materials that may have implications for the composition of the subsurface ice and ocean. However, current measurements are limited by the spectral coverage of ground-based observations, especially at wavelengths with no or reduced-quality data due to telluric absorptions in Earth's atmosphere, and by the relatively low spatial and spectral resolution and signal-to-noise ratio of spacecraft spectral measurements. These deficiencies motivate the need for a dedicated suite of advanced instrumentation to explore the composition of Europa's surface.

The majority of Europa's surface displays a high visible albedo (∼0.65) and prominent vibrational bands in the near-infrared (NIR), characteristics of H_2O, both as ice and in hydrated materials (e.g., Carlson et al. 2009). Measurements of water byproducts atomic oxygen (Hall et al. 1995) and atomic hydrogen (Roth et al. 2017) sputtered into the atmosphere further confirm the global presence of water ice (Sect. 2.1). Remote sensing observations in the ultraviolet to the infrared also reveal albedo variability, spectral signatures that are shifted from the wavelengths at which pure H_2O is expected to exhibit such absorption bands, and other spectral features that are indicative of non-ice materials on the surface (e.g., Nelson et al. 1987; Carlson et al. 2009; McGrath et al. 2009). Definitive identification of these materials, however, has been frustrated by limitations in the observational data and the lack of laboratory spectral data for the array of candidate materials acquired at relevant temperatures, pressures, and radiation environments and across the full spectral range of the observations. At present, it is unclear whether these non-ice materials are hydrated salts and/or solid acids, and how and from where they are formed (Sect. 2.2).

To address these outstanding questions, two primary objectives of the Europa Clipper mission are to characterize the global distribution of the non-ice components across the surface of Europa and to identify localized variations that may be associated with specific geologic landforms (Table 1 and Sect. 2.3). A fundamental goal of this work is to identify material exchanged between the surrounding cosmic space, atmosphere, surface and the subsurface, and possibly the underlying ocean. For this reason, it is important to identify which non-ice materials are inherent to Europa, possibly emplaced onto the surface through

Table 2 Brief descriptions of each of the Europa Clipper science investigations. For remote sensing instruments, we provide details such as the field of view (FOV), instantaneous FOV (IFOV), and the spectral range and resolution of sampling. For more details about an individual investigation, see the corresponding paper in this journal

Europa Clipper investigation	Investigation details			Primary compositional science measurements
Mapping Imaging Spectrometer for Europa (**MISE**)	Infrared imaging spectrometer FOV: 4.3° × 4.3° nominally, but along-track is variable IFOV: 250 μrad Spectral Range: 800 nm–5000 nm Spectral Sampling: 10 nm			Map the distribution and composition, including organics, acids and salt deposits, of materials on Europa's surface
Europa Imaging System (**EIS**)	Digital Camera Suite Bandpasses: Clear, NUV, BLU, GRN, RED, IR1,1MC			Capture stereographic images and photometry, global color mapping, associate compositional variations with geology
	Wide-angle Camera (WAC) FOV: 24° × 48° IFOV: 218 μrad	Narrow-angle Camera (NAC) FOV: 1.2° × 2.3° IFOV: 10 μrad		
Europa Thermal Emission Imaging System (**E-THEMIS**)	Multispectral thermal imager			Search for thermal variations and anomalies that could indicate warmer ice near the surface; support interpretation of observed compositional variation
	Band 1 Spectral Range: 7–14 μm Temperature ∼ 220 K	Band 2 Spectral Range: 14–28 μm Temperature ∼130 K	Band 3 Spectral Range: 28–50+ μm Temperature ∼90	
Europa Ultraviolet Spectrograph (**Europa-UVS**)	Ultraviolet spectrograph FOV: 0.1° × 7.3° + 0.2° × 0.2° (7.5° full length) IFOV: 0.16° (0.12° with High-resolution Port) at 130 nm Spectral Range: 55 nm–206 nm Spectral Resolution: ∼0.6 nm (point source); ∼1.2 nm (extended source)			Assess composition and structure of Europa's atmosphere; search for and characterize potential plumes
Radar for Europa Assessment and Sounding: Ocean to Near-surface (**REASON**)	Sounding	Reflectometry		Assess surface roughness, porosity, near-surface and subsurface structure/heterogeneities
	30 m vertical resolution and 2 km horizontal resolution or better down to 3 km depth; 300 m vertical resolution and 5.5 km horizontal resolution or better at depth greater than 3 km	Spatial resolution 10 km for VHF; 27 km for HF Horizontal baseline 5 m for VHF; 32 m for HF Near-surface depth 30 m for VHF; 300 m for HF Radiometric stability 1db for VHF and HF		

Table 2 (*Continued*)

Europa Clipper investigation	Investigation details	Primary compositional science measurements
Europa Clipper Magnetometer (**ECM**)	Magnetometer Measurement range: +/− 4000 nT per axis for each of the three sensors Sampling rate: 16 vector samples per second (high) or 1 vector sample per second (low)	Measure Europa's induced magnetic field to determine ocean thickness and conductivity, placing constraints on ocean salinity and temperature
Plasma Instrument for Magnetic Sounding (**PIMS**)	Plasma instrument consisting of four Faraday cups Energy resolution (magnetosphere): <15% Energy resolution (ionosphere): 0.3v Energy range: −2 keV to +6 keV 50 eV/q to 6 keV/q (ions; magnetospheric mode) −50 eV/q to −2 (electrons; magnetospheric mode) 1 eV/q to 50 eV/q (ions; ionospheric mode) −50 eV/q to −10 eVq/ (electrons; ionspheric mode) −2 ke/Vq to 6 keV/q (ions and elexctrons; transition mode) FOV: Four 90° cones	Measure charged particles in Europa's environment to support interpretations of ocean salinity and temperature data
Mass Spectrometer for Planetary Exploration (**MASPEX**)	High resolution mass spectrometer Mass spectral range: 2–500 u Mass Resolution (m/Δm) ≥ 4275 at mass 50 μ Surface Resolution: Equivalent to S/C closest approach distance Spectral Sampling Interval: <5 s at closest approach	Identify organics and other volatiles in Europa's atmosphere and local space environment
Surface Dust Mass Analyzer (**SUDA**)	*In situ* dust particle impact ionization mass spectrometer Grain Size Range: 100–1000 nm (Accuracy <20%) Mass resolution Δm: ≤ 1 u at m ≤ 200 u Mass spectral range: < 500 u Surface Resolution: better than spacecraft altitude FOV: +/− 23°	Create compositional surface maps of Europa's surface ice/dust grain ejecta particles; detect organic compounds and salts, if present
Gravity and Radio Science (**G/RS**)	Radiometric Tracking (Doppler, Sequential Ranging) and Radio occultations Frequency: X-band (7.2 GHz uplink/8.4 GHz downlink) Ka-band (31.9 GHz downlink only) Antennas: fanbeam (3), low-gain (3), medium-gain (1), high-gain (1) Doppler Accuracy: 0.1 mm/s @ 60 s integration time	Constrain ice shell thickness, density, and strength; measure plasma densities in the ionosphere
Radiation Monitor (**RadMon**)	Change Rate Monitor (CRM) and Distributed Total Ionizing Dose (TID) sensors Electrons intensity spectrum >∼1 MeV TIDskrad (Si)	Provide measurements of energetic particle inflow onto Europa, constraining the radiation- induced alterations of the surface composition

processes such as diapiric upwelling, cryovolcanism, or plume activities (Daubar et al. 2024, this collection), from those that originate from external sources such as micrometeoroids or from the other Galilean satellites, particularly from eruptions by active volcanoes on Io. The Europa Clipper science investigations also seek to understand how these surface materials are altered by their exposure to Jupiter's intense radiation environment and other processing, including impact gardening, sputtering, redistribution, and thermal processes (e.g., Carlson et al. 1999b).

The compositional investigation of ice- and non-ice material on Europa's surface will be primarily accomplished with the MISE dataset, which will consist of NIR spectral image cubes with a 10 nm spectral sampling between 800 nm and 5000 nm. Near-global (>60%) coverage of the surface will be acquired at spatial scales of <10 km/pixel. Regional (<300 m/pixel) and local-scale (<25 m/pixel) image cubes will be acquired during closest approaches to Europa (Table 2, Blaney et al. 2024, this collection).

Geologic context for these spectral maps will be provided through the EIS imaging datasets, which will deliver near-global coverage (80–90% monochromatic, >25% color) at <100 m/pixel, regional coverage (5–30% monochromatic, color as data volume permits) at 10–25 m/pixel, 10 km × 10 km sites (10 sites monochromatic, 10 sites color) at <10 m/pixel, and local sites (18+ sites mono) at <1 m/pixel (Table 2, Turtle et al. 2024, this collection). The EIS NAC is mounted on a gimbal that will provide off-nadir high-resolution observations up to 30° from nadir to preview ground tracks of future flybys.

These surface measurements will be complemented by high-spectral-resolution (1.2 nm spectral sampling) data collected by the Europa-UVS at wavelengths ranging from 55 nm to 206 nm, which can use its regular aperture port (AP; 0.16° resolution) or its high-resolution port (HP; 0.12° resolution) to achieve near-global coverage (>60%) with a spatial scale exceeding 90 km/pixel. During closest approaches, Europa-UVS will obtain localized surface observations with spatial scales exceeding 1 km/pixel (Retherford et al. 2024, this collection).

Surface temperature variations that may or may not be related to the composition will be assessed through E-THEMIS thermal measurements. Such observations will have scales of <100 m/pixel at closest approach.

Surface reflectometry measurements made by REASON will provide information on the bulk density (porosity) of surface ice and on other materials in the upper few hundred meters below the surface. Each surface reflectometry measurement is derived from km-long sections along each ground track (centered on the closest approach), which results in resolving the surface along-track to ≤10 km for the VHF band and ≤27.5 km for the HF band (Sect. 2.4; Blankenship et al. 2024, this collection).

The remote sensing instruments will operate in push-broom mode, collecting data as the nadir-point of the spacecraft moves across the surface over the course of the flyby. Additionally, two "Joint Scans" are planned for most flybys at an altitude of ~40,000 km; one during approach and one during departure from Europa (Fig. 3). These scans are implemented by offsetting the nadir-facing instruments from Europa, and then slewing across the satellite, enabling Europa-UVS, MISE, E-THEMIS, and EIS to obtain simultaneous, near-hemispheric NIR, UV, thermal and visible surface measurements. Most flybys will also include more distant ~10 minute scans primarily to slew the narrow field of view of Europa-UVS over the full hemisphere of Europa for UV surface, atmospheric, and auroral measurements of the satellite.

In situ measurements made by the SUDA and MASPEX investigations will detect and analyze the composition of grains and gases that have been ejected and sputtered by micrometeoroids from the surface, respectively (Kempf et al. 2024; Waite et al. 2024, both this

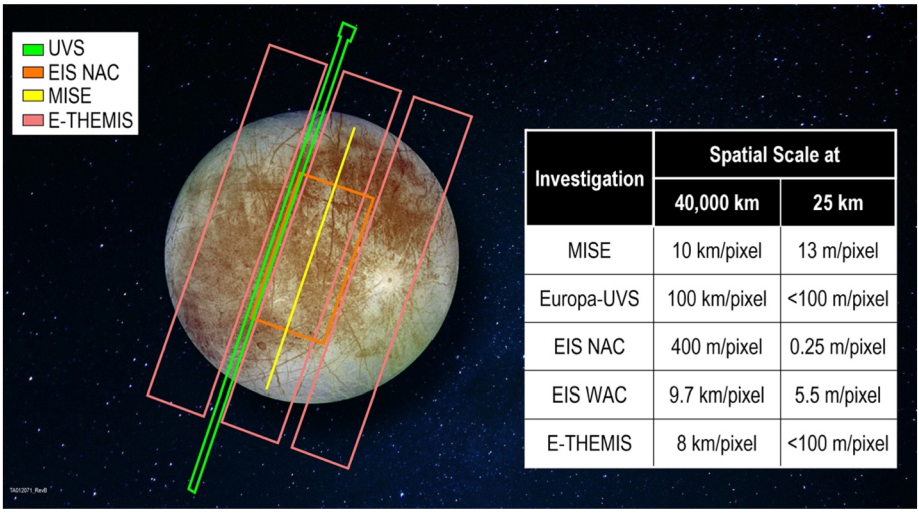

Investigation	Spatial Scale at	
	40,000 km	25 km
MISE	10 km/pixel	13 m/pixel
Europa-UVS	100 km/pixel	<100 m/pixel
EIS NAC	400 m/pixel	0.25 m/pixel
EIS WAC	9.7 km/pixel	5.5 m/pixel
E-THEMIS	8 km/pixel	<100 m/pixel

Fig. 3 The nominal projected fields of view for Europa-UVS, EIS NAC, MISE, and E-THEMIS when the Europa Clipper spacecraft is at an altitude of 40,000 km. Note that EIS WAC is not shown due to its size at this scale. The center of the Europa-UVS FOV is slightly offset from the spacecraft nadir in the along-track direction. 40,000 km is the approximate altitude for the joint scan observations, during which the spacecraft will slew the instrument FOVs across the surface of Europa. The table indicates the expected spatial scale for each investigation at the distance of the joint scan. It also provides a representative spatial scale that will be achieved by each investigation during the closest approach to Europa at 25 km altitude, accounting for the average expected relative ground motion

collection). Detections by SUDA can be traced back to Europa's surface through modeling of the 'grains' trajectories (Sect. 2.3.1), potentially identifying the source region of any non-ice material.

2.1 Europa's Ice Composition and Properties

Detailed characterizations of Europa's surface ice, including grain size and porosity, are necessary for studies of the geologic history of Europa because the ice properties are reflections of past and ongoing chemical and physical alterations of the ice through surface processing.

2.1.1 Europa's Water Ice Surface

The primary method for the identification and characterization of Europa's water ice surface has been with NIR spectroscopy, where water-ice vibrational bands near 1.04, 1.25, 1.5, 2, and 3 μm are prominent (Fig. 4). Shifts in the band-center, width, and depth of these water-ice spectral features will be used to constrain the temperature and crystallinity of water ice, as well as the grain size (Carlson et al. 2009). Due to its high spectral resolution, MISE observations will be sensitive to these subtle changes. MISE data will be used to map the grain size, crystallinity, and distribution of water ice globally, as is discussed in the following sections.

"Fresh" water ice on the surface can also be identified by Europa-UVS observations by measuring the strong, distinct 165 nm spectral edge of water ice seen in the laboratory and

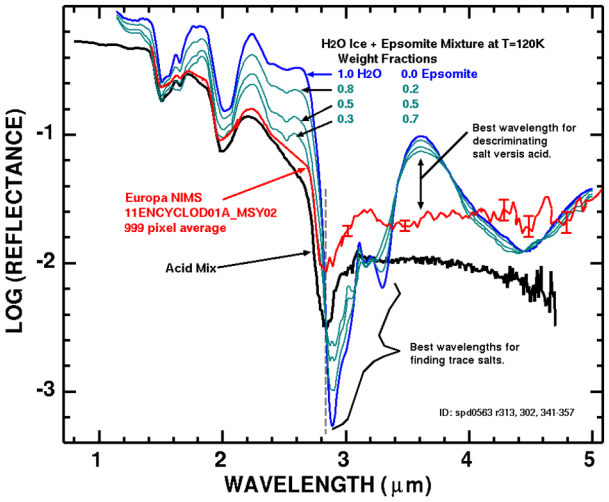

Fig. 4 Laboratory spectra and models compared to a Galileo NIMS spectrum, showing wavelength regions for discrimination between H_2O ice, solid acids, and hydrated salts. MISE observations will cover this spectral range (Blaney et al. 2024, this collection). Epsomite, $MgSO_4{\cdot}7H_2O$, is a hydrated sulfate mineral. The acid mix (ID = spd0563 record 302) is 50 wt% H_2O + 25 wt% HCl + 25 wt% HBr with trace amounts of MKS812 (Mauna Kea red soil) and Carbon Lamp Black to redden and darken the spectrum

observed in Saturn's rings and on icy surfaces such as the Saturnian moon Enceladus, which is presumably constantly coated with fresh, water-rich E-ring grains (e.g., Hendrix et al. 2010; Raut et al. 2018). Surprisingly, observations of Europa's leading hemisphere, which is considered the least-contaminated water ice based on IR and visible observations of the spectral water bands, does not display this strong UV feature in HST observations (Fig. 5; Roth et al. 2016; Becker et al. 2018, 2022). This may be due to some surface processing of ice, a surficial UV-absorbing lag deposit of a non-ice material, or UV-absorbers within the ice grains (Molyneux et al. 2020). The Europa-UVS spectral bandpass covers the wavelength of the water ice spectral edge and will be used to correlate any detections of "pristine" water ice with other key observations by Europa Clipper. In particular, the known water ice absorption features within the MISE bandpass and other thermal or geological anomalies observed by E-THEMIS and EIS, respectively, will be important for identifying any possible recent water upwelling or plume deposits (Sect. 5).

The deuterium to hydrogen (D/H) ratio of the water ice has implications for the history of the water on Europa because different processes will result in various fractionations (Sect. 6). The MASPEX instrument will collect bulk samples of volatiles derived from the surface via sputtering by using a cryogenic trap; mass spectrometry analysis of the trapped bulk sample will yield the D/H ratio for the collected water vapor. The cryo-trapped samples will also be able to reveal minor components such as HDO and $H_2{}^{18}O$, again with implications for the evolution of the ice. The mass resolution of the instrument is sufficient to resolve $H_2{}^{17}O$ from HDO. The MISE NIR data will be used to independently map D/H across Europa's surface using the band depth of the 4.12 μm absorption (Clark et al. 2019). Recent experiments show that impact ionization time-of-flight (TOF) mass spectrometers, such as SUDA, may be able to provide measurements of the D/H ratio of icy dust grains ejected from the surface when operating in the negative ion mode (Ulibarri et al. 2023), thus potentially providing a unique constraint for comparison with other Europa Clipper measurements. While the D/H ratio of water may be modified by radiolysis, combining these measurements with other isotopic enrichment information will aid in constraining details about the water that could help understand the formation and evolution of Europa (Sect. 6).

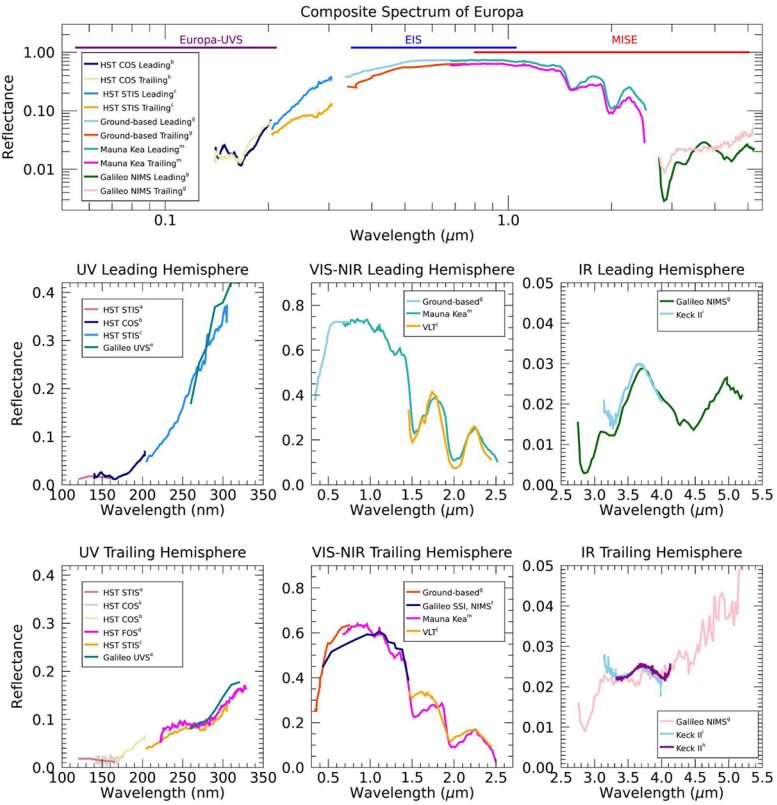

Fig. 5 (Top) A composite of selected spectra of Europa's leading and trailing hemisphere from the UV to the IR. Wavelengths covered by Europa Clipper investigations are indicated with horizontal bars. Note that EIS spectral coverage is not continuous; six bandpasses are used to cover this spectral region. (Middle row) Leading hemisphere spectra of Europa in the UV, VIS-NIR, and IR. (Bottom row) Trailing hemisphere spectra of Europa in the UV, VIS-NIR, and IR. The data in this figure were retrieved from the following: [a]HST Space Telescope Imaging Spectrograph (STIS) data from Becker et al. (2018), [b]HST Cosmic Origins Spectrograph data from Molyneux et al. (2022); [c]HST STIS data from Becker et al. (2022); [d]HST Faint Origin Spectrograph data digitized from Noll et al. 1995; [e]Galileo UVS data from Hendrix et al. (2005); [f]Galileo Solid State Imaging (SSI) experiment and NIMS data digitized from Fanale et al. (1999); [g]Data digitized from Carlson et al. (2009); the leading hemisphere visible data were collected by Spencer et al. (1995) at the Lowell Observatory, the trailing hemisphere visible data were collected using ground-based telescopes by Johnson (1970), Wamsteker (1972), and McFadden et al. (1980), the NIR data are from Galileo NIMS; [h]Keck II telescope NIRSPEC data from Trumbo et al. (2017); [i]Keck II NIRSPEC telescope data from Hand and Brown (2013), [j]Very Large Telescope/SINFONI data digitized from Ligier et al. (2016); [k]HST Cosmic Origins Spectrograph data from McGrath et al. (2015); [m]Mauna Kea Observatory data from Clark and McCord (1980). The trailing hemisphere data from Galileo-UVS have been normalized by a factor of 0.75. The trailing hemisphere Mauna Kea Observatory data were normalized to 1 at 1.2 μm, here they have been normalized to match the ground-based data with an approximate visible albedo of 0.6. The leading hemisphere Mauna Kea data was normalized to 0.7 to match the other ground-based leading hemisphere data published by Carlson et al. (2009). The Galileo SSI/NIMS data have been normalized by a factor of 0.65 to be consistent with the other datasets at 1.2 μm. Note that some of these data have been corrected for geometric albedo, while others are more simply reflectance, but they provide an overview of the general shape, absorption features, and hemispherical differences observed across Europa's spectrum. The Europa Clipper instrument suite will acquire spatially resolved data covering nearly the entire spectrum from 55 nm to 5 μm across the surface of Europa. Simultaneous observations at multiple wavelengths will reduce uncertainties introduced by differences in observational conditions including phase angle and local solar time across the spectral bandpasses

2.1.2 Surface Ice Porosity

Surface porosity is modified by multiple processes, including impact gardening (Sect. 6), deposition of fallout from possible plume activity (Sect. 5), and refreezing of brines associated with possible cryovolcanism. The magnitude of these effects, and the retention of porosity in general, depends on the local thermal conditions. Thus, variations in the porosity of Europa's surface ice may provide insight into local variations in thermal conditions and geologic history, both of which can influence composition. Furthermore, surface porosity also affects the interpretation of spectral measurements that will be acquired by the remote sensing investigations. Therefore, it is important to constrain the porosity in order to properly interpret Europa Clipper data in terms of the surface composition.

Models of radar backscatter observations have indicated that the porosity in the upper meter of Europa's ice shell could range from 33% to 94% (Black et al. 2001; Lee et al. 2005). Visible and UV observations suggest hemisphere-averaged surface porosities (at representative optical depths) of ~80–95%, assuming a uniform grain size distribution, with the sub-Jovian and anti-Jovian hemispheres having higher porosities than either the leading or trailing hemispheres (Domingue and Verbiscer 1997; Hendrix et al. 2005). Nevertheless, detailed spatial variations and vertical profiles of Europa's near-surface porosity remain poorly constrained. Models suggest that millimeter-to-meter scale voids (associated with porosities between 1% and 22%) may extend from hundreds of meters to kilometers into the subsurface (Aglyamov et al. 2017; Nimmo et al. 2003). The extent of porosity depends on the balance of the processes that either work to promote the creation of porous ice (e.g., impacts and tectonic fracturing) or those that tend to remove porosity (e.g., sintering, Sect. 6).

The porosity of surface ice will be constrained through multiple Europa Clipper investigations. The effective reflection coefficient at radar wavelengths depends primarily on the ice/void ratio at the surface, which relates nonlinearly to porosity (Cuffey and Paterson 2010). The wide radiometric range of REASON enables the distinction between compact ice from old fallout vs. from fresh, porous deposits (Grima et al. 2014a; Scanlan et al. 2022). Photometric modeling of the solar phase curve reflectances as measured by EIS, MISE, and Europa-UVS will provide an alternative method to constrain porosity (e.g., Domingue and Verbiscer 1997; Hendrix et al. 2005). An array of Europa Clipper flybys at a variety of geometries will enable robust, simultaneous spectral measurements of reflectance across phase angles and regions of the globe. This will provide the data for the photometric models to constrain variations in ice porosity (as well as grain size; Sect. 2.1.3). Additional constraints on porosity may be obtained from the thermal properties of surface materials determined from E-THEMIS data (Christensen et al. 2024, this collection).

2.1.3 Surface Ice Grain Sizes

Current best estimates for the grain size of ice on Europa's leading hemisphere were derived from Galileo Near Infrared Mapping Spectrometer (NIMS) spectra to be ~30–40 μm (Hansen and McCord 2004). On the trailing hemisphere, H_2O grains are thought to be ~20 μm in diameter near the equator, and the size increases to 100 μm nearer to the poles (Carlson et al. 2005, 2009).

Like porosity, surface grain sizes can be constrained by photometric modeling of the solar phase curve measurements, most notably using Hapke models (e.g., Hapke 1986), and by the strength and shapes of absorption bands (e.g., Clark 1999, and references therein). Modeled spectra of pure ice as a function of grain size are shown in Fig. 6. Different wavelengths, with different absorption strengths, probe to different depths (Fig. 7), and enable the dependence

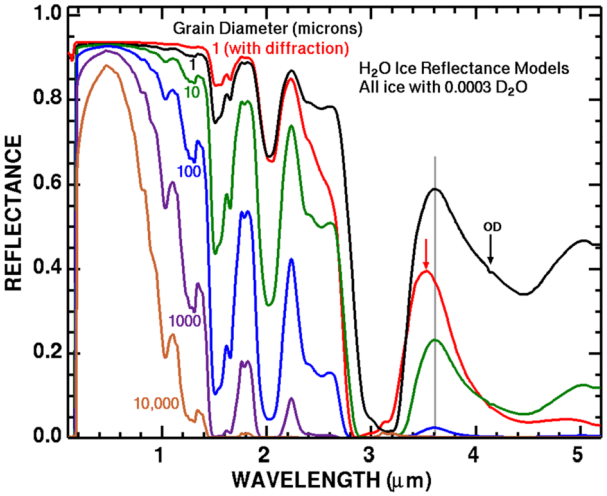

Fig. 6 Models of pure ice spectra at different grain sizes, covering the MISE and EIS spectral range and approaching the Europa-UVS spectral range. Assessments of the depths and positions of these spectral features will be used to constrain grain sizes across Europa. The strong OH stretch fundamental is located near 3 μm, and a strong absorption is seen at wavelengths shorter than 0.165 μm. All visible to NIR absorption bands are temperature sensitive; it is not known how temperature-sensitive the UV absorption may be (e.g., Ockman 1958; Clark 1981; Grundy and Schmitt 1998; Mastrapa 2004; Clark et al. 2012). Diffraction by small grains affects the position, shape, and strength of the absorptions (Clark et al. 2012). The OD absorption near 4.12 μm can be used to derive the D/H ratio in H_2O ice (Clark et al. 2019)

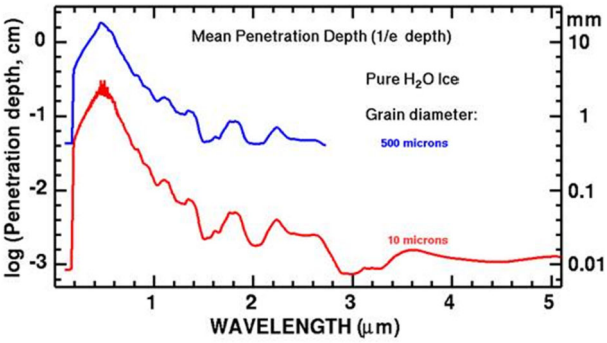

Fig. 7 The wavelength-dependent penetration depth (1/e depth) of photons into a water ice surface composed of one of two ice grain diameters: 10 μm (red) and 500 μm (blue). These wavelengths are covered by the EIS and MISE investigations in the visible and infrared spectral ranges, so simultaneous measurements will provide assessments of grain crystallinity and composition as a function of vertical depth in the uppermost surface regolith. Depths were derived using Hapke (2012) and Clark and Roush (1984) models. For a regolith composed of 10-μm diameter ice grains, the maximum depth probed ranges from ~12 mm at 0.8 μm to ~0.03 mm near 3 μm

of the grain size on depth to be derived. The ratio of EIS measurements made at 1 μm (950–1050 nm) to those made at IR1 (780–920 nm) will be used to infer surface ice grain sizes (Porco et al. 2006). The transparency of the ice at different MISE wavelengths will enable an even deeper probe (up to 10 mm deep, depending on grain size). Observations of surface reflectance at Lyman-alpha (121.6 nm) from HST have shown an anti-correlation

with the visibly dark and bright regions that may be caused in part by grain size (McGrath et al. 2009; Roth et al. 2014b; Becker et al. 2018). Higher spatial resolution observations by EIS and Europa-UVS may confirm these correlations and provide insight into the physical surface properties causing this albedo pattern, such as space weathering or grain properties, including size and porosity.

As discussed in the previous section, the multiple geometries and illuminations during the Europa Clipper flybys will enable robust solar phase curves to be generated across the UV, visible, and NIR wavelength spectrum. These in turn will be used to derive grain size and scattering parameters of the ice from models using Hapke's theory (Hapke 1986).

2.2 Europa's Non-ice Surface Materials

Two of the primary compositional goals of the Europa Clipper mission are to identify and map non-ice material on the surface, as well as sources in the atmosphere and local space environment. Some of these non-ice materials have likely been brought to the surface from below through various geologic processes (Sect. 6) and therefore represent an opportunity to constrain the composition of Europa's interior; other surface materials are exogenic in origin.

2.2.1 Sources of Non-ice Materials on the Surface

By leveraging the complete suite of investigations on the Europa Clipper mission, it may be possible to distinguish between the sources of the non-ice material found on Europa's surface. Endogenic materials on the surface have direct implications for the composition of the interior, as well as how the satellite (and the entire Jovian system) formed. The deficiency of impact craters on Europa compared with other airless bodies, including Ganymede and Callisto, suggests that resurfacing, which may be regionally or globally related to a subsurface liquid source, has occurred geologically recently (Bierhaus et al. 2009) or even continues to occur. It is noted that some of the geologic features are associated with variations in albedo, color, and composition (Fig. 8) and may represent avenues for which subsurface material is brought to the surface. Some hypotheses for the formation of geologic features on Europa's surface, such as chaos terrains, invoke mechanisms of brine transport towards the surface (Schmidt et al. 2011; Daubar et al. 2024, this collection). Laboratory experiments of flash-frozen brines produced near-IR features similar to those on Europa (McCord et al. 2002; Dalton et al. 2005; Dalton and Pitman 2012a; Orlando et al. 2005).

Exogenic sources of non-icy materials include material delivered from outside of the Jovian system by micrometeoroids and larger impactors and from within the system from material ejected and sputtered from other Jovian satellites (Pollack et al. 1978; Zahnle et al. 1998). Specifically, compounds containing C, H, O, N, S, Na, Al, Si, K, Mg, Ca, and Fe may come from a variety of sources including the other Jovian satellites, the solar wind, chondritic impactors, and cometary dust (e.g., Pierazzo and Chyba 2002; Carlson et al. 2009). A particularly large source of exogenic materials may be the volcanically active Jovian moon, Io. Nanograins originating from Io's volcanic plumes (e.g., NaCl) and detected in the Jovian system by Cassini (Postberg et al. 2006) can become charged and then be radially accelerated by the corotational electric field in Jupiter's magnetosphere and subsequently delivered to Europa (see Sect. 4). The number of iogenic neutral S and Na expected to interact with and be accumulated in some forms on Europa's surface is approximated to be $\sim 1 \times 10^6$ and $\sim 4 \times 10^4$ atoms, respectively (Cooper et al. 2001; Johnson et al. 2004).

Clues for distinguishing between the endogenic and exogenic origin of surface species come from: 1) association of materials with specific types of geologic features; 2) general,

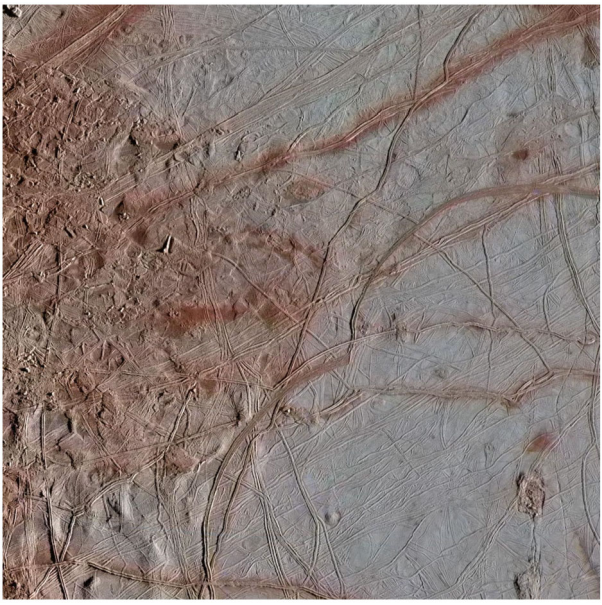

Fig. 8 Enhanced color image of Europa's surface from Galileo depicting a ~300 km transitional region between blocky chaos terrain (left) and ridged plains (right). The coloration, indicative of non-ice material, corresponds with much of the geological terrain whereas the more featureless part of the surface is associated with more "pristine" water ice. CREDIT: NASA/JPL-Caltech/SETI Institute

widespread patterns across the surface (e.g., hemispheric) that may reflect preferential emplacement or processing of material; and 3) investigations of the space environment, and Io's fluxes, in particular. The high-resolution images of geologic features on Europa to be achieved by EIS, combined with the high spatial- and spectral-resolution NIR measurements of these same regions afforded by MISE, will enable correlation of local landforms and compositions (Sect. 2.3). Europa-UVS and SUDA observations during close flybys of geologic features (Goode et al. 2021; Retherford et al. 2024; Kempf et al. 2024, both this collection) will be used to further investigate these correlations. However, it is important to consider processing of exposed endogenic species (Sect. 6). For example, the preferential radiolysis of the trailing hemisphere by Jupiter's magnetic field or the higher rate of impact gardening on the leading hemisphere (Johnson 1996) may alter how and where endogenic species are (or are not) detected.

The widespread hemispheric albedo and compositional patterns on Europa provide clues to the origin of some exogenic species. As Jupiter's magnetic field sweeps past Europa with a periodicity of ~11 hours, it deposits species from Io, including charged O, S, SO, SO_2, and nm-sized mineral dust (e.g., Hsu et al. 2012; Bagenal and Dols 2020). This deposition (and subsequent radiolysis) has resulted in the presence of S-bearing materials (sulfur allotropes, sulfuric acid hydrate, S-O species, likely SO_2), which are heavily concentrated on Europa's trailing hemisphere (Lane et al. 1981; Noll et al. 1995; Hendrix et al. 1999; Carlson et al. 2002, 2005, 2009; Becker et al. 2022). Meanwhile, exogenic material from outside of the Jovian system may be preferentially present on the leading hemisphere due to the orbital direction of Europa (Zahnle et al. 1998).

Further constraints on what material is endogenic versus exogenic will be obtained by studying Europa's space environment and assessing the influx of exogenic materials (Sect. 4). The PIMS instrument will measure the flux, composition, and origin of main plasma ions, electrons, and, if present, anions, and from these data, the surface sputtering rates from Europa may be determined to constrain surface alteration (Westlake et al. 2023, this collection). Measurements of Jovian O^+, S^{n+}, and e^- will be used in conjunction with

magnetic field models to produce precipitation maps onto Europa's surface. The precipitation maps will be compared with MISE NIR spectral imaging to identify regions that have been significantly weathered (Dalton et al. 2012b, 2013).

The Europa-UVS instrument will detect emissions from sulfur, oxygen, and hydrogen neutral atoms and ions in the environment surrounding Europa, including its neutral cloud and torus if present. Determining the Jovian distance at which these emissions peak potentially allows particles originating from Io to be distinguished from those originating from Europa (e.g., Szalay et al. 2022). The SUDA instrument will conduct survey measurements at distances farther from Europa specifically to determine the composition of submicron grains originating from Io and other Jovian moons, and of interplanetary dust grains, providing critical data on the composition of exogenic grains. These will be contrasted with endogenic grains during the closest approach flybys of Europa.

The ECM investigation will measure magnetic perturbations caused by the interaction of the incident Jovian plasma flow with the neutral and charged particles present at Europa; these measurements will help constrain particle origins to localized surface source regions (Kivelson et al. 2023, this collection). For example, geologically active source regions, if present, would support an endogenic origin, as was found by Cassini at Enceladus (Dougherty et al. 2006). Time-variability of species that are not associated with changes in the external plasma environment would provide further indirect evidence for an endogenic source.

2.2.2 Detecting Non-ice Materials on Europa's Surface

The Europa Clipper investigations will confirm and map spatial distributions of previously identified non-ice compounds and detect new species. Compounds that have been previously identified on Europa with a high degree of confidence include H_2O_2, CO_2, SO_2, O_2, NaCl, S_4, S_8, and polymeric sulfur, S_μ (Johnson and McCord 1971; Lane et al. 1981; Noll et al. 1995; Spencer et al. 1995; Smythe et al. 1998; Carlson et al. 1999a,b; McCord et al. 1999; Spencer and Calvin 2002; Hand et al. 2007; Hansen and McCord 2008; Carlson et al. 2009; Trumbo et al. 2022; Trumbo and Brown 2023; Villanueva et al. 2023). In addition, at least one or several hydrated sulfates have been identified (Carlson et al. 2009).

Sulfates: Fits to Galileo NIMS spectral data have suggested the presence hydrated sulfates and/or sulfuric acid hydrates on Europa's surface (Clark et al. 1980; Carlson et al. 2005; Dalton 2007, 2012a; Hibbitts et al. 2019; Shirley et al. 2016). Ground-based observations with the Keck II telescope indicate that radiolytically produced magnesium sulfate hydrate ($MgSO_4 \cdot 7H_2O$, epsomite) may also be present on the trailing hemisphere (Brown and Hand 2013), though a recent analysis of similar ground-based observations from the Very Large Telescope (VLT) question this interpretation in favor of a non-salt radiolysis product (Davis et al. 2023). The high spectral resolution of the MISE instrument will resolve the distortions of the NIR absorption bands on Europa's surface between 0.8 and 2.4 μm that are indicative of these materials (McCord et al. 1999; Dalton 2003; Carlson et al. 2009). MISE observations in the 3.5 μm region will discriminate between acid hydrates and hydrated sulfates, such as epsomite, that could precipitate from ocean-sourced water solutions (Fig. 4). MISE will also be sensitive to the the 4 μm SO_2 feature. SUDA will identify and distinguish sulfate salts and sulfuric acid (Napoleoni et al. 2023b).

Spatially resolved visible wavelength spectra from the HST show several features that are confined to the trailing hemisphere that may reflect sulfur-bearing species, with others following a distribution consistent with sulfur allotropes (S_4, S_8). Some materials show an association with geologic features, suggesting that they are radiolytically produced from a mixture of endogenic material and exogenic sulfur (Hendrix et al. 2011; Trumbo et al.

2020). Through mapping of the 280-nm UV absorption feature, SO_2 has been identified in concentrated abundance near the trailing hemisphere but is not detected on the leading hemisphere (Lane et al. 1981; Noll et al. 1995; Hendrix et al. 1999; Becker et al. 2022). Measurements of HSO_4^- and other S-bearing ions in the SUDA dataset will also constrain hemispheric distribution of sulfates (Napoleoni et al. 2023b).

Chlorides: Chlorides are also likely present on the surface of Europa (Fischer et al. 2015; Hand and Carlson 2015; Hanley et al. 2014; Ligier et al. 2016; Poston et al. 2017; Trumbo et al. 2019, 2022; Brown et al. 2022). Like some of the observed sulfates, chlorides are possibly derived from the subsurface ocean (Kargel et al. 2000; Zolotov and Shock 2001), although some surface chlorides could be from Io (cf. Postberg et al. 2006). Pure alkali halides, such as those found in Earth's oceanic evaporites (e.g., NaCl and KCl) are spectrally flat across much of the visible and infrared wavelengths and are not uniquely distinguishable from water ice in their visual appearance. When irradiated, however, these salts acquire distinct coloration and spectral features (Hand and Carlson 2015; Poston et al. 2017; Hibbitts et al. 2019; Brown et al. 2022) that will be evident in EIS color observations (e.g., Fig. 9). Similarly, visible (450 nm, 720 nm) and mid-UV (230 nm) spectral signatures of irradiated NaCl have been detected in HST data, with the highest concentration in the chaos of Tara Regio, suggesting an endogenic origin (Trumbo et al. 2019a, 2019b, 2022). Hyperhydrated NaCl species are predicted to be metastable on the surface of Europa and their putative presence may explain why there have been no clear identifications of NaCl on the surface at infrared wavelengths (Journaux et al. 2023). SUDA is very sensitive to any type of chlorides in both its cation (e.g., $(NaCl)Na^+$, Postberg et al. 2009) and anion (e.g., $(NaCl)Cl^-$, Napoleoni et al. 2023b) channels and can determine the distribution of different chlorides on the surface.

NaCl was also identified by the Cassini Cosmic Dust Analyzer (CDA) as the major dust grain constituent of Jovian stream nanograins (likely originating from Io), accompanied by minor sulfur- and potassium-bearing components (Postberg et al. 2006), although the CDA composition measurements were taken within 1 AU from Jupiter, and other constituent species might have been lost due to sputtering. The SUDA instrument can detect sub-ppm concentrations of chlorides (Napoleoni et al. 2023b; Kempf et al. 2024, this collection) and will constrain whether the material is exogenic to Europa by making measurements at Europa Clipper's orbital apoapsis and at closest approach to the satellite (Sect. 4.2.2)

Organic Compounds: Organic matter is widespread in the outer solar system and may exist on Europa's surface through impact delivery, radiolysis of implanted compounds, and/or upward transport of material from the interior (deep icy shell, an ocean, or sub-oceanic materials). JWST observations of Europa have been used to identify CO_2 on the surface that is concentrated near the chaos region Tara Regio, possibly indicative of a sub-surface, internal source of carbon (Trumbo and Brown 2023; Villanueva et al. 2023). The MISE bandpass includes the spectral features at 2.7 microns, 4.27 microns, and 4.25 microns that were used to identify CO_2 in the JWST data.

The 3–5 μm spectral range of the MISE instrument will be critical for detecting organic compounds because C–C bonds in aliphatic hydrocarbons can be distinguished from the stronger C = C (e.g., benzene, polycyclic aromatic compounds) and C ≡ C bonds in other hydrocarbons (cf. Clark et al. 2009; Kokaly et al. 2017). This offers an approach for distinguishing hydrocarbons from one another, as shown in Fig. 10, as well as from other dissimilar materials that may be present on the surface of Europa. SUDA measurements are sensitive to sub-ppm concentrations of a wide variety of organic constituents, including potential biomarkers inside ice grains (Dannenmann et al. 2023; Napoleoni et al. 2023a,b).

Other Materials: Data acquired by the MISE instrument will allow for the detection of absorption features associated with several other materials, including the 3.5 μm H_2O_2

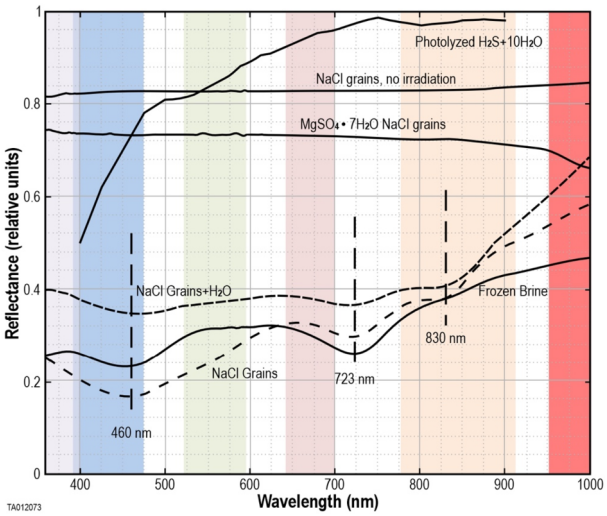

Fig. 9 Spectra of 10 keV electron-irradiated NaCl grains showing the absorption features at 460 nm and 720 nm for the F and M centers. Shown are results from three irradiation experiments that simulate a range of possible surface conditions on Europa: NaCl grains (dashes), NaCl grains with approximately 1 μm of water deposited on top (close dashes), and an NaCl evaporate (frozen brine) created by introducing a salt-saturated solution into the vacuum chamber and slowly removing the water (solid line). The presence and depth of these absorption features could be detected by EIS and used to identify very young terrains with endogenic or exogenic (e.g., Ionian) chlorides. The EIS spectral bandpasses are indicated by the vertical color bars. Also shown for comparison: a spectrum of NaCl before irradiation, spectrum of cryogenic magnesium sulfate heptahydrate (epsomite) grains, (~180 μm) and photolyzed hydrogen sulfide (from Carlson et al. 1999). Figure modified from Hand and Carlson (2015)

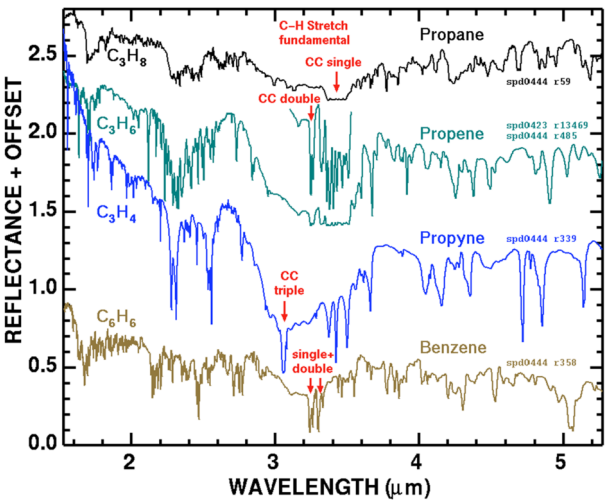

Fig. 10 Near-infrared spectra of four hydrocarbon compounds that would be detectable with the MISE instrument. As the C–C bond strength increases from propane through propene to propyne, the C–H stretching absorptions shift to shorter wavelengths. Spectral differences between the various carbon bonds are noted in red. Figure adapted from Clark et al. (2009)

feature. The 2.1–2.4 μm range of the MISE instrument will be sensitive to spectral features associated with phyllosilicates such as clay minerals.

2.3 Investigating the Composition of Local Landforms

2.3.1 Implications for Landforms Based on Compositional Information

Europa's surface comprises a collection of geologic constructs that provide clues to the evolution of its ice shell and the transport of material within and through the shell via melt (e.g., Schmidt et al. 2011; Buffo et al. 2020; Lesage et al. 2020, 2021; Chivers et al. 2021) and through ice dynamics associated with tectonic deformations, possible convection (e.g., Kattenhorn and Prockter 2014; Howell and Pappalardo 2018), and cryomagmatism (Muñoz-Iglesias et al. 2013, 2014, 2019; Lesage et al. 2020, 2021). Such features include ridges and double ridges, lineae, ridged plains, band-like structures, chaos regions, lenticulae, and frozen briny surface flows (Greeley et al. 2000; Fagents 2003; Figueredo and Greeley 2004; Quick et al. 2017, 2022; Leonard et al. 2018, 2020; Senske et al. 2019; Shirley et al. 2010; Lesage et al. 2020, 2021; Singer et al. 2021; Daubar et al. 2024, this collection). Evidence of ocean-sourced material on the ridged plains would support a thin ice shell at the time of their formation. Likewise, ocean-sourced material associated with band-like features would support a terrestrial mid-ocean-ridge-like genesis (Howell and Pappalardo 2018). The composition of chaos terrains will be integral for deciphering the formation mechanism(s) of these features. Some proposed chaos formation mechanisms (Daubar et al. 2024, this collection), including melt-through (Carr et al. 1998; Greenberg et al. 1999, 2003), liquid water sills, or melt lenses (Schmidt et al. 2011; Michaut and Manga 2014), may concentrate impurities in liquid water that is then refrozen within specific portions of the chaos (Buffo et al. 2020; Chivers et al. 2021). In comparison, dissolution and migration associated with chemical and/or thermal diapirism may result in the formation of more pure ice (Pappalardo and Barr 2004).

Stereo imaging of the various surface landforms by EIS, combined with the highest spatial resolution spectral data from MISE and Europa-UVS, will be used to correlate composition with geologic regions of interest. Further, the measurements of ice and dust grains by the SUDA instrument can be traced back to a specific region of origin on the surface by modeling their ballistic trajectories (Fig. 11). If the same region is flown over twice, using SUDA's anion mode during one flyby and the cation mode during another, it will be possible to constrain the salt and acid hydrate composition of a local feature on Europa's surface and hence the salinity, which may provide information about its subsurface source. Importantly, SUDA can detect NaCl with high sensitivity (Postberg et al. 2009; Napoleoni et al. 2023a).

2.3.2 Inferences of Surface Age from Composition

The Europa Clipper observations will provide a means to estimate relative surface ages. For example, high energy particles from Jupiter's strong radiation environment will damage materials on the surface and generate radiolytic products such as oxidants (O_2, H_2O_2) (e.g., Loeffler et al. 2006; Mastrapa and Brown 2006; Teolis et al. 2017b) and acid hydrates. Europa Clipper observations will constrain the abundance of these radiation byproducts on the surface with MISE and in the atmosphere with Europa-UVS and MASPEX (Sect. 2.2.2). The intensity of the existing, variable radiation environment will be directly accounted for through RadMon measurements (Meitzler et al. 2023, this collection). These measurements can then be used to quantify the radiolytic damage of a given feature as a function of time, providing a metric by which a rough geochronology of Europa will be constrained (e.g., Dalton et al. 2013). Complete saturation of the surface would provide a lower limit to the

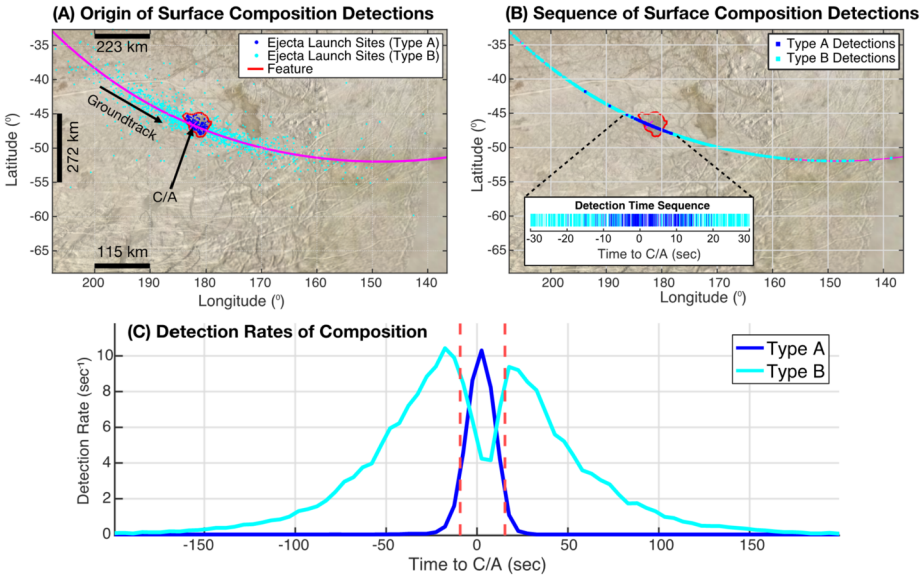

Fig. 11 A simulation of SUDA surface impact ejecta detections during a flyby over Thera Macula (feature outlined in red) demonstrating how SUDA will provide surface composition with spatial resolution over geologic features. Panel A shows the locations of origin on the surface of the grains detected by SUDA. Panel B shows the modeled detection sequence of two types of ejecta. The detections marked in dark and light blue colors originate from inside and outside Thera Macula, respectively. The closest approach altitude of 35 km in this model is close to the center of Thera Macula, making it an ideal trajectory to obtain its surface composition. Panel C shows the modeled detection rate of both types of composition. The vertical red dotted lines indicate when Europa Clipper is over Thera Macula. In this case, detections from Thera Macula dominate the detection rate by SUDA when over the feature. This figure demonstrates how the SUDA investigation will map Europa's surface composition through impact ejecta cloud measurements

surface age. Interpretation of these data, however, will require modeling of competing processes that expose fresh materials on the surface, such as impact gardening (Sects. 2.4 and 6.7).

Constraints on the D/H ratio (Sect. 2.1.1) will be used to infer surface age; older surfaces are expected to be enriched in D due to preferential H escape. The spectral signatures of non-ice materials exposed on Europa's surface tend to weaken as the surface ages, while the signature of mostly amorphous water ice increases. This has been interpreted to result from the build-up of a sputtered water ice layer on non-ice materials (Hansen and McCord 2004), which may be enhanced by radiation-induced desiccation of the hydrate. MISE measurements of the relative spectral signatures of the non-ice materials may constrain the relative importance of these mechanisms.

The relative surface age will also be estimated from measurement of the density and porosity of putative plume fallout deposits, which can be inferred from E-THEMIS and REASON data (Sect. 5). Fresh fallout deposits should progressively stiffen and densify with age through sintering (Sect. 6.6) (Cuffey and Paterson 2010), the rates of which depend on grain size and temperatures (Blackford 2007; Molaro et al. 2019; Choukroun et al. 2020). Plume fallout on Europa is expected to coalesce and build strength over time. Estimates of the timescales over which detectable plume deposits form range from decades to Ga (Bierhaus et al. 2009; Ashkenazy 2019; Molaro et al. 2019; Choukroun et al. 2020).

Several well-characterized radiolytic compounds, such as H_2O_2 and H_2SO_4, form and reach a saturation steady state on timescales that are short relative to the formation of all but the youngest surfaces (Carlson et al. 1999a; Hudson and Moore 2001; Hand and Carlson 2011; Trumbo et al. 2019b). Salts, however, may provide a useful geologic clock (Seinen et al. 1994; Hand and Carlson 2015; Poston et al. 2017). Alkali halides develop radiation-induced color centers that produce strong absorption features in the ultraviolet and visible regions of the electromagnetic spectrum. These color centers form when a vacancy in the crystal lattice is filled by a lone electron. The primary center, the so-called F center, forms first, followed by a dose and temperature dependent accumulation of additional electrons (and vacancies) that yield the M, R, N, and V centers, some of which overlap with EIS bandpasses (Fig. 10). The relative growth of these centers, and their corresponding absorption features, provide a metric for assessing surface ages on Europa. Based on laboratory experiments with NaCl, Poston et al. (2017) showed that comparisons between the F and M centers in that salt could be used to assess ages of very young surfaces (∼10–100 years). Many additional parameters explored in that work (such as surface temperature, color center bleaching, and radiation type and flux) indicate that color center band ratios can also be used to estimate higher surface ages. In addition, color centers in other salts (e.g., KCl) will be used in conjunction with NaCl to further enhance this technique for estimating surface ages. Interestingly, HST observations of Europa revealed the F center of NaCl, but found no evidence of the M center (Trumbo et al. 2019a,b). The distribution of the F-center absorption was heterogeneous, with the maximum absorption found near the equator in Tara Regio (∼85° W). One interpretation of this discovery is that the chaos features in that region could be delivering endogenous salt-rich oceanic material to the surface, after which the exposure to irradiation yields the observable F center. The EIS blue filter overlaps with the F center and whereas the red filter partially overlaps with the M center (see Fig. 10) giving the Europa Clipper mission the ability to potentially determine whether the material is sufficiently young and fresh so as not to have yet accumulated enough radiation to produce the M center.

2.4 Shallow Compositional Profile

Material on Europa's surface is affected by ion bombardment, sputtering, radiolysis, and overturn from meteorite bombardment, all of which are processes that can alter the composition to different depths (Sect. 6.6). The shallowest of these processes is energetic ion bombardment from species such as H^+, Na^{n+}, S^{n+}, and O^{n+}, which deposit all of their energy in the top hundreds of nanometers to microns, depending on the energy and type of particle. Ion bombardment is responsible for the majority of the sputtering of surface particles (Cassidy et al. 2013) that will be analyzed by SUDA and dominates the contribution to the atmosphere (Hall et al. 1995) that will be measured by MASPEX and Europa-UVS. Energetic electrons can penetrate more deeply (tens of centimeters to meters, depending on energy) than ions, and the secondary X-rays, which are produced when these particles interact with the ice (called Bremsstrahlung), can travel a few additional meters into the ice. The fluxes and energies of these particles vary with latitude and longitude on Europa, and their effects on the surface can range from extensive, centimeters-to-meters deep processing near the equator (particularly on the trailing side), to mild, ∼1-centimeter-deep near the poles (Nordheim et al. 2018). These particles can implant into the surface, sputter existing surface material, dehydrate minerals, break bonds, and generate free radicals, which can form new chemical species. As discussed above, variations in the presence of these new chemical species may help constrain the different surface ages. Over time, this leads to the increase in the abundance of more radiolytically-stable species at the surface such as sulfate, salts,

and sulfuric acid (Carlson et al. 1999b, 2002). Micrometeoroid bombardment is estimated to mix the upper ∼1 meter of the surface over the past $\sim 10^7$ yr (Sect. 6.6.2), whereby results from some recent models for impact gardening indicate that the gardening reaches varying depths based on location, with average mixing within 30 cm of the surface (Costello et al. 2021). This implies that the depth-dependence of the different processes described here may not persist but become muddled over time.

The mean penetration depth of electromagnetic radiation across the Europa-UVS to EIS to MISE wavelength range depends on grain sizes and absorption coefficient (Fig. 6). Europa's surface should exhibit considerable variability with depth from particle weathering within the top millimeters. Because of the varying transmission of ice across the IR wavelengths range, from near complete transparency at 0.8 μm to only penetrating mere microns at 3 μm, the MISE NIR spectral measurements will probe not only the top surface that is dominated by radiolysis but also deeper into grains that can be warmed by sunlight.

Deposition and thermal processing affect the compositional depth profile of the surface. Heating of the surface can cause sublimation of water and other volatiles and lag deposits containing salts and other non-volatiles. Re-deposition of these volatiles (or of species that were outgassed, sputtered, or ejected through meteorite bombardment) may be more pronounced in colder locations such as potential permanently shadowed regions and the poles, which can cause a global redistribution of volatiles and obscure underlying material in these regions (Spencer 1987). These types of deposits likely vary with latitude/longitude and local temperature, and the thicknesses are unknown. Regions subject to steady accumulation of ice will result in material density that increases continuously with depth, which will be evident in the radar reflection coefficient and a sharper dielectric gradient in the near-surface vertical column (Grima et al. 2014a). Thermophysical properties derived from E-THEMIS measurements will also be sensitive to such surface processing and allow detection of any low-density plume deposits (Sect. 5).

Thermal processes influence the ice phases exposed on the surface. Deposition of water vapor onto colder regions of Europa (<120 K) may result in amorphous ice, while exposure of ice to warmer temperatures converts the structure it to crystalline ice. The ice can again become more amorphous when exposed to radiation (e.g., Berdis et al. 2020; Hansen and McCord 2004). However, in cold environments on other satellites, such as the Saturnian and Uranian satellites, the ice is crystalline (e.g., Clark et al. 2012, 2013, 2014; Buratti et al. 2019; Cruikshank et al. 2020), and it remains a mystery as to why amorphous ice is not found in such cold environments. During the thermal amorphous-to-crystalline transition, any non-water impurities that are present may be displaced out of the ice lattice (Jenniskens and Blake 1996; Kouchi and Sirono 2001; Lignell and Gudipati 2015), increasing the likelihood of chemical reactions between impurities (Gudipati and Allamandola 2006) and outgassing of more volatile components and radiolytic products (Ghormley 1967; Hudson and Donn 1991).

Although these changes originate in tiny nanometer-to-micron-sized domains inside an ice lattice, their combined effects on reflectance spectra are observed as shifting absorption bands within the MISE spectral range (Clark et al. 2012; Mastrapa et al. 2008). Many wavelength ranges (for example, near 1.65 and 3.1 μm; Hansen and McCord 2004) can be used to determine ice temperature and/or crystallinity. Additionally, the measurements of surface temperatures derived from radiances in the range from 4.5 μm to 5 μm, which are elevated with respect to the background temperatures, could indicate the presence of active or recent resurfacing or near-surface advective processes. Together, these measurements can reveal the temperature of Europa's surface ice from below 50 K to melting.

The E-THEMIS instrument is sensitive to photons in the thermal infrared, which originate from the first few tens of microns of the surface materials. However, E-THEMIS is

designed to determine surface temperatures, which are controlled by the thermophysical properties down to ∼1–2 thermal skin depths (the depths at which the signal is attenuated by a factor of 1/e). Thermal skin depth is different than the NIR depth shown in Fig. 7 due to different optical properties at longer wavelengths. Therefore, the analysis of E-THEMIS data will constrain thermophysical properties (i.e., thermal conductivity, and to some extent, density, or porosity) for approximately the top meter of Europa's surface.

Surface echoes in the REASON shallow subsurface dataset will be used to identify regions of putative brines within the near-surface (on the order of one decameter to one hundred meters deep for the 60-MHz and 9-MHz signals, respectively). If present, brines will generate a stronger contribution to the total surface echo than those due to the effects of surface porosity (Grima et al. 2016), making them more easily detectable. Laboratory experiments of brine exposed to Europan surface conditions have confirmed precipitation of hydrated salts upon freezing (McCord et al. 2002; Vu et al. 2016; Thomas et al. 2017). Although the presence of hydrated salts may only have a relatively minor effect on the radar return echo, frozen brines could form ice layers that could interfere with surface reflections (Rutishauser et al. 2016). The observed echoes from REASON's VHF and HF frequencies will exhibit relatively distinct signatures that depend on layer depth and thickness (Mouginot et al. 2009), allowing REASON's two frequencies to identify regions of layering in Europa's near-surface. Detection of these layers may indicate regions where brines at depth have intruded into the porous surface and flash frozen.

The depth-dependent measurements detailed above will be used to assess the effects of radiation, impact gardening, and thermal processes on composition across Europa's surface. Details of the processes that affect the composition of the topmost ∼meter of the surface and how they impact the Europa Clipper measurements are given in Sect. 6.6, while the expected exploration of Europa's composition deeper into Europa's interior is described in Sect. 3.

3 Europa's Interior Composition

The current knowledge about the subsurface composition of Europa depends on models that typically do not have unique solutions. The interior composition will be estimated indirectly from Europa Clipper measurements of chemical speciation of surface and atmospheric materials and through the use of physical models that depend on the gravity, magnetic field, and density, and make use of the equations of states of relevant materials. These evaluations need to consider processes that formed the body and modify the original compounds as they approach the upper ice shell, surface, and the atmosphere (Sect. 6). For example, the composition of upwelling water solutions in the ice shell changes through freezing, while salts and organic compounds that may be delivered to the surface from Europa's interior are altered through radiolysis and polluted by exogenic ions, molecules, and grains originating from Io, other satellites, and from outside the Jovian system. While indirect, compositional constraints on the interior that will be inferred from Europa Clipper data are essential for understanding the formation, evolution, ongoing processing, and habitability of the moon.

3.1 Ice Shell Composition

The predominance of water in the surface materials suggests ice as the main constituent of the shell. However, other components are locally abundant at the surface in association with geologic features (e.g., ridges, chaotic terrains), and are expected to be endogenic (Sect. 2.3).

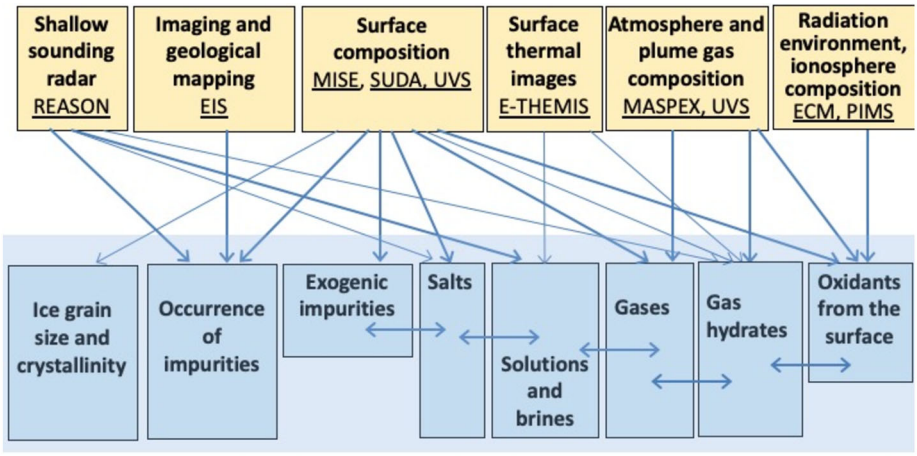

Fig. 12 Expected compositional datasets from Europa Clipper investigations and how they can be used to constrain the composition of the subsurface ice shell. The thin arrows indicate more indirect data sources. Horizontal arrows show that data on some impurities could inform studies of other impurities

Many features might not extend to the current ice–ocean interface, but rather reflect disruptions in an earlier, thinner shell (Daubar et al. 2024, this collection). The apparent thickening of the shell in the present epoch (Pappalardo et al. 1998) suggests elevated abundances of trapped oceanic impurities in the uppermost part of the shell and in geological features formed in a thin shell (Zolotov and Kargel 2009). The thickening of the ice and formation of a stagnant lid above possibly convecting ice could impede fluxes of radiolytic (H_2SO_4, O_2, etc.) and space-delivered (SO_2, NaCl, etc.) compounds to the deep subsurface.

Data from the remote sensing investigations such as MISE, REASON, Europa-UVS, and EIS in conjunction with *in-situ* observations by SUDA and MASPEX will be used to constrain the composition of the ice shell and the material from the surface sputtered into the atmosphere. The corresponding data together with contextual information from EIS and E-THEMIS will characterize materials associated with endogenic geological features. These data will provide information about the composition of the shell, accounting for processing of the surface, subsurface, and atmosphere (Sect. 6). An overview of the contributions of compositional datasets acquired by each investigation to a greater understanding of Europa's ice shell is illustrated in Fig. 12.

3.1.1 Salts and Brines

Multiple salts have been tentatively identified among non-ice constituents on Europa's surface (Sect. 2) and are likely present at depth within the ice shell. Endogenic salts, entrained in the ice through freezing of the oceanic water, are likely altered through radiolysis and mixed with exogenic compounds at the surface (Sects. 2 and 6). Models of ice shell salt entrainment, informed by terrestrial desalination processes (Petrenko and Whitworth 1999), show that the composition of salts in the ice shell somewhat reflect that of the underlying ocean, although the salinity of the ice is generally limited to a fraction of the overall ocean salinity. Variations in ice shell salinity with depth could indicate variations in the rate, conditions, and mechanisms of ice formation (Spiers and Schmidt 2021; Buffo et al. 2020; Wolfenbarger et al. 2022b). For instance, more salts are expected in the uppermost parts of

the shell that could represent a fast freezing of the ocean and formation of geological features (e.g., narrow ridges) when the shell was thin (Zolotov and Kargel 2009; Buffo et al. 2020). Similarly, only a small fraction of oceanic salts (∼5% in some models and <1% in others) will be retained within the ice shell during a slow ice shell thickening in the current geological epoch (Buffo et al. 2020; Wolfenbarger et al. 2022b).

Salts may be concentrated in discrete regions throughout the ice shell from partially or completely frozen melt lenses, dikes, or injected water bodies (Fig. 1) (Muñoz-Iglesias et al. 2013; Buffo et al. 2020; Lesage et al. 2020, 2021; Chivers et al. 2021). Both endogenic and exogenic salts may be submerged into the interior through processes such as putative subduction/subsumption of the ice crust (Kattenhorn and Prockter 2014). The composition of salts in the shell formed through freezing could reflect precipitation of salts from saturated brine (salt-brine partitioning) at corresponding temperature-pressure conditions (Zolotov and Shock 2001; Zolotov et al. 2004; Marion et al. 2005; Kargel et al. 2000; Wolfenbarger et al. 2022a, 2022b) and freezing rates that affect deviation from partitioning controlled by chemical equilibria. Less salt-brine partitioning is expected in the upper and colder parts of the shell due to rapid crystallization. However, equilibrium salt-brine partitioning is likely in brine pockets that are stable in the warmer parts of the shell that are expected to be closer to the ocean-ice interface (Zolotov et al. 2004; Marion et al. 2005; Wolfenbarger et al. 2022b). The presence of salts and brine pockets in the shell affects both thermophysical (Durham et al. 2010; McCarthy et al. 2011; Litwin et al. 2012) and electromagnetic (e.g., Blankenship et al. 2009; Pettinelli et al. 2015) properties that could be inferred from Europa Clipper data.

The data on surface salt composition obtained with the MISE, Europa-UVS, and SUDA instruments (Sect. 2.2), together with geological mapping based on imaging from the EIS investigation, will be used to extrapolate surface compositions to depth, especially below endogenic surface features such as ridges, domes, and chaotic terrains. The REASON shallow subsurface data will place additional constraints on non-ice components since the radar signals will be influenced by the presence of salts within the shell. Specifically, low concentrations of impurities (tens to hundreds of micromolar) within the ice lattice (e.g., chlorides, ammonium salts) can result in enhanced signal attenuation in warm ice (Moore 2000; Blankenship et al. 2009), whereas layers of ice with higher bulk concentrations of impurities accommodated interstitially represent potential reflectors within the ice shell. Because radar signal attenuation is highly dependent on temperature (Kalousová et al. 2017), using it to constrain composition is challenging. Lateral variations in attenuation could signify either heterogeneities in the concentration of lattice impurities within the ice shell or changes in the shell's thermal environment. Overlapping thermal measurements from E-THEMIS may help to disentangle the cause of the radar attenuation observed by REASON.

Variations in bulk ice salinity with depth are unlikely to produce detectable reflections, due to a low salinity hypothesized for the ice shell (Buffo et al. 2020; Wolfenbarger et al. 2022b), unless the salts become locally concentrated. Salt layers within the ice have been hypothesized to form because of the freezing of water bodies perched within the ice shell (Chivers et al. 2021). These water bodies are hypothesized to form through direct injection of oceanic water into the ice shell by basal fracturing (Michaut and Manga 2014; Manga and Michaut 2017) or through melting caused by diapirism (Schmidt et al. 2011). As water bodies within the ice shell freeze, salts precipitate and collect at the base of the liquid body and form a layer rich in hydrated salts (Chivers et al. 2021). The reflection coefficient associated with an ice–salt interface is governed by the salt layer thickness and the volume fraction of salt. Estimating the layer thickness using REASON measurements and constraining the size of the original reservoir with EIS images, may allow the bulk salinity of the original

reservoir to be constrained (Wolfenbarger et al. 2024). If a water body is formed through injection of oceanic water, this salinity constraint would apply to the salinity of the ocean.

At temperatures above the eutectic point, the composition and abundance of the relevant salts governs the amount of brine stable at a given temperature and pressure (Marion et al. 2005; Wolfenbarger et al. 2022b). The brightness intensity of a radar reflection from an ice-brine interface will be determined by the brine volume fraction (Culha et al. 2020). Detection of an ice–brine interface can serve as a constraint of bulk ice shell salinity and/or temperature if the composition of impurities is known. Putative bodies of water within the ice shell represent interfaces with the highest reflection coefficient. However, brines are only stable at temperatures above the eutectic of the corresponding salt system (e.g., 252 K for NaCl, 269 K of $MgSO_4$, and 236-239 K of modeled Europa's oceanic compositions; Kargel et al. 2000; Zolotov and Shock 2001; Marion et al. 2005; Fortes and Choukroun 2010; Drebushchak et al. 2017), thus frozen impurities concentrated in colder (i.e., less attenuating) settings may appear more reflective in radar (e.g., Pettinelli et al. 2016). Isostatic analysis, combining sounding, altimetry, and topography data from REASON and EIS may be necessary to discriminate between subsurface reflections from liquid water and salts.

3.1.2 Non-water Ice Volatiles, Clathrate Hydrates, and Organic Matter

The deep ice shell could contain volatile species (CO_2, H_2, CH_4, N_2, SO_2, etc.) of exogenic and endogenic origin. Thickening of the ice shell in the last 10^8 years through freezing from below (Sect. 6.5) does not imply a widespread occurrence of surface volatiles of radiolytic and/or exogenic origin (e.g., H_2O_2, O_2, CO_2, SO_2) below a shallow surface layer. Although a thermal evolution of Europa's interior suggests outgassing of the rocky interior (e.g., Kargel et al. 2000; Melwani Daswani et al. 2021; Sect. 6.3), the current geologically young shell may not contain much of those early-formed compounds (e.g., CH_4, CO_2). In the current epoch, low- and high-temperature aqueous alteration of suboceanic rocks would have the potential to release volatiles into the ocean that might make their way into the ice (Vance et al. 2016; Běhounková et al. 2021). Most volatiles in the shell could represent gases trapped through a downward freezing of the shell and via incomplete degassing of oceanic water during cryovolcanic events. As for endogenic salts, the highest concentrations of trapped oceanic volatiles are expected in the uppermost part of the shell formed through rapid freezing of the ocean and multiple disruptions of the thin ice that are observed in geological features. Trapped gases could be embedded in the ice crystal lattice, concentrated at grain boundaries and in brine pockets, and form clathrate hydrates (Prieto-Ballesteros et al. 2005; Prieto-Ballesteros and Kargel 2005; Sloan et al. 2007; Bouquet et al. 2019).

Both lithostatic pressure and temperature in the interiors of Europa and other ocean worlds (Tse and White 1988; Fortes and Choukroun 2010; Sohl et al. 2010; Choukroun et al. 2013) allow stability of gas hydrates if sustained partial pressures or concentration of dissolved hydrate-forming molecules (CH_4, CO_2, N_2, SO_2, O_2, H_2S, and noble gases) are achieved. Some gas hydrates (presumably mostly of CH_4, other light hydrocarbons, CO_2, and mixed compositions) could form upon freezing of oceanic water (Marion et al. 2012; Bouquet et al. 2019). Others could form in the shallow subsurface (Muñoz-Iglesias et al. 2019) and incorporate radiolytic products such as SO_2 and O_2 if they reach the subsurface (Prieto-Ballesteros et al. 2005; Prieto-Ballesteros and Kargel 2005; Hand et al. 2006). The presence of a clathrate layer might be inferred from REASON data if the layer is of a sufficient thickness to appear dielectrically distinct and if the ice above the layer is cold (i.e., attenuation is negligible). A clathrate-bearing reservoir could also produce a reflection if a clathrate is sufficiently abundant. Clathrates that contain polarizable molecules (e.g., CO_2)

may produce a stronger reflection due to a higher dielectric permittivity (Pettinelli et al. 2015). However, distinguishing a clathrate layer from a salt layer would be challenging from REASON data.

Spatially resolved measurements by MASPEX of atmospheric nonpolar inorganic and low-mass organic gases may hint at the presence of clathrate hydrates in a locally degassing ice shell. The ratio of water to hydrate-forming volatiles (e.g., CH_4, CO_2) for fully occupied cages in clathrates is expected to be about six, which reflects the gas hydrate composition (Sloan et al. 2007). Direct observations of CO, CO_2, and CH_4 in the atmosphere obtained through Europa-UVS observations of stellar occultations, Jupiter transits, and potential plume emissions (Sect. 4) may provide additional constraints on clathrate-forming gases. The relative abundances of hydrate-forming gases themselves, as compared to predictions for the ocean (Bouquet et al. 2019), could be another clue to clathrates contributing to the source of measured volatiles, as has been suggested for comet 67P/Churyumov-Gerasimenko (Mousis et al. 2016). Geochemical modeling of measured gases would constrain the fugacities of clathrate-forming gases at their interior source(s) (Bouquet et al. 2019). However, the interpretation of these measurements may be subject to uncertainties, unless all volatiles measured originate from a unique source consisting solely of clathrate hydrates.

The presence of CO_2 in endogenic non-ice surface materials (Hansen and McCord 2008; Trumbo and Brown 2023; Villanueva et al. 2023) could indicate delivery of organic matter from Europa's oceanic water followed by radiolytic oxidation (Sect. 6), though inorganic sources are possible. In either scenario, the shell may contain endogenic organic compounds in ice lattice structures (e.g., polar species), at ice grain boundaries together with salts, as hydrocarbon hydrates and hydrocarbon-rich bodies (layers, lenses, domes), and as an oil or paraffin-like layer at the ice-ocean interface (Zolotov and Kargel 2009). Data from the Europa Clipper on possible plume grains, gases, and recent plume deposits, if they are present, would be informative to constrain the composition of subsurface organic compounds. Observations of freshly delivered and/or exposed subsurface materials by the MISE, Europa-UVS, MASPEX, and SUDA instruments will aid in constraining the composition of organic matter in the upper shell. Although the REASON shallow sounding dataset will be used to investigate non-ice constituents, distinguishing a hydrocarbon-rich from a salt-rich body could be challenging due to their potentially similar reflection coefficients. Gas composition measured by MASPEX would indicate the origin of any possible plumes within the ice shell, and the data collected within the SUDA and MASPEX investigations would provide complementary information about organic compounds, salts, and gases in the shell. The diversity and chemical structure of organic matter (e.g., aromatic/aliphatic ratio) can indicate source environment, including the original formation mechanisms and subsequent thermal, aqueous and radiolytic processing (Sephton et al. 2018; see Sect. 6)

3.2 The Ocean Composition

The limited current knowledge of the inferred oceanic composition is based on the composition of non-ice surface materials related to endogenic surface features, and on the relative abundances of Na and K in the atmosphere (Zolotov and Kargel 2009). Evaluations of oceanic composition from these data are complicated by the influx of alkali chloride grains from Io (Postberg et al. 2006), together with S- and O-bearing ions, and by radiolytic oxidation of any ocean-sourced reduced S- and C-bearing species (e.g., sulfides and organic compounds). Oceanic compounds measured at different locations across Europa's surface could represent oceanic water of different compositions delivered at different times. Some

endogenic surface compounds might have come from the ice shell rather than directly from the ocean.

Despite these ambiguities, most inorganic solutes in the ocean are represented by ions, notably Mg^{+2}, Na^{+}, $SO_4{}^{-2}$, Cl^{-}, and $HCO_3{}^{-}$ (Kargel et al. 2000; Zolotov and Kargel 2009). The low solubility of metal sulfides (e.g., FeS, FeS_2) in cold ocean water suggests oceanic sources of abundant sulfates in colored endogenic surface materials (Zolotov and Kargel 2009). Several independent tentative detections of Mg salts in surface materials (Sect. 2) are consistent with oceanic sources of sulfates because abundant Mg would be present in sulfate-rich water, while a NaCl type and sulfate-poor ocean could be depleted in Mg (Zolotov and Kargel 2009). The presence of CO_2 in colored, non-ice surface materials associated with geological features (Hansen and McCord 2008; Trumbo and Brown 2023; Villanueva et al. 2023) implies an endogenic delivery of carbonate species (CO_2, $HCO_3{}^{-}$, $CO_3{}^{2-}$) and/or organic compounds. The ionic composition of oceanic water suggested from the available surface and atmospheric data is consistent with models for water–rock interactions (e.g., Zolotov and Kargel 2009; Melwani Daswani et al. 2021), although these models are based on the unknown composition of Europa's rocks (Sect. 3.3). The current knowledge of surface and atmospheric compositions does not allow a definite assessment of oceanic pH. Evaluations of the pH from water–rock interaction models depend on the assumed rock composition and excess inventories of volatiles that are sourced from mantle rocks (e.g., Rubey 1951). The permeability of a seafloor layer of rock that influences the degree of water–rock interaction is also a key unknown. The major ambiguities regarding oceanic composition are concentrations of sulfate, Mg, and inorganic and organic carbon species. The data obtained by the Europa Clipper will enable a big step toward constraining the composition of Europa's ocean. The level of detail that can be revealed will depend on how closely the ocean composition is reflected by materials that are accessible to the spacecraft.

3.2.1 Major Solutes and Acidity

If an ocean-sourced plume is detected, data from the SUDA, MASPEX, and Europa-UVS investigations can provide specific and complementary information on the ocean's ion and neutral (e.g., dissolved gas) constituents (Sect. 5), as was demonstrated at Enceladus (Postberg et al. 2009, 2011a; Waite et al. 2017; Hansen et al. 2020). Major target analytes detectable by SUDA include Na^{+}, Mg^{+2}, K^{+}, Ca^{+2}, Fe^{+2}, Cl^{-}, $HCO_3{}^{-}$, $SO_4{}^{-2}$, and $CO_3{}^{-2}$ in grains. The MASPEX investigation will seek to measure H_2, CH_4, NH_3, H_2S, CO_2, N_2, O_2, and noble gases. Both instruments are capable of detecting organic compounds (e.g., Waite et al. 2009; Postberg et al. 2018b; Khawaja et al. 2019). If detected, *in situ* plume measurements might be complemented by remote sensing constraints on the gas (CO, CO_2, CH_4, N_2) composition determined from Europa-UVS data through techniques described in Sect. 4.1.1, and the composition of salts and organic compounds in plume fallout material on the surface by MISE and Europa-UVS (Sect. 5.2.2). These approaches were demonstrated at Enceladus (e.g., Brown et al. 2006; Hansen et al. 2020).

The abundances of chlorides, sulfates, and carbonates in possible ocean-sourced plume(s) and endogenic surface salts detected by the Europa Clipper investigations may enable the resolution of the dominant ions in oceanic water. These have implications for redox conditions in the ocean, as S(VI) in sulfate is the most oxidized form of sulfur. If the ocean is extremely oxidized, then perchlorate ($ClO_4{}^{-}$) might be present (Ligier et al. 2016). In contrast, the presence of ferrous iron, methane, organic compounds, ammonia, or abundant hydrogen sulfide would suggest more reducing conditions (Fig. 13), perhaps similar in some ways to Earth's ocean prior to the Great Oxidation Event (Lyons et al. 2014). A specific knowledge of organic compositions aids in probing oceanic oxidation states. A predominance

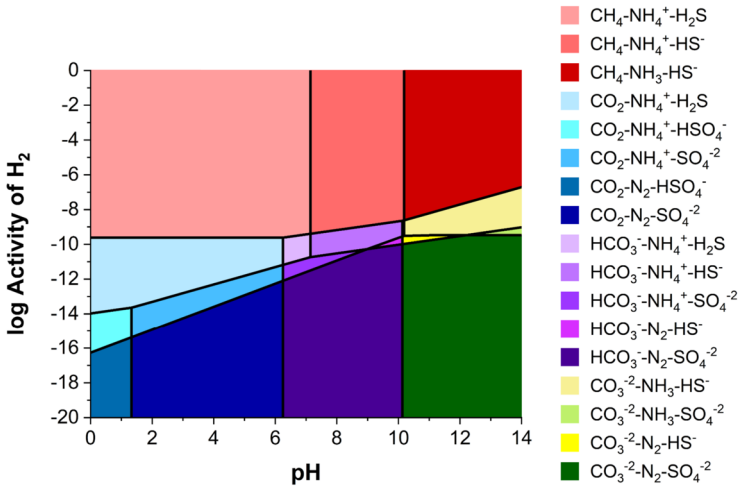

Fig. 13 Equilibrium predominance assemblages of C, N, and S aqueous species as functions of redox conditions and solution acidity at 0 °C and 1000 bar. Predominance means that the species shown in the legend have the highest aqueous activity for the element of interest. The assemblages shown are the most stable ones; note that a species can still be present outside of its region of predominant abundance. As an example, if Europa Clipper observations allow the H_2 activity and pH to be constrained, then the dominant equilibrium forms of C, N, and S in Europa's ocean can be predicted. On the other hand, if CH_4, NH_4^+, and HS^- are found to be the most abundant forms of C, N, and S in the ocean, then chemical equilibrium would imply that the conditions in the ocean fall inside the medium red region of this diagram. Other combinations of the most abundant forms of these elements would map to differently colored regions. It should be noted that complete chemical equilibrium is not guaranteed in the ocean. Equilibrium is an initial assumption that can be used to guide quantitative interpretation, and subsequently improve modeling approaches if disequilibria are observed in various parts of the system. Measurements of more species enable tighter constraints on equilibrium conditions or provide additional consistency tests of equilibrium. This figure was made using equilibrium constants that were computed using the slop07 database (Widman and Shock 2008) for the program SUPCRT92 (Johnson et al. 1992), and the nitrogen speciation was calculated for a total N concentration of 1 mmole/kg H_2O

of aliphatic hydrocarbons (e.g., alkanes) would point to more reduced conditions, while a more oxidized ocean would favor higher abundances of alkenes, aromatic compounds, and oxygen-bearing organics such as alcohols, ketones, aldehydes, and carboxylic acids (Shock et al. 2013, 2019). Measurements of H_2 or O_2 in a plume by MASPEX and Europa-UVS could provide a more direct quantitative indication of redox conditions in the ocean (e.g., Glein et al. 2018). Such observations would need to be complemented by E-THEMIS thermal measurements of the surface temperature at locations of any plume venting (Christensen et al. 2024, this collection), or SUDA measurements of carbonate species concentrations (Postberg et al. 2009), to enable estimation of the oceanic concentrations of dissolved gases from their plume mixing ratios (Waite et al. 2017; Glein and Waite 2020). The radiolytic fluxes of O_2 and H_2 from the icy surface would also need to be accounted for to determine how much of these gases in a plume emanate from the subsurface (Sect. 6.6). Diffusion rates of these volatile species through the bulk ice as well as through the cracks and voids need to be constrained through laboratory studies to better estimate surface and subsurface chemical exchange.

It is important to measure or infer the pH because this fundamental geochemical parameter drives the speciation of elements throughout the periodic table. Data from SUDA will constrain the pH of ocean-derived ice grains via analysis of certain ion clusters (e.g.,

$(NaOH)Na^+$ and $(NaCl)Na^+$) in the mass spectrum, as their relative abundances depend on pH in a source aqueous reservoir (Postberg et al. 2009).

If the ocean is alkaline, corresponding ocean-sourced salts would be rich in Na carbonates that are abundant in soda lakes on Earth (Kempe and Kazmierczak 1997; Toner and Catling 2020), detected in the plume emissions of Enceladus (Postberg et al. 2009, 2011a, 2011b), and dominate aqueously deposited salts on Ceres (De Sanctis et al. 2016). On Europa, Na carbonate and bicarbonate could be observed by MISE in surface materials and by SUDA in sputtered surface solids and plume grains. Ocean-sourced salts would contain abundant $(NaOH)Na^+$ in SUDA data, as it was observed at Enceladus by the Cassini CDA instrument (Postberg et al. 2009). In contrast, Ca carbonates are not expected in salts delivered from an alkaline ocean owing to their low solubility. As in the Saturnian system (Hsu et al. 2015), silica grains could be detected by SUDA because silica is significantly more soluble in alkaline solutions than in acidic water. As for the E ring grains sourced by Enceladus' plumes (Postberg et al. 2008, 2023), SUDA will be able to detect sodium phosphates that have been found in soda lakes (Toner and Catling 2020; Postberg et al. 2023) and in the alkaline ocean on Enceladus (Hao et al. 2022). Corresponding plume gases would be depleted in CO_2, which is not abundant in alkaline waters and may contain NH_3 (Fig. 13). A low NH_4^+/NH_3 ratio inferred from combined MISE, SUDA, and MASPEX data on surface and plume materials would characterize an alkaline ocean.

If Europa's ocean is highly acidic (pH < 3), CO_2 could be abundant in plume gases owing to dissolution of carbonate minerals at the ocean floor and higher abundance of dissolved CO_2 compared to HCO_3^- and CO_3^{-2} ions. Abundant aluminum and/or ferric iron ($Fe^{+3} \gg Fe^{+2}$) could be detected in plume and surface materials (Napoleoni et al. 2024). By analogy with Martian materials, detections of jarosite and/or alunite in Europa-sourced dust by SUDA and/or in freshly-deposited surface materials in MISE spectra would indicate formation in acidic aqueous environments. However, a high Fe^{+3}/Fe^{+2} ratio of surface-sourced dust would be indicative of radiolysis (Sect. 6) rather than of the pH. If the ocean is acidic, the acidity could be caused by a supply of surface oxidants (O_2, H_2O_2, H_2SO_4) and a limited acid-neutralizing capacity of the ocean floor rocks/sediments (i.e., high water/rock ratio at low rock permeability) to enable sufficient oxyanion formation (Pasek and Greenberg 2012). An elevated Fe content of ocean-derived samples with other evidence of neutral to basic pH would indicate a high concentration of Fe^{+2} in the ocean because Fe(III) would be immobile at those pH levels. In addition, a combination of MASPEX (CO_2), Europa-UVS (CO_2), SUDA (carbonate species or alkalinity), and E-THEMIS (plume vent temperature) data could provide a complementary approach to estimating pH through consideration of carbonate equilibria in the ocean water (Glein et al. 2015; Glein and Waite 2020).

Independent of any plume investigations, SUDA and MISE observations will be used to constrain the endogenic surface composition, from which the ionic composition and acidity of oceanic water may be inferred. In particular, the dominant oceanic water speciation (e.g., $SO_4^{-2} + Cl^-$ vs. Cl^-; $Mg^{+2} + Na^+$ vs. Na^+) could be assessed, though radiolysis and exogenic contamination of surface materials (Sect. 6.6) would need to be considered. Constraints on oceanic chemistry from MASPEX and Europa-UVS observations of the atmospheric composition would also need to be interpreted carefully in the context of radiolytic processing of surface and exospheric compounds.

3.2.2 Secondary Ocean Floor Mineralogy

Constraining concentrations of major ions in oceanic water will provide new clues about the mineralogy of the ocean floor and rocky interior. For example, SUDA measurements

of ion concentrations in plume ice grains will be used to evaluate the ion activity products of minerals that contain these ions (e.g., calcite, gypsum). These could then be compared to theoretically calculated solubility products to assess whether the presence of different minerals is likely or not. With an additional constraint on the silica (SiO_2) concentration from SUDA measurements (e.g., Hsu et al. 2015), the stability of silicates and related oxides and hydroxides (e.g., brucite) can be assessed. The stability relationships among silicates could provide insights into dynamical processes at the ocean floor, depending on whether complete acid-base type equilibrium is achieved, or certain minerals that are known to form relatively slowly (e.g., quartz, talc; Tosca et al. 2011; Leong and Shock 2020) are found to be supersaturated.

Mass balance modeling, including Europa Clipper observations, will increase our understanding of the geochemical evolution of the ocean. By combining data on the ion concentration from the SUDA and MISE instruments and the gas concentration measured by MASPEX and Europa-UVS with constraints from REASON, ECM, PIMS, and Gravity Science observations on the mass (or volume) and electrical conductivity of the ocean, estimates can be made of the oceanic inventories of observed elements. Note that upper limits can also be useful. Comparing these estimates to the results of previous models will provide tests of earlier assumptions of element extraction to the ocean (Zolotov and Shock 2001), and lead to more refined models. If appropriate assumptions are made on the sources of key elements, then pathways of their delivery and retention in the ocean can be constrained. Some promising chemical probes for constraining the fraction of volatiles delivered from the rocky interior are chlorine (Clay et al. 2017; Lodders and Fegley 2023) and noble gases, particularly ^{40}Ar (Marty 2012). A potential upper limit on the ratio of water to reacted rock could be obtained using the Na or Mg inventories in the ocean, based on the requirement of sufficient leaching from a sub-oceanic layer of rock. SUDA data will be used to estimate the silica (SiO_2) concentration in oceanic water (cf. Hsu et al. 2015), which may hold the greatest information content for estimating the extent of water-rock reactions in Earth's seafloor hydrothermal systems (Milesi et al. 2021) and may for Europa as well. This type of information can influence geophysical perspectives (McKinnon and Zolensky 2003; Vance et al. 2016, 2018) to gain deeper insight into how ocean water accesses rock on Europa.

3.3 Bulk, Mantle and Core Composition

The composition of Europa's deep interior provides constraints on the formation and the physical and compositional evolution of the body. Our current knowledge about the bulk composition is mainly based on estimates of Europa's bulk density ($\sim$3 g/cm^3), moment of inertia, and the existence of an icy envelope, all of which will be refined by the Europa Clipper investigations. The bulk density of Europa's rocky interior is currently uncertain (3.6–3.9 g cm^{-3}, Gomez Casajus et al. 2021) and further data are needed to constrain that value. Interior models that consider these data together with equations of state for water, silicate mantle, and core materials have considered several types of chondrites as analogs for the rocky interior. Europa's derived rock density (bulk minus ocean) is low compared to a suggested density of water-less carbonaceous Ivuna-type (CI) chondrites (Zolensky et al. 2017) that are similar to the composition of the solar photosphere (except H, C, N, O, and noble gases, Lodders 2021). Kuskov and Kronrod (2005) concluded that density of LL-type ordinary chondrites with a low Fe content provides a more consistent fit than other meteorite types. Similarly, recent interior structure models for Ganymede, Titan (Néri et al. 2020) and Ceres (Zolotov 2020) consider CI carbonaceous chondrite compositions with added carbon-rich material that decreases the rock density. Europa's relatively low rock density could also

be explained by additional carbonaceous material rather than by a deficiency of Fe in its initial rocky constituents. Abundant C-bearing species (e.g., CO_2 and carbonates) in endogenic surface materials (e.g., Trumbo and Brown 2023; Villanueva et al. 2023) and possible plumes investigated with the MISE, SUDA, Europa-UVS, and MASPEX instruments would discriminate end-member compositions of Europa. For example, a detection of abundant methane by the MASPEX or Europa-UVS investigations in any plume originating from the ocean or through decomposition of crustal clathrates would be consistent with a significant contribution of organic-rich material from the outer Solar System and with a C-rich bulk composition of the moon. Indirect signs of methane clathrates in the ice shell (Sect. 3.1.2), if found, would support such a contribution of C-rich materials.

Several types of suboceanic rocks have been discussed in the literature. Earlier models (Kargel et al. 2000; Zolotov and Shock 2001) considered aqueously altered carbonaceous chondrites to provide plausible constraints on oceanic composition. The possibility of tidally-driven silicate volcanism (Behounkova et al. 2021) suggests a mafic (basaltic) composition for seafloor rocks (Zolotov and Kargel 2009). Chemical sediments (e.g., low-solubility salts and carbonates) at the ocean floor were considered in models of formation and freezing of oceanic water (e.g., Spaun and Head 2001; Melwani Daswani et al. 2021). Metamorphic devolatilization of carbonaceous chondrites before igneous differentiation could have led to the deposition of chemical sediments (Kargel et al. 2000; Melwani Daswani et al. 2021) and to hydrothermally altered suboceanic rocks (cf. Zolotov and Mironenko 2015) that could be rich in carbonates. Io-like volcanism in terms of petrology and an Earth-like redox state of igneous environments (Zolotov and Fegley 1999) could result in a sulfur or SO_2-clathrate layer at the seafloor (McKinnon and Zolensky 2003). These and other sedimentary and hydrothermal scenarios do not exclude subsequent mafic volcanism at the ocean floor (Behounkova et al. 2021). More exotic organic-rich sea-floor materials (Zolotov and Kargel 2009) could, as mentioned above, represent possible C-rich bulk compositions of Europa.

Gravity measurements analyzed within the Europa Clipper G/RS investigation will improve the constraints on Europa's density structure. Current understanding of the interior structure of Europa is based on the Galileo data on gravity and bulk density, which allowed estimation of the dimensionless moment of inertia, suggesting a differentiated body (Anderson et al. 1998; Gomez Casajus et al. 2021). Europa Clipper observations will yield a "true" estimate of Europa's moment of inertia, instead of relying on the assumption of hydrostatic equilibrium for deriving the moments of inertia from the degree 2 gravity coefficients. At present, even the value of Europa's second-degree gravity coefficient, C_{22}, upon which this assumption relies, is imprecisely known (Mazarico et al. 2023, this collection). Constraints on the density of the metal core would provide indirect clues to its composition, mainly the Fe/FeS ratio and possible C and O contents. However, the inversion of the gravity data into a density profile remains a challenging problem, and it is less sensitive to the second order impact of light elements on the core density (Mazarico et al. 2023, this collection). Achieving an independent constraint on the hydrosphere thickness from ECM measurements, and tidal monitoring with Gravity Science (Mazarico et al. 2023; Roberts et al. 2023, both this collection) and REASON altimetry measurements (Blankenship et al. 2024, this collection) will narrow down the parameter space of possible bulk rocky mantle plus metallic core compositions. Constraints on salt composition and the density of oceanic water obtained from SUDA investigations of the salt-ice grains in a potential plume would further constrain these evaluations. Chemical and phase compositions of rock types are manifested in oceanic composition, and will be assessed through the MISE, SUDA, Europa-UVS, and MASPEX investigations of endogenic compounds in surface, atmospheric, and possibly

plume materials. Compositional data on endogenic salts (Sect. 2) together with MASPEX and Europa-UVS data on $H_2/CO_2/H_2O$ ratios in possible plumes will constrain the composition of suboceanic rocks (Sect. 3.2). Elevated H_2 content, low CO_2/H_2O ratios, and a low SiO_2 abundance in Europa-sourced grains (SUDA data) would indicate ultramafic rocks. Low Mg and H_2 content, and elevated SiO_2 in grains would be consistent with silicic rocks. An elevated CO_2/H_2O ratio could characterize silicic materials at the ocean floor formed through an acidic aqueous alteration of a variety of igneous silicate rocks (Sect. 3.2). A high CO_2/H_2O ratio could characterize interaction of CO_2-rich oceanic water (e.g., melted cometary ices) with silicate rocks at elevated water/rock ratios that reflects low permeability of oceanic floor rocks. The latter case would suggest a late formation of the ocean through accretion of ice-rich cometary materials (see also Sect. 6.2). ^{4}He in a possible plume, if measured by MASPEX, could indicate an enrichment of felsic U- and Th-rich materials at the seafloor. Detection of ^{40}Ar by MASPEX will be informative for abundances and behavior of K-bearing substances in the history of the moon, including processes in sub-oceanic rocks and ocean water.

4 The Composition of Europa's Atmosphere and Space Environment

The composition of endogenic materials in Europa's atmosphere, especially if detected within possible plumes, has direct and indirect implications for the habitability of Europa's ocean. The Europa Clipper mission will identify the composition and sources of key non-ice constituents in the atmosphere, including carbon-containing compounds. Assessments of the vertical and temporal characteristics of the atmosphere will be used to constrain ongoing surface and atmospheric processes that may alter the relative abundances of any ocean-derived materials which are lofted into the atmosphere. Investigations of Europa's local space environment beyond its Hill sphere will be used to determine the abundance and distribution of exogenic materials at Europa and differentiate them from the endogenic matter observed in the atmosphere and on Europa's surface. Several investigations on the Europa Clipper mission will contribute synergistically to our understanding of Europa's atmosphere, dust exosphere, neutral clouds/tori, and plasma tori.

The composition of Europa's atmosphere and local space environment includes neutral atoms and molecules, positively and negatively charged atoms and molecules, electrons, and solid ice and non-ice grains both inside and outside Europa's Hill sphere. The Hill sphere is the region inside ~8.7 Europa radii where the moon's gravity dominates, i.e., the atmosphere, ionosphere, and dust exosphere. Outside of Europa's Hill sphere are the Europa dust cloud, neutral particle clouds, neutral torus, and the Jovian plasma torus, which originates primarily from Io. It is to be noted that the terms exosphere and atmosphere are synonymously used to represent the tenuous $\sim 10^{-9}$ mbar environment extending from the surface to the boundary of Europa's Hill sphere and includes the ionosphere.

Europa's gaseous atmosphere and the neutral clouds are produced by similar processes, primarily from plasma sputtering, with possible contributions from putative plumes. Ice and mineral dust grains are lofted into the atmosphere by micrometeroid impacts onto the surface, and perhaps by plume venting (Sect. 5). Most of the material stays bound to the satellite, but a small fraction escapes Europa's gravity field to form the neutral and dust clouds, neutral tori, or to become part of the Jovian plasma tori. The atmospheric composition therefore is directly linked to the surface composition, and depending on the state of interior-surface interchange and plume activity, it can provide a constraint for ocean composition (Sect. 3). The various processes that affect the atmospheric composition are captured in Fig. 14.

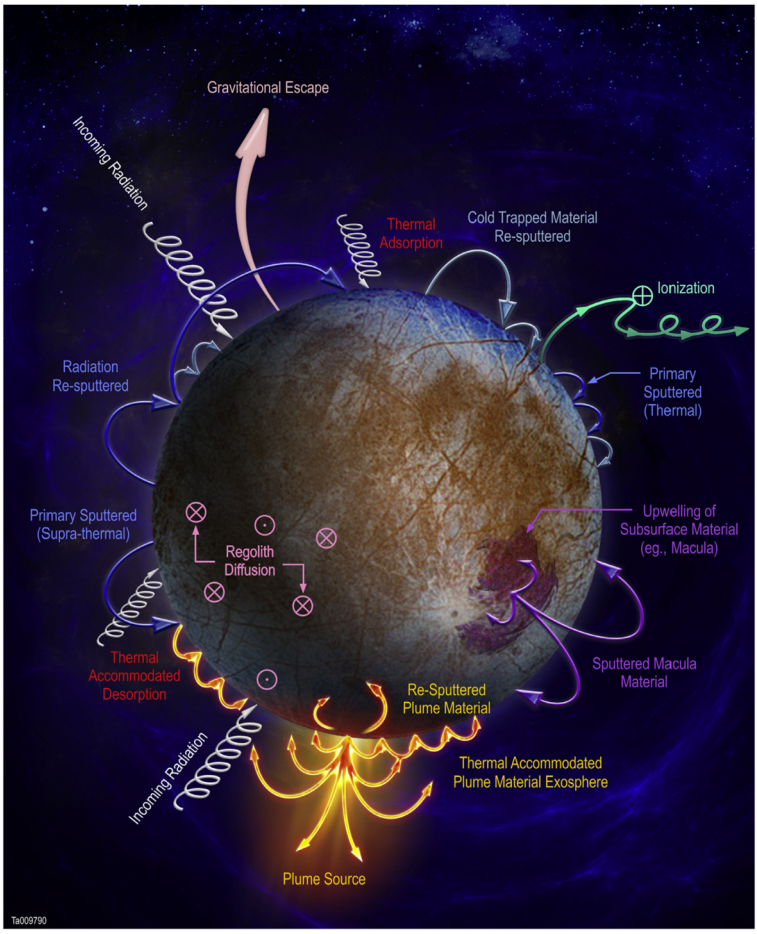

Fig. 14 Multiple physical processes that could affect Europa's tenuous atmosphere. The Europa Clipper investigations will be able to detect sputtered material and potentially plume material in the atmosphere to assess surface and possibly sub-surface compositions. Figure from Teolis et al. (2017)

Gas that has been liberated from a solid surface can typically be more easily detected and identified than when observed on the surface. For example, most molecules in the gaseous phase have a very distinctive and relatively narrow line/band spectral structure, with pronounced emission or absorption features that can be measured (e.g., by UV spectroscopy with Europa-UVS). The same molecule bound in Europa's icy surface may have a less distinct, broad-band structure that can make unique identification more challenging.

Through *in situ* measurements, the MASPEX and SUDA investigations will sample the local environment with parts per billion sensitivities, making the detection of some trace species, such as hydrocarbons, possible. Other molecules with high absorption cross sections can be more readily detected in the large column lengths observed by the remote sensing investigations. The PIMS investigation of particle precipitation will determine the neutral source rates from the surface and will be used for tracking variations in the ions that sputter atmospheric neutrals from the surface, providing observations complementary to those by MASPEX and SUDA. Thus, the suite of *in situ* and remote sensing investigations on Europa

Clipper complement each other in detecting a much broader range of atoms and molecules, providing a more complete understanding of the atmospheric composition of Europa.

4.1 Europa's Atmospheric Volatiles

The volatiles in Europa's atmosphere are dominated by molecular oxygen, which was first detected in 1994 (Hall et al. 1995) and has since been observed extensively (Hall et al. 1998; McGrath et al. 2004, 2009, Hansen et al. 2005; Roth et al. 2014b, 2016; Roth 2021). It is widely accepted that the primary process for creating Europa's atmosphere is sputtering of surface water ice (Brown et al. 1977, 1982). Sublimation of water ice is a secondary source of O_2 in the sunlit hemisphere, especially near the sub-solar point (Yung and McElroy 1977; Johnson et al. 1981; Teolis et al. 2017). If present, and depending on their activity level, plumes may dominate contributions to the atmosphere over the sputtering source (Fig. 15; Teolis et al. 2017). Sputtering of the surface produces a more energetic, non-thermal particle distribution with relatively larger scale height than sublimation does, with lighter particles, such as H, lofted higher than heavier species (such as hydrocarbons). The sublimated material has a thermal particle distribution with a lower scale height. The vast majority of sputtered or sublimated particles do not escape but follow ballistic trajectories. Because the atmosphere is only marginally collisional; most particles never encounter another particle and eventually re-impact the surface. A small fraction of the sputtered species escapes to form neutral clouds or tori (Sect. 4.3). As discussed below, remote sensing and *in situ* Europa Clipper investigations of the O_2 abundance as a function of altitude and local solar time will constrain the processes contributing to the formation of Europa's collisionless atmosphere.

Within Europa's Hill sphere, only four atomic species have been detected through emissions: atomic hydrogen, oxygen, sodium, and potassium (Hall et al. 1995; Brown and Hill 1996; Brown 2001; Roth et al. 2017). Upper limits have also been determined for atomic sulfur, chlorine, and carbon (McGrath et al. 2015). Na, K, Ca, and Mg have all been observed near Europa (Volwerk et al. 2001; Leblanc et al. 2005; Cipriani et al. 2009), and these ions are expected to be abundant in the ionosphere. The relative strength of atomic oxygen emission lines in the ultraviolet has been used to infer that the atomic oxygen derives from O_2 (Hall et al. 1995). A recent analysis of the spatial properties of the oxygen emissions across Europa's disk suggest H_2O to be more abundant than O_2 around the sub-solar region (Roth 2021). An ionosphere has also been inferred from electron density profiles derived from Galileo radio science measurements (Kliore et al. 1997; McGrath et al. 2009, Fig. 7). The ionized atomic or molecular species that must be associated with the electrons comprising the ionosphere have not been directly detected. Kliore et al. (1997) considered scenarios with O_2^+ or H_3O^+ as the primary ionospheric species, with additional contributions from H^+ and O^+. Unlike bodies with robust atmospheres, Europa's ionosphere extends all the way to the surface of the satellite. These species will be studied through Europa Clipper investigations (Sects. 4.1.1, 4.1.2) to better understand the distribution of these materials in Europa's atmosphere.

Numerous detailed models have been developed to help fill in the observational gaps and develop observing scenarios for the Europa Clipper mission. A few notable models include Smyth and Marconi (2006), Shematovich et al. (2005), Plainaki et al. (2018), and Teolis et al. (2017). Plainaki et al. (2018) provide a comprehensive summary of models of Europa's atmosphere published prior to 2017.

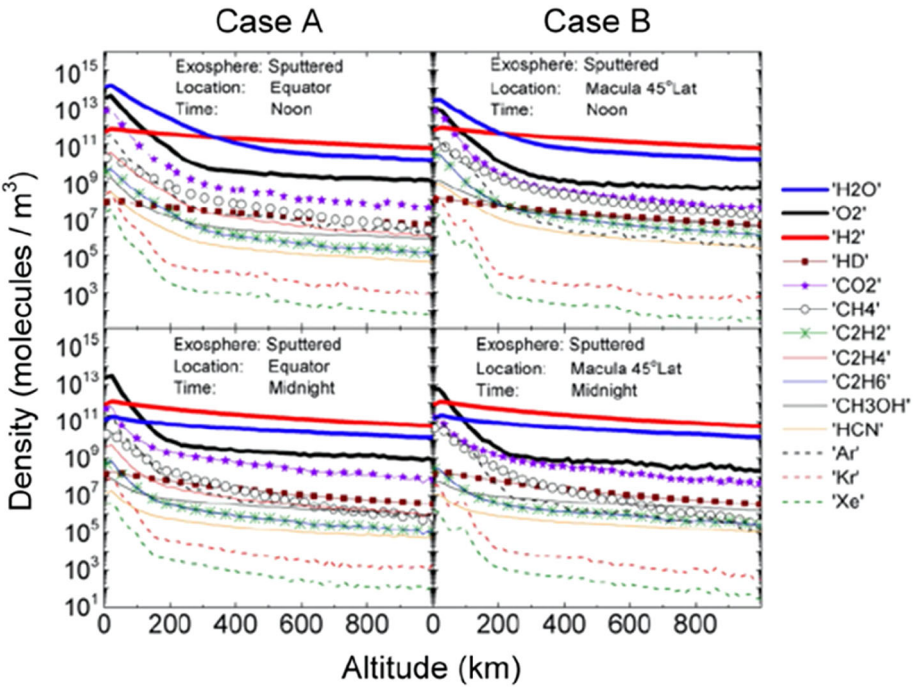

Fig. 15 Exospheric density (molecules per unit volume) versus altitude at the spacecraft point of closest approach, for selected exospheric species for an equatorial flyby through a sputtered-only exosphere (Case A) and for a flyby over a localized sputtered macula terrain enriched in non-ice species (Case B). Figure adapted from Teolis et al. (2017)

4.1.1 Remote Sensing Observations

Many of the expected atmospheric species have strong absorption cross sections at FUV wavelengths that will be detectable by the Europa-UVS investigation. In the UV, the composition of the atmosphere will be constrained using two separate techniques at these wavelengths: emission and transmission spectroscopy (Retherford et al. 2024, this collection). The Europa-UVS emission spectroscopy observations of fluorescence and electron excitation are capable of detecting many known and potentially present atmospheric neutral species, including O, H, H_2, S, CO, C, Cl, Ca, Mg, N_2, and N. These FUV airglow and auroral emissions will be monitored when the Europa-UVS is pointed toward the satellite and during scans when the spacecraft slews the instrument's field of view across the entire disk of Europa. These stares and scanning observations will occur multiple times each flyby and over the duration of the mission to continually monitor the spectral emissions as Jupiter's magnetic field sweeps past the satellite (see Sect. 4.3.1). Low and high phase angle observations made using MISE may also be used to constrain exospheric composition, but the extent of those constraints will be evaluated following instrument performance measurements in flight.

Other species, including H_2O, O_2, O_3, H_2O_2, SO, CO_2, NH_3, CH_4, and C_2H_2, have strong absorption features in the FUV that can be detected during occultation and transit events. Stellar and solar occultations occur when a background star or the Sun passes behind Europa's atmosphere from the perspective of the spacecraft. These occultations will provide

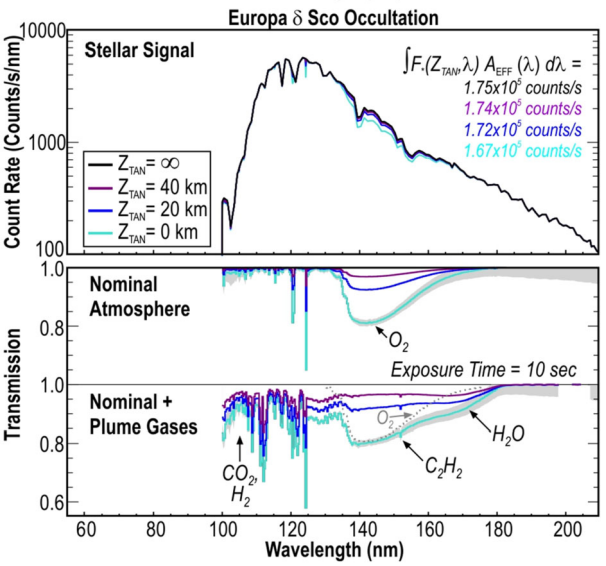

Fig. 16 (Top) Simulated Europa-UVS spectra for a star at several tangent altitudes (Z_{TAN}) during an occultation of the star δ Scorpii by Europa. (Bottom) Transmission spectra are shown for both a nominal global atmosphere (Smyth and Marconi 2006) and for an Enceladus-type plume vapor composition using a tangential column density that aligns with those measured for the putative Europa plume detected by Roth et al. (2014b). The observed transmission spectra are diagnostic of the composition of the atmosphere and plume material, if present

localized, vertical profiles of the atmospheric composition as the various species attenuate the background starlight (Fig. 16, Retherford et al. 2024, this collection). Similarly, the Europa-UVS will be used to observe the satellite as it transits in front of Jupiter, during which the gases in Europa's atmosphere will attenuate the background Jupiter dayglow and reflected solar signal. The amount of absorption detected as a function of altitude above Europa's surface during transits and occultations will constrain the vertical composition, density and temperature profiles of the satellite's atmosphere. Observations of more than 100 stellar occultations are planned over the course of the mission in order to measure these properties at globally-distributed latitudes and longitudes and to track the variability of the atmospheric composition and structure over time.

Additional measurements of the atmospheric structure will be derived from signal distortions observed in REASON observations. These distortions are from the regular ionosphere or a localized ionized plume and can be used to measure the total electron content in the vertical column above its surface ground track. This provides information about the ionosphere, which ultimately derives from ionization of the neutral atmosphere and can constrain regular ionospheric variability.

4.1.2 *In Situ* Observations

In situ measurements of volatiles by the MASPEX investigation (Waite et al. 2024, this collection) will offer an even more sensitive probe of Europa's atmosphere at the locations where it can be sampled directly. The Cassini *in situ* mass spectrometer measurements of the Enceladus plume were used to obtain mixing ratios on the order of one part per million (ppm) for trace hydrocarbons (Magee and Waite 2017). The major atmospheric species (O_2, H_2O, H_2) will be readily detectable by MASPEX during Europa flybys, thus allowing detailed characterization of the nominal horizontal and vertical atmospheric density and temperature structure. The instrument's atomic mass range extends up to 500 u, and the measurement sensitivity is 10 s of ppm. Compounds such as NH_3, HCN, N_2, CO, CH_4, CH_3OH, C_2H_5OH, CH_3CO_2H, and CO_2 are specifically targeted, and the instrument's variable mass

window and mass resolution will enable surveying of the Europan environment for previously unknown compounds. Measurements by the MASPEX instrument will also be used to spatially resolve less abundant atmospheric constituents. Material will be captured and cryogenically trapped ("cryotrapped") during flybys for bulk detection of compounds present at levels of ppm or lower for flybys at an altitude of 25 km. Because these *in situ* measurements will take place at a variety of altitudes above Europa's surface, the vertical profile of the atmosphere will also be established for these trace species.

4.2 Ice and Dust Grains

4.2.1 Atmospheric Dust Composition

A dust exosphere around Europa was first detected during close flybys of the satellite by the Dust Detector System (DDS) onboard the Galileo spacecraft (Krüger et al. 2003b). The dust exosphere is produced by hypervelocity micrometeroid (dust) impact ejecta, and possibly by plume sources (Roth et al. 2014b; Sparks et al. 2016, 2017; Jia et al. 2018) that might loft dust grains into the atmosphere. While compositional information is not available from the Galileo DDS, the impact ejecta are expected to be material from the satellite's surface given that the mass ratio between ejecta and the high-speed impactor is on the order of 10^3–10^4 (Sremčević et al. 2003, 2005; Krivov et al. 2002, 2003), implying that the impactor contribution to the ejecta will be small. The impact ejecta that do not escape contribute to a dust exosphere around Europa, providing another technique to study the surface composition from orbit (Postberg et al. 2011b; Sect. 2).

The SUDA investigation will map the ejecta composition distribution during close flybys and provide direct compositional constraints on various surface features (Fig. 6), complementing remote sensing spectroscopic measurements. Such measurements will provide a strong constraint on the roles of endogenic and exogenic processes shaping the surface of Europa, since the dust measurements will be made at varying distances from Europa, including those outside of the closest approach period. The analysis of ice/dust grains that are detected during targeted "Io particles" and "ring particles" observation campaigns will provide grain particle characteristics such as size, charge, and velocity, as well as chemical composition, which will constrain the relative flux of grain particles originating from Europa's surface compared with those from exogenic sources.

While the chemical composition of icy dust grains has yet to be determined, Cassini CDA observations of icy dust grains in the Saturnian system can be used as a rough proxy for the measurements that the SUDA investigation will obtain at Europa (Postberg et al. 2011b; Kempf et al. 2012). As discussed in Sect. 2.2, in addition to sub-ppm measurements of salts, the SUDA instrument will be able to measure simple and complex organic compounds, such as amino and fatty acids, as well as their possible associated breakup products (if present) in icy dust grains lofted in the atmosphere. It will also be able to detect Cl^-, HSO_4^-, Na^+, Mg^+, $MgOH^+$, and K^+ among other ions that could form from dust constituents during a hypervelocity impact onto the instrument (Napoleoni et al. 2023a, 2023b; Kempf et al. 2024, this collection).

4.2.2 Exogenic Ice and Dust Grains

Io, the volcanically active innermost Galilean satellite, serves as the major source of neutral gas, plasma, and high-speed nanodust in the magnetosphere of Jupiter (Hillier et al.

2018). Geochemical modeling suggests that sodium chloride is a major constituent in Europa's subsurface ocean (Zolotov and Shock 2001), and its detection on the surface has been considered an indication of endogenous activities of Europa (Trumbo et al. 2019a, 2019b, 2022). It is therefore necessary to understand the exogenous supply of NaCl and KCl from Io nanodust, as well as related implications of its bombardment for Europa's surface properties.

Nanodust emitted from Io forms from condensation in the volcanic plumes (Fegley and Zolotov 2000; Postberg et al. 2006). It can then acquire electric charge through interactions with ambient plasma, and when the nanodust grains reach about 10 nm radius in size, the dynamics is governed by the Lorentz forces and the nanodust grains become coupled to Jupiter's wobbling magnetic field. Positively charged nanograins are accelerated outward by the magnetospheric co-rotating electric field (Horányi et al. 1993) and are traveling at a velocity of ∼100 km/s when they reach Europa's orbit. Results from the Cassini CDA during the brief Jupiter flyby in 2000 suggest that these so-called Jovian stream grains (Grün et al. 1993) are mainly composed of sodium chloride, accompanied by S- and K-bearing components (Postberg et al. 2006).

Similar to the magnetospheric plasma, a fraction of nanodust from Io will deposit on Europa as well as the other Galilean moons. The deposition likely occurs on the trailing and sub-Jovian quadrant with a mass flux of ∼1 g/s (Horányi and Juhasz 2022) and is expected to vary with Europa's magnetic latitude and the level of Io's volcanic activity (Krüger et al. 2003a). To improve our understanding of the composition and deposition flux of nanodust from Io and other Jovian satellites (Liu et al. 2016), observations by the SUDA instrument will be scheduled both during Europa's closest approach and when the spacecraft is farther from Europa in the Jovian system. The SUDA monitoring requires the instrument to be continuously pointed towards the Jupiter line-of-sight for more than half of Jupiter's rotation period, i.e., more than 5 hours, in order to account for the changing magnetic field configuration.

Measurements from the Galileo DDS over the span of seven years indicate that the Io nanodust production rate varied by more than a factor of 100, possibly correlated with Io's volcanic activity (Krüger et al. 2003a). Regular monitoring of Io nanodust using SUDA, in conjunction with measurements from the European Space Agency's Jupiter Icy Moons Explorer (JUICE) mission and ground-based campaigns to monitor volcanic activity from Io, will provide further constraints on the variability of Io nanodust production rates, and the long-term effects, together with plasma ions and neutrals, on Europa's surface composition.

4.3 Neutral Clouds, Neutral Tori, and Plasma Torus

Neutral clouds and tori form when neutral particles escape from a moon and establish a population that co-orbits with it. If these particles survive long enough, they can form a partial or full ring (or "torus") of particles along the moon's orbit. Conversely, if their lifetimes are too short, they form a neutral cloud centered on the satellite. The presence of Europa's neutral torus was inferred using Pioneer 10 plasma osbservations (Intriligator and Miller 1982) and Cassini energetic proton (Lagg et al. 2003) and energetic neutral atom (Mauk et al. 2003) observations.

Because neutral cloud and tori distribution and composition are directly linked to surface composition and source mechanisms (including source variability), they can potentially provide insight into a source process that might not be directly observable and thus into the moon's composition and processes (Johnson and Sundqvist 2018). For example, the shape of the neutral Na cloud associated with Io has been directly related to the strength and frequency of Io's volcanic activity (Wilson and Schneider 1999).

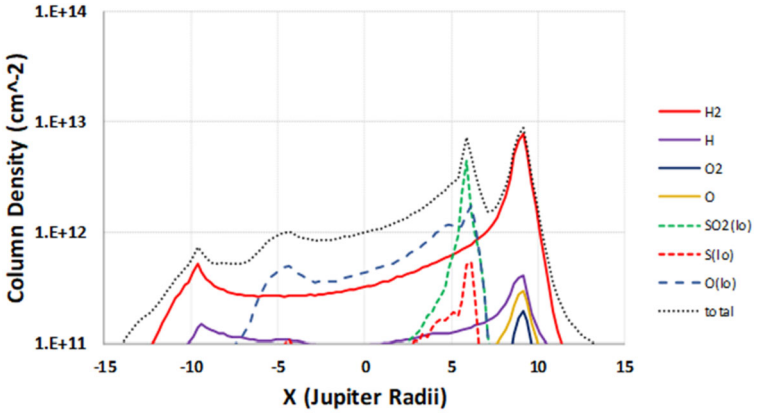

Fig. 17 Model equatorial column densities (cm^{-2}) from Smith et al. (2019) as a function of distance from Jupiter (Rj): Europa H_2 (solid red), Europa H (solid purple), Europa O_2 (solid black), Europa O (solid yellow), Io SO_2 (dashed green), Io O (dashed blue), Io S (dashed red) and all species combined (dotted black). The data represents a time when both Io and Europa are in the XZ Plane (i.e., perpendicular to the line of site along the equatorial plane or $Z = 0$, $-Y$ points toward the observer), with Io at $X = +5.9$ Rj and Europa at $X = +9.4$ Rj. This shows that the Io-generated neutrals do not contribute significantly at Europa's orbit

The primary source mechanism of Europa's neutral torus is sputtering of its water ice surface by magnetospheric ions (Johnson 1996). Most of the water particles liberated by sputtering re-impact and freeze onto the surface (Cassidy et al. 2013). A small fraction of hydrogen and oxygen atoms escape and are distributed into neutral tori through particle interactions such as charge-exchange (Dols et al. 2008, 2016; Smith et al. 2019; Bagenal and Dols 2020). It is also possible that plume activity, if occurring (Intriligator and Miller 1982; Roth et al. 2014b; Sparks et al. 2016, 2017; Jia et al. 2018), could produce a source of neutral water particles that might escape to form water-product neutral tori.

Even though Io's neutral particle source is much larger than Europa's, these two features can be distinguished because near Io the ionization lifetimes are so short that most neutral particles originating from Io are ionized long before they can be transported to the Europa torus region (Smyth and Marconi 2006; Smith et al. 2019), as shown in Fig. 17. Smith et al. (2019) report that the dominant neutral particle processes at Europa's orbit have lifetimes >2–8 days while the neutral particle lifetimes at Io are as short as 8–13 hours.

Mauk et al. (2003) reported the first detection of a Europa neutral torus using hydrogen energetic neutral atom (ENA) observations. However, there was concern that these observations could have resulted from the interaction with a plasma torus because of the relatively large plasma densities. Subsequently, Smith et al. (2019) confirmed the presence of a Europa-generated neutral torus based on available observations and computational modeling of relevant source species (Fig. 17). They constrained the resulting highly asymmetric H, H_2, O, and O_2 neutral tori and verified that while some of the Mauk et al. (2003) observations were produced by interaction with a plasma torus, a neutral torus must be present to reproduce the ENA observations at Europa.

The plasma torus is tilted with respect to the satellite orbital plane at Io due to Jupiter's tilted magnetic field, but at Europa's orbit, it is no longer as tilted and is more in the form of a plasma sheet. Since plasma is formed through ionization of neutral particles, this plasma population can be directly correlated to the neutral torus composition. Since sputtering of Europa's atmosphere and surface produces a neutral torus, detection of resulting ionized

material from the neutral clouds and tori will provide insight into Europa's composition as well as satellite sources. Recent direct detections of H_2^+ by the Juno Jovian Auroral Distributions Experiment (JADE) were attributed to H_2 pickup ions originating from Europa's neutral cloud (Szalay et al. 2022).

4.3.1 Europa Clipper Observations

Observations of Europa's neutral clouds and tori will constrain the source processes and composition of material coming from Europa. Expected species include H, H_2, O_2, O and trace species such as Na (Brown and Hill 1996). Most of the plasma at Europa is expected to originate at Io, but some hydrogen and oxygen could also come from Europa. Far from Europa, a goal of the Europa Clipper PIMS, SUDA, MASPEX and Europa-UVS investigations is to help disentangle whether the origin of the neutral and plasma species is at Io or at Europa.

The highly structured and variable plasma environment surrounding the satellite will be probed by the Europa-UVS instrument through direct measurements of ion emissions near Europa and through observations of the aurora morphology. The morphology is controlled by the way the magnetic field lines guide electrons onto Europa, and is modified by Europa's induced magnetic field, causing intrinsic variability of the aurora to occur twice over the Europa-Jupiter synodic period ($\sim$11.2 hours). Scanning observations with Europa-UVS have been designed to occur every 2 hours or less over a half-synodic period ($\sim$6 hours) for either the inbound or outbound portion (or both) of many of the Europa flybys to investigate how the aurora responds over that time. Measurements of the magnetic field and plasma environment around Europa by the ECM and PIMS investigations will provide complementary information to interpret the Europa-UVS aurora and plasma ion and neutral emission measurements. The PIMS investigation will measure ionized species, which derive ultimately from the neutral source at Europa, both within and beyond the Hill sphere, providing indirect information on structure and variability of the atmosphere and ionosphere as well as its sources.

Farther from Europa, the Europa-UVS investigation will perform long integrations ("stares") of the regions along Europa's orbit where the neutral clouds would be located to search for trace species and constrain the abundances of the neutral cloud and/or torus. Similarly, the MASPEX investigation has dedicated observations timed to collect data at >3 distinct locations along Europa's orbit around Jupiter, primarily searching for H_2 as the expected dominant neutral species in the neutral clouds or torus.

5 Europa's Possible Plumes and Their Compositional Implications

The search for and characterization of current activity on Europa is one of the primary science objectives for the Europa Clipper mission and is primarily focused on the potential presence of localized, cryovolcanic plumes, general outgassing, or thermal anomalies. Over the last decade, evidence has emerged that Europa might potentially be venting sub-surface material into space in the form of such plumes, which would provide valuable information about Europa's composition because fresh and accessible sub-surface material could be observed by the remote sensing and *in situ* instruments onboard the Europa Clipper spacecraft. These compositional measurements would therefore provide a unique and powerful dataset for assessing the habitability of the plume source regions. However, there are few constraints on the structure and composition of Europa's putative plumes, so activities to identify and characterize plume materials must consider a wide range of potential materials.

5.1 Current Knowledge

The first potential detection of a plume at Europa came from Hubble Space Telescope observations at ultraviolet wavelengths. These observations found signals in emission lines from both atomic hydrogen and oxygen that were consistent with material derived from a localized enhancement of water vapor lasting for at least seven hours (Roth et al. 2014b). Thus far, water vapor remains the only compound that has been identified in the putative plumes. However, repeated follow-up surveys with HST have been unable to detect such emissions using this technique (e.g., Roth et al. 2014a).

Later HST observations found additional candidate plume signals where material beyond the limb of Europa's disk blocked reflected light from Jupiter as the moon passed in front of the planet (Sparks et al. 2016, 2017). The opacity of these potential plumes measured during these Jupiter transits were roughly consistent with the column densities inferred from the earlier emission signals if they were composed primarily of water vapor (Sparks et al. 2016). However, subsequent analysis of these candidate plume signals indicate that they may be statistical fluctuations and thus might not provide independent evidence for plumes (Giono et al. 2020).

Further evidence for the existence of plumes was detected by Jia et al. (2018) following a re-analysis and modeling of magnetic and plasma wave signatures from the closest Galileo flyby (<400 km altitude) of Europa. The location, duration, and variations of the magnetic field and plasma wave measurements from this analysis were found to be consistent with plumes with similar characteristics to those inferred from the putative plume detections from HST.

The first efforts to detect signatures of water molecules at infrared wavelengths provided only upper limits on the abundance of water vapor (Sparks et al. 2019). A marginally significant direct detection of water vapor in infrared spectral data from the Keck Observatory was later interpreted to originate from general outgassing (Paganini et al. 2020). However, there was insufficient spatial information in these data to constrain or characterize the water vapor source. Recent observations by the JWST have failed to detect the IR signatures of an active plume (Trumbo and Brown 2023; Villanueva et al. 2023).

Despite the limited observational evidence for water vapor in Europa's possible plumes, it is reasonable to expect that water vapor will be a major component of the material launched from beneath the moon's surface. Not only is water ice a dominant constituent of Europa's surface layers, but water vapor is also by far the dominant component of the plumes detected by Cassini at Saturn's moon Enceladus (Postberg et al. 2018a, and references therein), which are some of the closest analogs to the potential activity on Europa.

Currently, there are no constraints on any other constituent of Europa's potential plumes; however, based on compositional measurements of Enceladus' plumes, it is reasonable to expect that the vapor phase of Europa's plumes would contain volatiles like CO_2, CH_4, NH_3, and H_2 (Waite et al. 2017). Furthermore, the active plumes of Enceladus, Triton, and Io also contain solid grains in addition to gas. For Enceladus, these grains are composed of various combinations of water ice, salts, organic compounds (Postberg et al. 2009, 2011a, 2018a; Khawaja et al. 2019); and silica nano-sized grains of likely Enceladean origin are detected in the Saturnian system (Hsu et al. 2015). The chemistry of solid materials ejected in any Europan plumes will depend on the composition of the subsurface sources, and so could include various combinations of water, organic compounds, and salts. While such plume grains have yet to be observed directly, certain diffuse dark patches on Europa's surface could be interpreted as deposits of low-albedo plume material (Fagents et al. 2000; Quick et al. 2013; Quick and Hedman 2021). If this hypothesis is correct, then this could

mean that plume fallout has a distinctive composition. At present, however, the data are too sparse to make reliable inferences about those compositional variations. New and upcoming observations by JWST would be useful for searching for such surface variations prior to the arrival of Europa Clipper.

5.2 Remote Sensing Searches and Characterization of Plume Composition

5.2.1 Active Plume Searches and Characterizations

Remote-sensing searches for plume vapor will be conducted primarily through the Europa-UVS investigation using techniques similar to those already employed to identify plume signals in data acquired by Earth-based telescopes. Similar to the HST detections of auroral emissions from excited atomic O and H resulting from the dissociation of water vapor plumes by electron impacts, which provided the first evidence of plumes at Europa (Roth et al. 2014b,a), Europa-UVS will search for coincident UV detections of emissions from O and H above the Europa's limb during nadir-pointed stares. Spacecraft scans (Sect. 2) across the moon will provide constraints on the spatial distribution and variability of any plumes, and will constrain the column density of the plumes' water vapor.

Additionally, the Europa-UVS instrument will acquire transmission spectra through Europa's atmosphere (Sect. 4.1.1) that will be used to search for and characterize the composition of plumes during stellar and solar occultations and during Jupiter transits. Species including H_2O, O_2, H_2, and a variety of hydrocarbon and nitrogen compounds (e.g., CO_2, C_2H_2, CH_4, N_2) that may be present in potential plumes have absorption features in the Europa-UVS bandpass and could therefore be detected with these techniques (Fig. 16). Similar to the HST transit observations (Sparks et al. 2016, 2017), light absorbed off of the limb of Europa during a Jupiter transit can not only be used to constrain the column density of a discovered plume, but also be used to constrain its composition as well since Europa-UVS acquires spectral and spatial information simultaneously.

Spectral information from stellar and solar occultations are highly sensitive to composition and will provide a high spatial resolution slice through Europa's atmosphere, especially for long-duration occultations. If the occultation chord happens to cut through a plume or a part of the atmosphere that was recently affected by a plume (Sect. 5.5), then measurements by Europa-UVS can be used to identify its constituents. Similarly, stellar and solar occultations by Enceladus' plume observed with the ultraviolet instrument onboard Cassini provided strong constraints on the plume's structure and composition (Hansen et al. 2019, 2020).

Remote-sensing searches for solid grains in any active plume will be primarily conducted at visible wavelengths by the EIS investigation, which will look for light scattered by plume dust particles near Europa's limb and terminator. Such observations can reveal tenuous populations of plume ice/dust grains, but directly determining the composition of lofted plume particles will be much more challenging due to both the reduced scattering efficiency of solid grains compared to free molecules and the suppression of diagnostic spectral features at high phase angles. Similarly, any high-phase angle observations from the MISE investigation can be used to constrain grain sizes in the plume. The Galileo SSI experiment conducted high phase observations of the limb that would enable a search for plumes (Phillips 2000) but did not detect any, which may be consistent with the apparent sporadic nature of putative plume activity (e.g., Roth et al. 2014a; Sparks et al. 2016).

5.2.2 Potential Surface Signatures of Recent Activity

Most of the solid grains ejected in a plume are expected to fall back to the surface near the plume vent, producing fresh deposits whose structures and compositions can be measured by the various remote-sensing and in situ instruments. At ultraviolet wavelengths, the spectrum of water ice is dominated by a sharp spectral edge near 165 nm. This spectral feature has been observed on the surface of Enceladus, which is thought to be coated by relatively fresh material from the plume-sourced E-ring (Hendrix et al. 2010). However, this feature has not been found in the present, low-resolution global surface spectra of Europa. This may be due to degradation of the signature by radiation, contamination by salts or other materials, or a thin, UV-absorbing lag deposit resulting from processing of the uppermost layer of the surface (Becker et al. 2018; Teolis et al. 2017). Localized surface areas displaying the strong water ice spectral edge may be visible in the Europa-UVS data and 'purer' H_2O ice signatures may be detected by MISE; these would indicate relatively fresh surface plume deposits or recent cryvolcanic activity (Prockter et al. 2017; Quick and Hedman 2021; Raut et al. 2023).

The SUDA investigation will model the surface origins of ice grains lofted into the atmosphere through micrometeoroid impacts. Abrupt changes in surface composition due to fresher, less-altered plume deposits will be detectable, and the specific origin of a plume fallout can be identified if the detections occur when the spacecraft altitude is less than or equal to the plume deposit size (Sect. 2.2.2; Fig. 11). Indeed, the Cassini CDA instrument (same operating principle as SUDA) observational data were successfully modeled to map fresh plume deposits on Enceladus (Kempf et al. 2010).

At visible and near-infrared wavelengths, Europa exhibits spectral absorption bands due to a variety of hydrated compounds and/or salts (Carlson et al. 2009; Trumbo et al. 2019a,b), and the distribution of these non-icy materials varies on a wide variety of spatial scales (McCord et al. 1998). The shape and intensity of these spectral features are affected by exogenic processes, and localized areas with unusual spectral properties could therefore be indicative of recent plume deposits; such features might be detected by the MISE investigation. Furthermore, since plume fallout is composed predominantly of small grains, plume deposits may have distinct regolith textures, including high porosities and low effective scattering lengths. These phenomena can alter the deposits' brightness and spectral parameters in ways that could be detected by the EIS and MISE investigations (Quick and Hedman 2021), as well as produce localized anomalies in the surface thermal behavior that could be revealed with the E-THEMIS instrument.

At even longer wavelengths, the plume fallout deposits are expected to influence the surface radiometry measurements by REASON through either modification of the surface porosity and through near-surface layering (i.e., a fallout deposit layer overlying ice). At wavelengths emitted by the instrument (VHF: ~5 m in vacuum, HF: ~33 m in vacuum), the effective reflection coefficient responds primarily to the ice/void ratio at the surface. This sensitivity to porosity is nonlinear, and owing to its wide radiometric range, REASON is sensitive to the various compaction stages of plume fallout as calibrated from Earth observations (Cuffey and Paterson 2010). For example, compact ice is approximately 5 dB more reflective than old fallout that is dominated by sintering and plastic deformation (porosity $> 50\%$). In turn, older, more compact deposits are approximately 13 dB more reflective than fresh, porous deposits (porosity $>90\%$; Grima et al. 2014a; Scanlan et al. 2022). Furthermore, surface radar reflectivity is sensitive to the existence of a near-surface layer when its thickness is less than the range resolution of the radar (Mouginot et al. 2009; Chan et al. 2023). Hence, surface radiometry measurements from the REASON instrument will provide insights into the relative activity and geographical extent of formerly active zones.

5.3 *In Situ* Searches for Plumes and Characterization of Plume Composition

While the existence of plumes at Europa remains presently uncertain, the spacecraft's multiple flybys will provide opportunities to measure the content of any active or recent plumes using *in situ* techniques, which will inform the composition of both the vapor and grain components of possible plumes. If the spacecraft happens to traverse through a plume, then SUDA and MASPEX will directly sample material from the plume's source region, which could be located within the ice shell or in the ocean.

During plume crossings, the SUDA instrument can record the mass spectra of cations and anions produced by the hypervelocity impact of dust grains onto the instrument's target plate at a rate of hundreds of grains per second. The high sensitivity of the SUDA instrument enables the detection of inorganic compounds like salts and other minerals, as well as simple and complex organic constituents. As a result, the SUDA investigation will enable a better quantification of the salt composition of ice grains from any active plumes and constrain their sources. Similar measurements with the Cassini CDA instrument at Enceladus have provided valuable information about the inorganic and organic composition of the moon's subsurface ocean (Postberg et al. 2009, 2018b, Hsu et al. 2015; Khawaja et al. 2019). Recent laboratory and theoretical work suggests that biosignature molecules such as amino acids and fatty acids, if present, could be identified with SUDA measurements (Klenner et al. 2020b,a; Jaramillo-Botero et al. 2021). The abundances of major (e.g., H_2O, CO_2, CO, N_2, H_2, CH_4) and trace gases in any plume vapor will be detected in the MASPEX investigation. The instrument also has a special mode to measure volatiles released from ice grains that enter the instrument, if encountered.

5.4 Understanding Plumes Through Global Atmospheric Effects

Active plumes can significantly alter the global composition of Europa's tenuous atmosphere (Teolis et al. 2017; Li et al. 2020). As such, *in situ* compositional measurements of the atmosphere from close flybys or from remote sensing observations like stellar occultations could provide evidence for recent plume activity anywhere on the moon (Sect. 4.1). Atmospheric modeling suggests that water and multiple other plume species, including noble gases and multiple nitrile and organic species, would be enhanced globally by plume activity, and would be detectable far from the plume. Intriguingly, models suggest that a recent plume could temporarily produce signatures in the ratios of major species like H_2O and O_2 that could be detected in the global atmosphere. For example, models suggest that if a plume recently erupted at the southern high latitudes, then the ratio of H_2O:O_2 would be $>$15:1 globally (Teolis et al. 2017).

5.5 Characterizing Plumes from the Local Plasma Environment and Magnetic Field

In addition to the neutral ice grains and gas molecules, some fraction of the molecules and small ice grains in a plume can become ionized, generating localized enhancements in the plasma density and abrupt changes in the magnetic field orientation and strength. Such variations may have been observed during the Galileo E12 flyby (Jia et al. 2018), and similar phenomena could be reflected in the PIMS plasma and ECM magnetic field data. The PIMS investigation will provide compositional measurements of plasma generated from any plume material, while the ECM's high temporal resolution magnetic field data will contribute to information about plasma composition by measuring ion cyclotron waves that may be generated by pickup ions associated with a plume (e.g., Volwerk et al. 2001).

Both the REASON and Gravity/Radio Science investigations have the ability to observe localized enhancements in the plasma density. The REASON investigation will provide an estimate of the total electron content (TEC) within the vertical column between the Europa Clipper spacecraft and the nadir surface in order to correct for dispersive plasma distortion occurring along the radio signal propagation path (Grima 2017; Scanlan 2019; Blankenship et al. 2024, this collection). As such, the instrument can search for perturbations in the local plasma environment, possibly related to plumes present along the spacecraft ground track. The ingress radio occultation by the Galileo spacecraft on flyby E6a measured notably large ionospheric electron densities in the vicinity of Pwyll crater (Kliore et al. 1997; McGrath and Sparks 2017), where several independent observations have suggested signatures of a plume (Sparks et al. 2016, 2017; Jia et al. 2018). Similar radio occultation observations by the Europa Clipper G/RS investigation will determine the vertical profiles of ionospheric electron density at a wide range of geographic locations. These observations have the potential to detect enhanced ionospheric electron densities associated with plumes. Such measurements can constrain the ionization state of possible plume material.

6 Processes Affecting the Composition of Europa

6.1 Overview

Over its history, the composition of Europa has been affected by its initial formation conditions, orbital and interior evolution, the formation of its hydrosphere, and ongoing and geologically recent processes in the coupled atmosphere–ice–ocean–rock system. The Europa Clipper mission will constrain the origin, evolution, and current processing of the satellite through compositional measurements. These observations will enhance our understanding of chemical and physical pathways between Europa's subsurface ocean, ice shell, surface, atmosphere, and space environment.

The main scenarios proposed for the origin of Europa are summarized in Sect. 6.2. Each scenario would imply different compositional evolution pathways, especially for the origin of the hydrosphere: accreted water vs. water resulting from thermal dehydration of rocky materials (Sect. 6.3). An important process expected during accretion is the loss of water and other volatiles. Accretion should be accompanied and followed by a phase of aqueous alteration of primordial reduced and anhydrous solids. Previously altered (oxidized, hydrated, and carbonated) asteroidal materials could be reworked if they were accreted. Subsequent, at least partial, dehydration of the rocky mantle expanded or even entirely produced the hydrosphere. In addition to inorganic ions, the hydrosphere could have contained inorganic carbon species, CH_4, NH_3, and/or N_2 (Sect. 6.4) whose fates depended on conditions in the ocean and processes driving the evolution of the ice shell (e.g., outgassing). The formation of a metallic core through igneous differentiation was likely and compatible with (if not demanded by) the Galileo gravity data (Anderson et al. 1998). The composition and size of the core depend on the nature of the accreted material and the fate of S, O, and C during the metamorphic evolution of the mantle (Sect. 6.3). Orbital evolution has been a major factor affecting tidal dissipation of heat, endogenic activity, and thickness of the ice shell (Hussmann and Spohn 2004). Geological observations and data suggest that the current shell is geologically young (Bierhaus et al. 2009) and has been thickening (Pappalardo et al. 1998; Doggett et al. 2009). Additional input of material of exogenic origin (e.g., comet/asteroid impactors) and from mantle evolution is expected to be small, although the long-term interaction between the ocean and the upper mantle is possible over Europa's history. Additional

discussion on the evolution of the deep interior can be found in Roberts et al. (2023, this collection).

Apart from these major evolutionary phases, little is known about the evolution of the ice shell before the past 10^8 years. As the current shell freezes, oceanic solutes concentrate. Hence, the current salinity of the ocean is in part determined by the extent of tidal heating as a key long-term heat source in the shell as well as heat transfer modalities. The heat transfer is influenced by the state of the Laplace resonance and the presence of non-ice compounds that may affect the thermophysical properties and viscosity of the shell. Heat transfer also determines geodynamic processes in the shell, ocean-surface exchange processes, and partial melting in the shell. Several mechanisms may allow the exchange of material between the ocean and the surface (formation of ridges, chaotic terrains, bands, liquid water sills or melt lenses, and diapirism) and have strongly affected an earlier thin shell (Sect. 6.5). Oceanic material exposed on the surface is altered by a variety of processes: heavy irradiation, impacts by dust and large-size objects, and thermal processing (Sect. 6.6,6.7, 6.8). These processes are limited to the upper millimeters to meters of the surface. Energetic charged particles alter surface material and sputter radiolytic species into the thin atmosphere. Gardening by micrometeoroid impacts exposes subsurface material and can also temporarily loft grains into the atmosphere. The atmosphere itself is also subject to radiolytic processes that ionize the neutrals, which can then be coupled to Jupiter's magnetic field (Sect. 6.8). These various interactions affect the atmospheric, surface, and subsurface environments.

6.2 Formation of Europa

Understanding the physical-chemical conditions encountered within the Jovian circumplanetary disk (CPD) is key to constraining processes that have shaped the properties of the Galilean satellites. Models for the formation of Europa must account for the density gradient observed across the four Galilean satellites: denser with a high fraction of rocky material closer in (Io) and dominated by ices and volatiles farther out (Callisto). In common models, the density gradient reflects the temperature gradient in the CPD.

One end-member category of the Galilean moons' formation scenarios (*Case 1*) advocates for high pressure-temperature gas chemistry reactions in the CPD (Prinn and Fegley 1981; Lunine and Stevenson 1982; Szulagyi et al. 2016) in which the volatile portion of the satellites's building blocks is condensed within the CPD. These scenarios predict a D/H ratio close to the protosolar value ($\sim 2 \times 10^{-5}$) (Mousis et al. 2002) and formation of Io and Europa from volatile-poor materials condensed *in situ*.

Another set of models (*Case 2*) suggests a warm, low-pressure CPD without chemical reactions that produce volatiles (e.g., CH_4) (Canup and Ward 2002) and accretion of materials from both sides of the solar accretion disk. Io and Europa would have formed from condensates of the protosolar nebula that devolatilized through their drift to inner warm regions of the CPD (Coradini et al. 1989; Canup and Ward 2002, 2009; Mosqueira and Estrada 2003a,b; Mousis and Gautier 2004). A significant fraction of such building blocks could have had a comet-type chemical (rock + organics + ices) and isotopic (Mousis and Gautier 2004; Mousis et al. 2009a,b) composition. Within the broad framework of *Case 2*, formation of the Galilean moons could have occurred through agglomeration of centimeter-sized pebbles that are dragged into the CPD (Ronnet et al. 2017; Anderson et al. 2021). The small size of solids implies efficient thermal devolatilization during the inward drift. This scenario imposes the accretion of the moons from pebbles after several Myr evolution of the protosolar nebula (Ronnet et al. 2017), and a fast accretion ($<10^5$ yr). Another parameter

to be considered in satellite formation models is the possible migration of Jupiter before the dissipation of the protosolar nebula. Heller et al. (2015) argue that Jupiter and the Galilean moons had to form beyond their current location 4.5 ± 0.5 AU before the proposed Grand Tack migration (Walsh and Morbidelli 2011) of Jupiter and Saturn. In this formation and migration scenario, Galilean moons should have been affected by influxes of carbonaceous bodies formed beyond Jupiter and thermally processed bodies formed between Jupiter and the Sun. It is also possible that organic and ice rich bodies formed Galilean moons during their sunward motion driven by giant planet movement away from the Sun at the last stage of the Grand Tack migration. Formation of Galilean moons from large bodies from the outer solar system implies devolatilization during (e.g., Bierson and Nimmo 2020) or after accretion (Sect. 6.3).

The possible formation models for the Galilean system differ in nature and abundance of accreted 'rocks', volatiles, and organic matter. Building blocks of Europa could include unaltered, aqueously altered (hydrated), and thermally dehydrated chondritic materials, cometary H_2O-dominated ices, and organic matter (Table 3). These materials could be accreted in different proportions, and each compositional assemblage could be linked to an accretion scenario. Formation from altered and/or thermally processed chondrites requires the accretion of large bodies, while unaltered icy and organic rich materials could accrete as large bodies and/or pebbles. Pebble accretion from partly devolatilized solids in inner parts of the CPD would correspond to a devolatilized cometary composition; i.e., water plus some remaining volatile ices, CI-type 'rocks', and abundant carbonaceous matter. Formation of Jupiter in a gap in the solar accretion disk (e.g., Desch et al. 2018) suggests a drag of materials from both sides of the disk. Primitive (anhydrous, reduced, organic- and ice-rich) comet-like materials could be supplied from the outer solar system, while thermally processed (ice-free, hydrated, aqueously oxidized, dehydrated, and organic-poor) materials were dragged from the Sun-facing side. In other words, the moons could accrete a mixture of cometary and thermally processed chondritic materials. Those chemically and isotopically diverse materials (e.g., Desch et al. 2018) likely contributed to the formation of Galilean moons. However, a late formation of Galilean moons during giant planet migration away from the Sun suggests a greater contribution from large bodies with at least partially aqueously altered materials with cometary and/or C-rich CI-type carbonaceous chondrite composition.

Europa Clipper data on the chemical and isotopic composition of current surface, atmospheric and possible plume materials may narrow the range of formation scenarios and constrain sources of Europa-building solids. Further, measurements of Ganymede and Callisto by JUICE will be extremely valuable for constraining the composition of the building solids and the possible compositional gradient in the Jupiter system. Several kinds of measurements can potentially discriminate between the origins proposed for Europa in the framework of *Case 2* (Table 3). Surface composition measurements can indirectly constrain types of volatiles accreted in Europa. A detection of abundant endogenic organic matter, carbonates, and ammonium salts through MISE, Europa-UVS, and SUDA measurements would be consistent with cometary-like constituents delivered from the outer solar system and would be consistent with the formation of the Galilean moons at larger heliocentric distances (*Case 2*). Additional constraints will be obtained from atmospheric and plume gases (MASPEX and Europa-UVS measurements) that may or may not be enriched in specific compounds (e.g., NH_3), that may indicate an outer solar system origin. However, NH_3 could be produced through interior high-temperature alteration of cometary/chondritic organic matter (Miller et al. 2019) and caution is needed in interpretation of measurements in terms of Europa's origin.

Table 3 Summary of possible Europa-building materials, accretion scenarios, and potential observables by the Europa Clipper's payload

Formation scenario in the framework of *Case 2*	Accreted materials	Measurable compositional signatures	Notes
2.1. Late accretion from parent bodies similar to those of carbonaceous chondrites	Carbonaceous chondritic material (hydrated) without ices	Mg-Na sulfate-rich salts at locations indicative of ocean composition (**MISE**, **SUDA**)	Considered in Melwani Daswani et al. (2021). Does not explain ice-rich Ganymede and Callisto, unless a volatile gradient in Jupiter's CPD is invoked.
2.2. Pebble accretion with limited drag from the outer solar system	Unaltered carbonaceous chondritic material with some ices	NaCl rich salts and ocean with limited sulfates (**MISE**, **SUDA**)	
2.3. Accretion of ice-rich pebbles delivered from the outer solar system	Cometary material: unaltered carbonaceous chondritic material with abundant organics and ices	NaCl-carbonate type endogenic salts and corresponding oceanic water (**MISE**, **SUDA**); Organic-rich endogenic materials (**SUDA**, **MISE**, and **MASPEX**); Cometary signatures in light stable isotopes (**MASPEX**, **Europa-UVS**)	Consistent with interior structure models for Ganymede, Titan (Neri et al. 2020), and Ceres (Zolotov 2020)
2.4. Accretion of material dragged from both the inner and outer solar system. Mixture of pebbles and thermally-processed bodies	Mixture of cometary and thermally processed chondritic material		Consistent with the models of Jupiter' formation and with meteoritic data (Desch et al. 2018). Consistent with ice-rich Ganymede and Callisto if extensive water loss from Europa is invoked ("hot accretion")

Note: Cases 2.3 and 2.4 may not be unambiguously distinguished based on Europa Clipper compositional measurements; however, Case 2.3 does imply a higher C content, both organic and inorganic.

Isotopic ratios D/H, $^{12}C/^{13}C$, $^{14}N/^{15}N$, and $^{16}O/^{18}O$ measured by the MASPEX investigation could constrain the ratio of chondritic material to cometary ice in accreted materials. For example, an elevated ^{18}O content would indicate abundant cometary sources and, possibly, a loss of water after accretion. The nitrogen isotope ratio may constrain the primary source of nitrogen – whether it was N_2 from the protosolar nebula (^{15}N-poor) or ammonia ice and HCN from cometlike materials (^{15}N-rich) (e.g., Prinn and Fegley 1989; Mandt et al. 2014). An elevated D/H ratio would be indicative of abundant cometary ice, though other mechanisms affecting the D/H ratio during Europa's evolution need to be considered. For example, water loss resulting from possible escape during accretion, or early in the moon's history because of Jupiter's luminosity (Bierson et al. 2023), would lead to an elevated D/H ratio in the remaining hydrosphere (Bierson and Nimmo 2020). Incorporation of D-rich primordial organix matter could also affect the hydrogen isotpic mass balance (Glein et al. 2024). If Europa did not accrete abundant ices, these stable isotope ratios could characterize chondritic building materials (cf. Ireland et al. 2020), their sources in the early solar system, and formation scenarios of the moon.

6.3 Thermo-Chemical Evolution of Europa and Formation of the Hydrosphere

Analogies for the thermo-chemical evolution of Europa and the formation of the hydrosphere can be drawn from other bodies for which we have more extensive observations and models, such as the parent bodies of carbonaceous chondrites, Ceres, and other icy moons. Carbonaceous chondrites provide a wealth of information about the aqueous alteration of reduced and anhydrous solids and organic materials that accreted together with water ice containing CO_2 and other volatiles (e.g., Brearley 2006; Zolensky et al. 2017). Aqueous processes on parent bodies of carbonaceous chondrites included at least partial consumption of liquid water through hydration of Mg-rich silicates and Fe sulfides and oxidation of Fe-Ni metal and sulfides. The alteration led to the formation of Mg-Fe phyllosilicates, hydrated Fe sulfides, ferric oxides (magnetite) and salts (carbonates, sulfates, and chlorides). Molecular hydrogen (H_2) forms in these oxidation reactions, becomes a dominant gas as water is consumed, and can then escape to space to potentially drive the system to higher oxidation states. The formation of sulfates requires strong oxidants such as O_2 in accreted ices (Zolotov 2016). Sulfate-free carbonaceous asteroid Ryugu, as evidenced by returned samples from the Hyabusa-2 mission (Nakamura et al. 2022), suggest that a fraction of Europa-building materials could be sulfate-poor. The Europa Clipper will search for endogenic sulfates on the surface through the MISE and SUDA investigations and efforts will be made to distinguish exogenic and endogenic sulfates, primarily through their potential association with geologic features (Sect. 2.2.2). All these processes could have occurred on Europa-building bodies (but not pebbles, *Case 2.1* in Table 3) and/or *in situ*, shortly after the accretion of Europa from unaltered rocky solar nebula materials and ices (McKinnon and Zolensky 2003). Thermally metamorphosed carbonaceous chondrites can inform our understanding of possible compositional changes on Europa caused by radiogenic heating of aqueously altered materials (Velbel and Zolensky 2021, and references therein). Heating of aqueously altered chondrites causes dehydration of phyllosilicates to Fe-bearing silicates (e.g., olivine), reduction of sulfates to sulfides, decomposition of carbonates, and oxidation (aromatization and graphitization) of high molecular weight organic matter. These processes affect the fractionation of stable isotopes (N, H, O, C, and S) between the remaining materials and released gases, which will be measured using the MASPEX and Europa-UVS investigations of Europa's atmosphere. These investigations will also assess the concentration of H_2O, CO_2, light hydrocarbons, and N_2 (Sect. 4), which are likely products of such metamorphic reactions.

The formation scenarios of Europa described above imply distinct evolutionary paths (1) because the scenarios differ in the amount of heat generated during and following formation (e.g., accretional heat and ^{26}Al decay) and (2) because water may be "free" or in the form of "water of hydration," in minerals. Europa's current water to rock ratio implies water could not play a major role in moderating early heating; a large part of the water was likely used in aqueous alteration processes in hydration (e.g., formation of serpentine and saponite) and oxidation of accreted materials (e.g., formation of Fe oxides and ferrous silicates from Fe-rich metal). However, it is possible that Europa accreted with more water (Sect. 6.2). Hence, early evolution of Europa formed in the CPD and pebble accretion scenarios (*Case 2.3* in Table 3) could have started with the differentiation of a thin hydrosphere, followed by the input of water released during metamorphism of the rocky mantle within the first billion years of Europa's evolution. In the case of accretion from hydrated chondrite material (*Case 2.1*), the quantity of additional ices that was accreted is unclear. Kargel et al. (2000) and Melwani Daswani et al. (2021) suggest that potentially all of Europa's hydrosphere stemmed from the release of water and other volatiles upon metamorphic dehydration.

Different evolution pathways for the ocean may be linked to different outcomes for the separation of a metallic core. The thermal evolution model of Trinh et al. (2023) suggests a protracted heating and delayed differentiation of a metallic core on Europa. This is due to the combined effects of a colder start (slow accretion) than assumed in earlier studies and more accurate tracking of Europa's heat budget over time. In particular, the large latent heat involved in dehydration of silicates such as serpentine represents a significant heat sink. This study highlights the dependency of Europa's internal evolution on key parameters (e.g., sulfur abundance, tidal heating) and shows that the presence of a metallic core is not a warranted outcome. The reanalysis of the Galileo gravity data by Gomez Casajus et al. (2021) also suggests a less differentiated Europa than inferred in previous studies (e.g., Anderson et al. 1998).

6.4 Water, Rock, and Organic Interactions

The large internal heat and inferred differentiated structure of Europa, with a water shell and rocky interior, together with a possibly carbon-rich interior, imply that water/rock/organic interactions occurred throughout its history. Initial aqueous processes and hydration of rocks (if they accreted anhydrous, *Cases 2.2–2.4* in Table 3) could have occurred during accretion and post-accretional cold fluid upwelling into a primordial ocean (Zolotov and Kargel 2009). Subsequent thermal dehydration of rocks before igneous processes and core formation could have caused alteration of inorganic materials and organic matter by upwelling fluids that further contributed to the ocean (Kargel et al. 2000; McKinnon and Zolensky 2003; Travis et al. 2012; Zolotov and Mironenko 2015; Melwani Daswani et al. 2021). Throughout history, low-temperature water–rock interactions within the upper tens of km of the oceanic floor have been discussed (Vance et al. 2007, 2016; Bouquet et al. 2017), although the permeability of suboceanic materials could be limited because of hydrostatic pressure. Local hydrothermal activity (e.g., Lowell and DuBose 2005) could have been associated with suboceanic tidal heating that may even cause silicate volcanism (Běhounková et al. 2021). Finally, salt–brine–gas type reactions could have occurred during freezing, thawing, or outgassing in the ocean and in the ice shell.

In analogy with parent bodies of meteorites (Sephton 2014; Alexander et al. 2017) and terrestrial sedimentary basins (e.g., Price and DeWitt 2001), water-soluble and insoluble organic compounds could have been altered in aqueous processes. As in carbonaceous chondrites, aqueous alteration of accreted high molecular weight organic matter could have enhanced aromaticity of surviving low-solubility organic compounds (Alexander et al. 2017). Other likely reactants are volatile compounds that could have accreted with ices (e.g., CO_2, CO, NH_3, CH_4, and other volatile organic species) and formed through aqueous processes and pyrolysis (e.g., CO_2, H_2, CH_4, NH_3). For example, H_2 and CH_4 could form as byproducts of oxidation of ferrous minerals and organic matter by water. Components such as CO_2, H_2, CH_4, NH_3, N_2, and an array of light organic compounds would form through hydrothermal water–organic reactions in the presence of rocks or sediments. The likelihood of commonly inefficient hydrothermal abiotic synthesis of CH_4 from CO_2 and/or CO in heated fluids (Seewald et al. 2006; McCollom 2016; McCollom and Seewald 2007) depends on whether the fluid residence time exceeded the chemical kinetic timescale for the geochemical environment. Europa Clipper data on gaseous or condensed products of aqueous reactions in the atmosphere (Sect. 4), any plumes (Sect. 5), or on the surface (Sect. 2) will be used to constrain preceding aqueous reactions.

Speciation of products of aqueous reactions (ions, neutral species, gases, minerals, and organic matter) depends on the compositions and amounts of reactants (water–rock–organic

ratios), temperatures, pressures, and durations of the interactions. Even short-term acid–base type interactions could reach chemical equilibrium at the low temperatures typical for oceanic water. Identification of reaction products (e.g., salts, gases, ions), which originated from likely acid-base equilibrated solutions, could constrain such alteration parameters as initial rock type, secondary mineralogy and pH of oceanic water or crustal brines. For a set of initial compositions, temperature, pressure, and duration of alteration, reaction products could be assessed through reaction path modeling that includes reaction rates and chemical equilibria constraints. Comparison of model results with speciation of plume and/or atmospheric gases measurements by MASPEX and Europa-UVS and/or solid phases in surface and sputtered dust materials observed by MISE and SUDA will constrain parameters of aqueous alteration. With these data, it will be possible to evaluate if subsurface (e.g., oceanic) water is saturated with respect to certain solids and assess mineralogy that could coexist with the solution (see also Sect. 3.2). For example, ultramafic, mafic, or evolved (SiO_2-rich) compositions of suboceanic rocks will be distinguished from the composition of endogenic salts observed on the surface by the MISE and Europa-UVS instruments, and in atmospheric grains by SUDA, together with potential measurements of $H_2/CO_2/CH_4/H_2O$ ratios in the atmosphere and possibly in plume gases by the MASPEX and Europa-UVS instruments. The Na/K ratio in the atmosphere, plume, and sputtered particles will be indicative of the prevailing temperature and mineralogy of water–rock reactions at the ocean floor (Zolotov 2012).

Many oxidation-reduction (redox) reactions are inhibited at low (e.g., oceanic) temperatures. CO_2–CH_4, CO_2–organic, sulfate–sulfide, and H_2–O_2 interactions are slow below ~500 K and do not reach chemical equilibrium in low-temperature natural and experimental systems (e.g., Seewald et al. 2006; Ohmoto and Lasaga 1982; Foustoukos et al. 2011; McCollom 2016). Measured abundances of corresponding species in endogenic materials (e.g., any plume emissions) will provide information about the degrees of redox disequilibria, some of which are known to provide metabolic energy for organisms. Some ratios of reduced and oxidized compounds (e.g., H_2/H_2O and C_2H_6/C_2H_4) could be indicative of redox conditions (e.g., H_2 fugacity, fH_2) in suboceanic hydrothermal environments, if they exist. For example, H_2/H_2O ratio could be used to constrain a dominant iron mineralogy and in hydrothermal systems that may control fH_2 in the fluid phase. Aqueous reactions with participation of strong oxidants (O_2, H_2O_2, etc.), which could be delivered through accreted ices or from the irradiated body's surface, are rapid. In interior aqueous environments, they should have been consumed via oxidation of reducing Fe, S, and C-bearing compounds (Ray et al. 2021; Zolotov and Shock 2004). Detection of a strong oxidant (O_2, H_2O_2) in any plume materials (Sect. 5) would indicate their radiolytic rather than aqueous origin.

The diversity of organic compounds in carbonaceous chondrites (Sephton 2014) and their suggested transformation pathways provide insight into Europa's processes. Higher temperature causes a decrease in the H/C, O/C, and N/C ratios in the insoluble organic matter (IOM), affecting the isotopic composition of IOM and its alteration products (e.g., Alexander et al. 2017). Chemical and isotopic composition of reaction products (e.g., CH_4, other hydrocarbons, organic acids, NH_3, H_2) detected in potential plume gases could inform the transformation of organic matter in Europa's interior. Temperature and/or fH_2 of aqueous reactions could be estimated from the concentrations of multiple inorganic compounds (Glein et al. 2008), if they can be measured in plume gas by the MASPEX and Europa-UVS instruments and in grains with the SUDA instrument. Even without a plume, SUDA measurements of positive and negative ions in sputtered surface salt grains will constrain the composition and pH of subsurface ocean, though we note that since SUDA cannot measure cations and anions simultaneously, such results will be inferred from ground-track crossovers of the same region that occur on different flybys (see Sect. 3.2).

6.5 Evolution of the Current Ocean-Ice Shell System

The chemical evolution of Europa's ice shell and ocean is influenced by the satellite's thermal history and is dependent on the moon's orbital evolution, tidal response, composition of Europa-building materials, physical-chemical processes in the rocky interior, and the processes that move material within and through the shell. The paucity of large craters on Europa's surface (Bierhaus et al. 2009) imply that major changes in Europa's ocean-ice shell system over the last 10^8 years have been primarily endogenic in nature. Little is known about the processes occurring in the ice shell prior to this time period because no obvious geologic evidence remains, possibly as a consequence of resurfacing events (Pappalardo et al. 1999).

6.5.1 Energy Sources and Shell Thickness

Europa's energy budget has several potential sources that vary in strength over the satellite's history, and each plays a critical role in its chemical evolution. Over the last 10^8 years, tidal dissipation in the mantle and/or ice shell has been expected to be most prominent with radiogenic heating, ocean tides, and ohmic dissipation orders of magnitude weaker over this time period (e.g., Nimmo and Manga 2009; Gissinger and Petitdemange 2019; Rovira-Navarro et al. 2019; Chyba et al. 2021). As a result, the intensity and distribution of tidal dissipation will crucially inform the physical process that may occur. Whether tidal dissipation primarily occurs in the rocky mantle or the ice shell, heat production from the Laplace orbital resonance with Io and Ganymede may be approaching a minimum (Hussmann and Spohn 2004). This orbital resonance may be a primary factor in controlling the thickness of the ice shell, which has a major influence on potential ocean–surface exchange processes (Chyba and Phillips 2001) that would affect the composition of the ocean–ice shell system over time.

Interpretations of the ice shell's surface geology may support the general thickening of the ice shell over time (Pappalardo et al. 1998; Greeley et al. 2000; Figueredo and Greeley 2004; Leonard et al. 2018, 2020; Senske et al. 2019). This thickening could increase oceanic salinity through time. However, it is unclear if the ice shell is currently thickening. Shell thinning could be driven by dissipation of tidal heat in the rocky mantle (Běhounková et al. 2021) and by high dissipation in the ice shell. In such a case, ocean salinity would decrease and some materials from the upper shell could be introduced to the ocean. Knowledge of the variability of ice salinity through the REASON investigation and overall compositional constraints on material in the ocean can therefore constrain models of current or past ice thickening.

Shell thickening over the last 10^8 years has further consequences for the composition of the ice shell. Faster freezing near the surface could retain up to ~50% of oceanic salts (Zolotov and Kargel 2009; Buffo et al. 2020), while smaller amounts of salts (~5% or less) could be retained during slower freezing in the deeper shell (Buffo et al. 2020; Wolfenbarger et al. 2022b). Once the shell thickness reaches a critical value estimated between 10–30 km, depending on the unknown ice viscosity, subsolidus convection of the ice is likely promoted (e.g., McKinnon 1999; Barr and Showman 2009). A convecting layer would not only tend to mix impurities or remove them through processes like dissolution (e.g., Pappalardo and Barr 2004) or melt migration (Zolotov and Kargel 2009; Kalousová et al. 2016), but may promote melting of salt-rich ices closer to the surface (e.g., Schmidt et al. 2011). Non-ice constituents of Europa's ice shell, such as salts and clathrate hydrates, could participate in the chemical storage and transport of ionic and volatile species, and affect the thermal and mechanical properties of the ice shell. The low thermal conductivity of salts and clathrate

hydrates could produce highly insulating layers near the surface, or at the top of the ocean as suggested for Pluto (Kamata et al. 2019). Salts and clathrate hydrates also have a much higher viscosity than water ice (Durham et al. 2010), thus potential layers or lenses of these non-ice constituents (Sect. 3.2) could effectively impede convection within the ice shell (Pappalardo and Barr 2004; Formisano et al. 2020). However, if these compounds are scattered within the ice, their impact on thermal and mechanical properties could be limited. For instance, low amounts (approximately 10% or less) of impurities would not make the rheology of the shell depart substantially from that of pure water ice of type I_h (hexagonal ice crystal, Durham et al. 2010). At present, the likelihood that individual layers of clathrate hydrates and salts exist within the ice shell is not well understood (Sect. 3.1). If such layers only exist locally as "lenses" from refreezing of brine pockets and conduits, their impact on bulk transport processes through the ice shell may be limited, and the I_h ice-like rheology commonly assumed in modeling efforts may remain valid. REASON sounding data will be able to constrain geometry of impurity-rich regions in the ice shell (e.g., lenses vs. layers) (Roberts et al. 2023, this collection).

The pattern of ice convection determines the composition of the ice shell–ocean system: a "stagnant lid" regime, where exchange may be limited by the cold brittle conductive layer, or a "mobile lid" regime, where the subduction of crustal material may occur and promote surface-to-ocean exchange. The stagnant lid regime is likely favored and the subduction of the buoyant crust is likely difficult to achieve (McKinnon 1998; Johnson et al. 2017; Howell and Pappalardo 2019), although the thickness of the ice shell and its constituent layers remain heavily debated (e.g., Billings and Kattenhorn 2005; Howell 2021). REASON data on possible physical (dielectric) anomalies within the ice shell (e.g., melt- and/or salt-bearing regions) would constrain the compositional structure and thickness of the shell.

6.5.2 Geologic Processes That Affect Composition of the Shell

Geologic evidence suggests at least three major resurfacing epochs over the last 10^8 years: early building of the ridges, lineae, and ridged plains; followed by the formation of the band-like structures; and finally, chaos formation (Greeley et al. 2000; Figueredo and Greeley 2004; Leonard et al. 2018, 2020; Senske et al. 2019). Many of the formation mechanisms suggested for ridged plains require a thin ($\lesssim$10 km) ice shell (Kattenhorn 2002; Leonard et al. 2020; Daubar et al. 2024, this collection), although double ridges appear to have formed throughout history (Figueredo and Greeley 2004). Presence of a thin ice shell may suggest that oceanic and surface materials were easily exchanged during this early period of ice shell history. The similarity of band-like structures with extensional mid-ocean ridges on Earth (Prockter et al. 2002) suggests formation of Europa's counterparts through incorporation of oceanic material from beneath (Howell and Pappalardo 2018) that is consistent with the low albedo and reddish color of some bands. A few described convergence (Sarid et al. 2002) and subsumption (Kattenhorn and Prockter 2014; Mével and Mercier 2005) bands may accommodate extension of the ice shell from bands along with thickening and folding of the shell and may cause transfer of surface materials to the depth (Bland and McKinnon 2013). Formation of chaos terrains may include chemically- and/or thermally-induced diapirism (Pappalardo and Barr 2004), melt-through (Carr et al. 1998; Greenberg et al. 1999, 2003), and liquid water sills or melt lenses (Schmidt et al. 2011; Michaut and Manga 2014). Each of these mechanisms implies different ice shell thicknesses that could have occurred at different times in geological history. Most of these involve liquid water, and once refrozen, will likely concentrate and leave behind traces of the water composition (Buffo et al. 2020; Chivers et al. 2021), while diapirism may leave behind fresher ice than the

surrounding shell (Pappalardo and Barr 2004). For more details on how the Europa Clipper mission will investigate the geological processes within the shell, we refer to Daubar et al. (2024, this collection).

Processes that transport material through the ice shell's interior are likely to leave fingerprints in the form of locally variable concentrations of salts, clathrates or melts (e.g., Fagents 2003; Schmidt et al. 2011; Buffo et al. 2020; Chivers et al. 2021), though surface non-ice materials will be modified by radiolysis and space weathering (Sect. 6.6). Spectra obtained by the MISE investigation will inform the composition and relative ages of features at <1 km resolution (e.g., Geissler et al. 1998; Hansen and McCord 2004; Dalton et al. 2013; Blaney et al. 20242024) (see Fig. 3). Color images obtained by the EIS investigation will constrain abundances of non-ice species at meter scales (Trumbo et al. 2019a,b; Hibbitts et al. 2019; Turtle et al. 2024, this collection). If oceanic water is chemically evolved through ice thickening, more chlorides are expected in younger endogenic features. By determining stratigraphic relationships derived from EIS images of geologic formations it may be possible to constrain the compositional evolution of the ice-ocean system. However, the link between salt assemblage at the surface and the initial salt composition in the crystallizing solutions is not trivial (e.g., Zolotov and Shock 2001) as it depends on transport processes and cooling rate (e.g., Vu et al. 2016). Any systematic relationship between salt assemblage and stratigraphy will be valuable information but should not be considered as a direct constraint on ocean composition.

Thermal emissions from current and/or recent geologic activity potentially measured by the E-THEMIS instrument in combination with MISE and EIS measurements could constrain the composition of the freshest surface material. Radar reflections obtained with REASON within the ice shell could inform about compositional stratigraphy (e.g., refrozen melts, disconformities) and about compositional variations such as a layer of salts or the presence of melt (e.g., brine pockets) (Blankenship et al. 2009). Data on specific geologic features observed by EIS, MISE, Europa-UVS, MASPEX, SUDA, and E-THEMIS would constrain formation mechanisms of these features and surface–ice–ocean exchanges. If detected with REASON, salt-water eutectic interfaces could inform about geological processes in the icy shell such as convection. Attenuation of the radar signal could constrain both temperature and the concentration of impurities (Moore 2000; Pettinelli et al. 2015) as well as porosities and voids (Heggy et al. 2017).

6.6 Surface Processes

Much of the compositional information about the geological processes on Europa will be inferred from observations of the surface and atmosphere, which are physically and chemically affected by heavy irradiation, impacts, mass wasting, and thermal processing. These types of processes, though they may be constrained to the uppermost layer of Europa's surface (Sect. 2.4), have strong effects the surface composition and complicate interpretations of the remote sensing data. It is therefore important for Europa Clipper investigations to constrain the extent of these processes and to acknowledge that measurements of Europa's surface and atmospheric compositions must be interpreted within the context of the following processes.

Some of these processes, and the depths to which they change the surface material, are shown in Fig. 18. For comparison, the maximum observable penetration depth as a function of wavelength is also shown, indicating how different investigations on Europa Clipper will be sensitive to, and constrain, different surface processes. Here, the penetration depth describes the decay of the intensity or power of the electromagnetic waves inside a material, which decays to 1/e of its surface value. For the visible range, it means that about 63% of

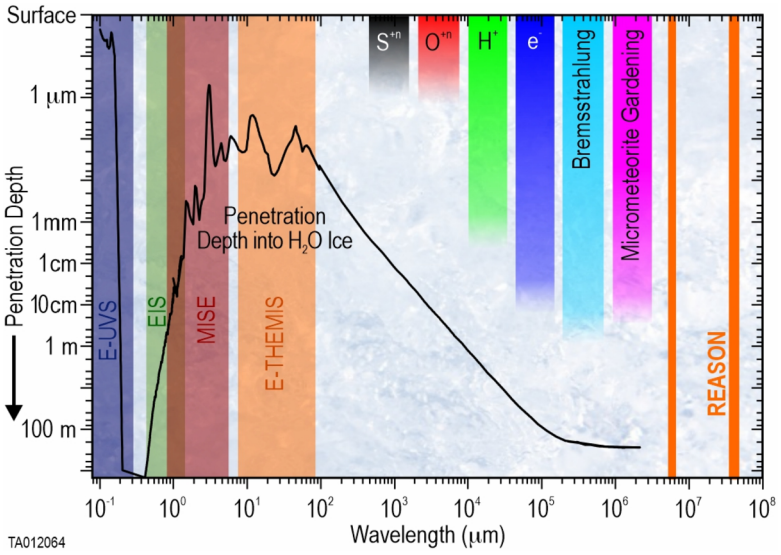

Fig. 18 The maximum penetration depth into bulk H_2O ice of remote sensing observations as a function of wavelength. This curve was created based on the imaginary optical constants from Warren and Brandt (2008) at 1/e attenuation, assuming the ice is a perfect glass, not granular, with no internal scattering or surface roughness. The bandpasses of the Europa Clipper investigations are indicated by the transparent vertical bars and labeled. The vertical bars that begin at the top of the figure indicate the depths at which different surface processes can affect the surface material and composition. The radiation processing depths are approximated to the maximum stopping ranges of S^+, O^+, H^+ (NIST PSTAR online program), e^- (NIST ESTAR online program), and Bremsstrahlung (NIST X-ray attenuation factors). Micrometeoroid gardening data are from Costello et al. (2021)

light is absorbed or scattered. We note that the calculation shows the maximum depth because it assumes the ice is a perfect glass with no internal scattering or surface roughness. Therefore, properties like grain size, which affect penetration depth as is shown in (Fig. 7), are not considered here.

6.6.1 Radiation-Induced Processes

Energetic charged particles trapped in Jupiter's magnetosphere continually irradiate Europa's surface, altering its physical state and chemical composition through radiolysis while also ejecting surface material into the exosphere. The flux of energetic particles onto Europa will be constrained using data acquired by the RadMon and other opportunistic radiation data from science instruments (Meitzler et al. 2023, this collection). The RadMon is an engineering instrument that will also provide a coarse energetic particle spectrum, which can be used to assess Europa's radiation environment and surface weathering by charged particles greater than ∼1 MeV. Charged particles at lower energy (less than ∼6 keV) will be measured by the PIMS instrument, while Europa-UVS is sensitive to penetrating electrons in the ∼10 MeV range. While the investigations will not directly measure the full energy spectrum of these particles, the data will 'bracket' the energetic bombardment that the Europa Clipper spacecraft will experience. Observations by the MISE, EIS, and Europa-UVS instruments will synergistically map Europa's surface albedo, maturity, and ice crystalline fraction, which are affected by the impinging plasma (Sect. 2).

Much of the ice on Europa appears crystalline in the interior of grains while the uppermost layer appears amorphous due to continuous exposure to radiation that destroys its crystal structure (e.g., Leto and Baratta 2003; Hansen and McCord 2004; Ligier et al. 2016). This is likely the result of competing radiation-driven amorphization and temperature-driven crystallization processes. Potential detections of areas with crystalline ice on the grains' very top surface in MISE data could be indicative of a recent deposit of water ice from the subsurface and/or plumes, which can potentially be confirmed with other MISE and/or Europa-UVS observations, and/or an anomalously warm surface, the existence of which may be confirmed with E-THEMIS data. In addition, REASON reflectometry data could reveal fresh (low density) icy plume deposits (Blankenship et al. 2024, this collection). At surface temperatures higher than ∼130 K, any amorphous ice will irreversibly transition to crystalline ice (likely cubic or possibly hexagonal) within hours (Mastrapa et al. 2008), while at temperatures below 110 K this conversion could take years or longer. It should be noted that there are still inconsistencies between the spectral observations of Europa's surface and models incorporating radiation-induced amorphization measurements in the laboratory (Berdis et al. 2020). This indicates the need for continued laboratory irradiation studies at the appropriate temperatures and with the appropriate array of candidate surface materials and mixtures on the surface of Europa.

Radiation processes can also contribute to thermal sintering of near-surface ice and/or hydrate. For a porous Europa surface composed primarily of water ice, thermal sintering rates and surface consolidation may operate over timescales ranging from decades to hundreds of millions of years (Clark et al. 1983; Molaro et al. 2019; Choukroun et al. 2020). On Saturn's moon Mimas, the near-surface water ice appears to have been partially sintered by induction heating by electrons from the Saturnian co-rotating magnetic field (e.g., Schaible et al. 2017). Near the surface of Europa, it is possible that ice and even the hydrated materials could be sintered by Jupiter's much stronger magnetic field and/or by 'hot spots' above diapirs bringing warm ice close to Europa's surface. Derivation of thermal inertia from E-THEMIS data could provide insight into this process, and REASON reflectometry data will provide information on porosity of the near-surface layer (Sect. 2.1.1) and inform the investigation of sintering processes across the surface.

Continuous bombardment of the ice and non-ice surface materials could also result in surface-bound radiolytic products in their electronic and vibrational excited states. As a result, luminescence from these excited atoms, molecules, and ions is expected across a wide portion of the electromagnetic spectrum, which could constrain compositional information of the surface (Nulsen et al. 2020; Gudipati et al. 2021). Spectral color centers, which are optically active crystal defects in halide salts such as NaCl, can form through irradiation by high energy electrons and ions but can subsequently relax through thermally induced defect center migration (e.g., Poston et al. 2017). NaCl has been tentatively identified on Europa's surface through the presence of a shallow absorption feature near 460 nm and 230 nm (Trumbo et al. 2019a, 2019b, 2022; Brown et al. 2022; Denman et al. 2022; Sect. 2). The shallowness of the band, yet absence of a 720-nm feature, could be indicative of thermal relaxation, or healing of the crystal defects responsible for the color centers. EIS observations that capture these bands could therefore constrain both surface composition and radiation effects on surface compounds.

Energetic ions release radiolytic species from the surface into the exosphere through sputtering. Investigations of atmospheric gases by MASPEX and Europa-UVS will constrain the abundance and distribution of radiolytic volatiles (e.g., H_2O_2, H_2, O_2, CO_2; see Sect. 4) and identify salts, acid hydrates, and trace organic compounds that result from radiolytic processing and sputtering, if they are present. Organic matter in the atmosphere can be studied

to reveal chemical modifications that indicate a history of irradiation (e.g., Court et al. 2006). Abundance and vertical structure of the exospheric species and their spatiotemporal variations (especially on the night side hemisphere), coupled to the plasma environment, may constrain source processes and rates, including sputtering. These investigations are critical to decoding the compositional relationship between Europa's exosphere and surface and how their compositions are altered via radiolytic processing. Interpretation of these measurements made by the Europa Clipper instrument suite will depend on continued laboratory experiments and computational modeling efforts that provide a foundational understanding of the role of radiation-induced processes on the chemical and physical changes of candidate materials on Europa's surface.

6.6.2 Impact Gardening, Thermal Processing, and Mass Wasting

In addition to bombardment by charged particles, bombardment by micrometeoroids and larger impactors serves to mix the material at Europa's surface. This process, referred to as "impact gardening," buries irradiated surface material and exposes fresher subsurface material to depths ranging from centimeters to meters (Chyba and Phillips 2001; Cooper et al. 2001; Phillips and Chyba 2001; Costello et al. 2020, 2021). Impact gardening affects the composition, grain size, crystallinity, and porosity in the upper surface layers, all of which will be assessed by the Europa Clipper investigations (Sect. 2.1). SUDA measurements of the abundance, trajectory and composition of exogenic grain particles in the Jovian system (e.g., grains from Io's volcanoes) will constrain physical and chemical effects of those grains on the garnering. Evaluations of impact gardening rates, sputtering rates, and diffusion rates through the ice, in conjunction with geological resurfacing rates, are needed to estimate delivery rates of radiolytic compounds (e.g., O_2, H_2O_2, H_2SO_4) to the deeper subsurface and in the ocean (Chyba and Phillips 2002; Hand et al. 2007; Greenberg 2010). Compositional data from MISE and Europa-UVS in combination with high-resolution ELS images will be used to constrain gardening of surface materials.

Europa's surface of ice and hydrated non-ice material is susceptible to thermal processing. At the maximum surface temperature observed at Europa of ∼132 K (Spencer et al. 1999), water ice will sublime at a rate of greater than 1 km/Ga (Vasavada et al. 1999) with the molecules potentially traveling global distances to contribute to the ice at the poles or more local cold traps. This rate is likely a lower limit for Europa because irradiation and micrometeoroid bombardment should enhance the sublimation. Sublimation of water ice from Europa's surface results in the concentration and eventually mass movement of the residual non-ice material, or lag. Lag deposits have been identified at the bases of fresh linea and in older regions, where they accumulate over time (e.g., Greeley et al. 2004) and protect the underlying terrain from weathering processes. Volatile segregation and migration should produce distinct deposits. The refractory lags created by volatile sublimation might provide strong spectral signatures of the non-ice components of features of interest. Non-volatile lag deposits can be observed through remote spectroscopy conducted by the MISE and Europa-UVS instruments, imaged by the EIS cameras, and sampled above the surface after sputtering by both the SUDA and MASPEX instruments. The exposure of hydrated salts of oceanic origin at the surface could lead to their dehydration and formation of lag deposits with a hydration profile that increases with depth (Zolotov and Shock 2001). This prediction will be tested with high spatial and spectral resolution data from MISE observations and complemented by EIS imaging. The condensation of sublimed and sputtered water molecules in polar regions creates surface frost deposits. The smallest ice patch due to cold trapping of sputtered or sublimed ice may be tens of centimeters wide (e.g., Spencer 1987). Sufficiently

cold polar frost deposits may even trap more volatile species than H_2O (e.g., CO_2, light hydrocarbons), and could be targeted for observations by MISE and Europa-UVS to identify some of these frosts (Sect. 2).

Mass wasting on Europa will likely fall into two categories: classic down slope movement of loose material, and volatile (e.g., H_2O, CO_2) segregation and migration, whereby the latter could initiate the former. Geologically recent large down slope movements may exhibit fresh exposures of compositionally distinct materials (Sect. 2.3.2). However, such materials may be difficult to observe because the scarp or cliff from which they are exposed may also block that material from view of the spacecraft due to the observational geometry.

6.7 Photochemical and Radiation Processing in the Atmosphere/Exosphere

The science investigations of the Europa Clipper mission will provide important insight into the composition of Europa's exosphere (Sect. 4). Processes in this region are dominated by interactions with photons, electrons, and ions, which are currently not well characterized, particularly with respect to their relative abundances. This complex and dynamic region encompasses the transition between Europa and Jupiter's magnetosphere. Compositional measurements of Europa's atmosphere and local space environment will provide key insight into local interaction processes, particle escape, and magnetospheric interaction, which in turn facilitates the ability to distinguish between endogenic and exogenic material. Close flybys over large endogenic geological structures (e.g., chaotic terrains) will inform the contribution of endogenic materials in data obtained with MASPEX and UVS for atmospheric gases. These compositional observations will help resolve relative particle interaction rates, the significance of each process, and ultimately how the exosphere is populated.

Multiple exospheric particle interaction processes increase the probability of escape and thus interaction with the magnetospheric environment. In particular, the interaction with solar UV photons and ionospheric and magnetospheric electrons ionizes and/or dissociates Europa's endogenic particles (Smyth and Marconi 2006). Previously observed neutral particles (H, O; Hansen et al. 2005) and minor species, such as Na (Brown and Hall 1996) and K (Brown 2001), tend to have larger energies and attain higher altitudes, thus increasing the possibility of escape. Detection of additional particle species would identify currently unknown interactions and source processes. Additionally, neutral particles can interact with surrounding ions through charge-exchange processes, which neutralize the ion and charge the neutral particle (Schreier et al. 1993). The neutralized ions can thereby have a higher velocity than neutral source particles. MASPEX data on neutral species will inform about particle interactions and will enable the differentiation of particles originating from Europa from those with external sources. Europa-UVS observations of auroral variations and of stellar occultations and Jupiter transits that vary in time, longitude, latitude, and altitude are essential to interpret Europa's dynamic exosphere and space environment. Compositional data obtained using the PIMS instrument could provide an understanding of the ambient plasma environment, which constrains the charge-exchange and ionization processes, while the REASON measurements will constrain the ionospheric electron density in the vertical column between the spacecraft and Europa's surface. Additionally, grain composition data obtained by the SUDA investigation could possibly identify minor species more difficult to identify from data collected by the other investigations.

The photochemical and radiation processes described in the previous sections increase the number of atoms and molecules escaping from Europa's tenuous atmosphere. Compositional data collected by MASPEX, Europa-UVS, and PIMS will be used together with spatial, directional, and energy information to quantify escaping particles, while the SUDA investigation will capture ice/dust grains that achieve escape velocity.

Escaping particles together with magnetic fields will constrain the interaction of Europa with the Jovian magnetosphere. Such interactions affect the local exospheric, atmospheric, surface, and subsurface environments, and they must be understood to make inferences on the subsurface ocean and, ultimately, Europa's habitability. Measurements by MASPEX, Europa-UVS, PIMS, and SUDA may also help to distinguish the flux of exogenic material and particles entering the atmosphere from other sources, including from Io's volcanoes.

6.8 Volatile Transport Within the Atmosphere and Cold Traps

As with Mercury (e.g., Ingersoll et al. 1992; Paige et al. 2013), the Earth's Moon (e.g., Watson et al. 1961; Hurley et al. 2012), and Ceres (e.g., Platz et al. 2016), the small obliquity of Europa leads to the possibility of long-term cold traps near its north and south poles in permanently shadowed regions (PSRs). Volatiles from localized endogenic (e.g., irradiated, low-latitude regolith, outgassing, and possible plumes) and exogenic (e.g., comet and asteroid impacts, dust accretion) sources can migrate to PSRs through ballistic transport, a process referred to as thermal hopping. A recent model (Ashkenazy 2019) suggests polar surface temperatures on Europa of 46 K compared with equatorial temperatures between ~86 K and 130 K. At temperatures this low, CO, CO_2, SO_2, NH_3, HCN, CH_2O, CH_3OH, Kr, Xe, and some low order hydrocarbons could migrate across the surface and would be long-lived at Europa's pole (e.g., Zhang and Paige 2009). Cassini's Ion and Neutral Mass Spectrometer data provided evidence of seasonal trapping of CO_2 at Rhea's poles (Teolis and Waite 2016) at similar temperatures that were verified by the Cassini Visible and Infrared Mapping Spectrometer (VIMS) investigation (Howett et al. 2010) and modeled by Miles et al. (2020). Migration and trapping have been modeled for the case of Europa's plumes (Teolis et al. 2017).

Both the MASPEX and Europa-UVS investigations will be used to track volatiles in Europa's atmosphere, which may also be detected on the surface with the remote sensing investigations (Sect. 2). The MASPEX investigation has the capability to detect noble gases *in situ*, including their isotopes. In addition, the Europa-UVS investigation is capable of detecting He through its EUV resonance line at 58.4 nm, as has been demonstrated at the Moon using LRO-LAMP (e.g., Grava et al. 2021). Transport of these gases will be inferred from either time-dependent behavior (i.e., if a sudden change in abundance is observed) or by spatial abundance gradients, along with modeling using E-THEMIS surface temperature measurements. The MISE and Europa-UVS spectral investigations will be used to determine the presence of surface volatiles by their spectral signatures in the cold trap or PSR regions. In addition, it is likely that the sublimation and condensation volatiles could affect the microstructure of the surface, e.g., the porosity, in a detectable way, as has been observed with the lunar PSRs (Gladstone et al. 2012; Sect. 2).

Vapor pressure differences spanning many orders of magnitude are to be expected across Europa, owing to surface temperatures ranging from ~46 K at the poles, to between ~86 and ~132 K at the equator for the nightside and dayside, respectively (Ashkenazy 2019; Spencer et al. 1999). Massive icy planetary bodies like Europa have sufficient gravity to retain thermally accommodated molecules in the exosphere, and most volatiles heavier than H_2 have scale heights no more than a few tens of kilometers, impacting and interacting with the surface many times before escaping into space (Shematovich et al. 2005). Europa's exosphere may contain a number of as yet undetected sputtered and possibly plume-supplied species, such as CO_2 and NH_3 (Teolis et al. 2017), which are semi-volatile over Europa's surface temperature range. These minor species, and to an extent, even H_2O, may sublimate on Europa's dayside surface and refreeze on the nightside (Teolis et al. 2017). This same

physics determines the distribution of the lunar argon exosphere (Grava et al. 2015) and the CO_2 exospheres of the icy moons Dione and Rhea (Teolis and Waite 2016), which also have gas densities far greater over the dayside hemisphere because of dayside sublimation process. We may therefore anticipate that some semi-volatile species in Europa's exosphere would likewise exhibit a highly nonuniform distribution centered on the dayside, or a diurnally 'pulsating' exosphere.

Temporal changes of Europa's entire exosphere may be driven by localized gas sources, such as localized outgassing or possibly high-speed plume sources, or 'Macula' type terrains from which a unique suite of volatiles are sputtered. Any time-variable plumes (Paganini et al. 2020; Roth et al. 2016; Sparks et al. 2016, 2017) would add another source for variations in global exospheric dynamics.

Measurements by the Europa-UVS and MASPEX investigations will be used to verify the density of H_2O and other species relative to the amount of radiolytic O_2. In a sputtered exosphere, the amounts of H_2O and O_2 are expected to remain fixed relative to one another as they are both ejected in relatively consistent proportions from the surface ice. Based on modeling and analysis of laboratory data on ice, Teolis et al. (2017) suggest that an H_2O/O_2 ratio greater than $\sim$15 would indicate a source of H_2O other than sputtering, which might suggest a nearby plume. If such a plume is detected, measurements from early flybys could be used as inputs into exospheric models to predict the evolution of the atmospheric species and establish if observations later in the tour are consistent with (1) a changing or constant exosphere, and (2) the presence or absence of a localized gas source. With the species column densities measured along the spacecraft track to provide rough constraints on exospheric composition, exospheric models will be iterated to fine-tune both the composition of material supplying the exosphere and the surface residence time of each species, which may depend on surface composition and regolith structure. Observations over the course of the mission enable the assessment of the atmosphere as a function of Europa's local time, and whether localized sources produce diurnal variability in the exosphere. Measurements of the spatial distribution and temporal responses of many different species with drastically different volatilities will help considerably to constrain exospheric models.

7 Conclusions and Broader Relevance

The Europa Clipper mission will assess the habitability of the enigmatic, icy moon of Jupiter through detailed studies of Europa's composition, geology, and interior. The unique and complementary suite of *in situ* and remote sensing investigations facilitate a powerful and robust set of observations to achieve the mission's primary goal.

The compositional investigations focus on identifying the composition and sources of key non-ice constituents on Europa's surface and in its atmosphere and local space environment. High spatial-resolution maps covering the majority of Europa's surface will be constructed from the Europa Clipper's remote-sensing suite and complemented by *in situ* measurements. The distribution of surface materials and correlation with local geological landforms will provide key insights into sources and ongoing processes on Europa's surface and interior, including radiation effects, space weathering, geological processes, and thermo-chemical evolution. Through the characterization of the composition and sources of volatiles, particulates, and plasma in Europa's atmosphere and local space environment, the Europa Clipper mission will determine the structure of Europa's atmosphere, constrain the relationship between the subsurface, surface, atmosphere, and local environment, and provide information about photochemical and radiation processing of materials on Europa's

surface and in its atmosphere. The possible presence of plumes, which may be directly observed or indirectly detected by their effects on the atmosphere or fallout on the surface, will enable a unique compositional study of material recently expelled from within Europa, possibly sourced from its underlying ocean. These compositional measurements of the moon's environment, atmosphere, surface, subsurface, and activity enable key analyses for assessing the habitability of Europa.

7.1 Connection with Habitability

Compositional measurements by the Europa Clipper investigations will be used to assess the habitability of Europa's interior (Vance et al. 2023; Pappalardo et al. 2024, both this collection). Data from the Europa-UVS, MASPEX, and SUDA instruments, with contributions from PIMS and REASON, on non-ice species in the atmosphere and local environment, together with spectral, geological, and thermal measurements of surface materials from MISE, EIS, Europa-UVS, and E-THEMIS, will be used to distinguish endogenic compounds, yielding implications about habitability at depth. The composition of salts in endogenic surface features and possible plume deposits as observed by the MISE, Europa-UVS, SUDA, and REASON investigations will be used to assess inorganic speciation and the pH of oceanic water, composition, and salinity of brine pockets in the icy shell, and evaluate mineralogy of suboceanic rocks and/or sediments.

The ratios between sulfate/chloride/carbonate and Ca/Mg/Na/K in salts will provide insight about the oxidation state, geologic history of oceanic water, and habitability of Europa through time. Relative abundances of oxidized and reduced species in plume and fresh surface materials (e.g., sulfate/sulfide, sulfate/organic matter, SO_2/H_2S, CO_2/CH_4, N_2/NH_3, H_2O/H_2) will be used to assess redox conditions, redox disequilibria, and chemical sources of energy that could support metabolism in the shell, in oceanic water, and at the ocean–rock interface. MASPEX, Europa-UVS, and SUDA data on organic compounds, which may be found in potential plume emissions, would constrain the organic composition in the ocean and the ice shell, together with possible origins and transformation pathways of organic matter. REASON measurements that are sensitive to the electromagnetic properties and structure of the ice shell will highlight the presence of any brine pockets and major impurities that could affect the moon's habitability. The abundances of radiolytic compounds observed in surface and local atmospheric materials by MISE, EIS, Europa-UVS, SUDA, and MASPEX and their association with geological features or hotspots observed by E-THEMIS will help assess whether the delivery of strong oxidants and acids to habitable niches in the ice shell, and even to oceanic water upon a major ice melting event, could have been a major process at Europa.

7.2 Supportive Laboratory, Telescopic, and Mission Science

Previous missions and telescopic observations of Europa not only provide the foundational knowledge for the planned investigations at the satellite, but also contribute independent results at different wavelengths and capture changes over time that can bolster findings from the data returned by the Europa Clipper mission. The observations made during close flybys by NASA's Juno mission, with its own unique suite of instrumentation, add new, high quality data of Europa and the Jupiter system, including the intensity and variability of the radiation environment anticipated for the Europa Clipper mission (e.g., Kollman et al. 2022).

The JUICE mission, led by the European Space Agency, launched in April 2023 and will arrive at Jupiter in 2031. Its anticipated simultaneous presence with Europa Clipper

in orbit around Jupiter presents unparalleled opportunities for concurrent observations of the system from two separate vantage points. The JUICE and Europa Clipper spacecraft carry complementary instrumentation, and the ultraviolet spectrographs on these missions are nearly identical (Retherford et al. 2024, this collection). The data that JUICE will collect during multiple flybys of Europa and Callisto, and following a year-long orbit of Ganymede (Grasset et al. 2013), should provide new, independent insights into the primordial material and evolution of all of the Galilean satellites. Further, the inherent differences between the icy satellites will help us to better understand and characterize the uniqueness of Europa.

Exploration and monitoring from Earth-based facilities and space telescopes (e.g., HST, JWST) continue to produce exciting possibilities for the interpretation of Europa's composition and habitability, which may pose new questions for the Europa Clipper mission to explore and provide the necessary, complementary data to address those puzzles. The detailed information gained about Europa's composition, interior, and geology through Europa Clipper data will provide critical constraints for any future missions to Europa, especially a possible lander (Grima et al. 2014b; Hand et al. 2022; Phillips et al. 2023).

New and ongoing laboratory studies will continue to support the interpretation of the Europa Clipper to enhance its scientific return well into the future. Current efforts to identify species and constrain grain properties under Europa-relevant temperatures will be important for deciphering the observed non-ice material on Europa (e.g., Dalton et al. 2007, 2012b, 2012a; Clark et al. 2013) and potentially the material spewed from within subsurface water in the form of plumes. Cryogenic fallouts or other geologically recent emplacement of surface material may appear to have different spectral properties in the ultraviolet to the infrared, offering a new approach for potentially detecting and dating recent geological activity with Europa-UVS, EIS, and MISE, and should continue to be studied in the lab (e.g., Raut and Baragiola 2013). Laboratory studies that simulate the processing of surface material by space weathering and Jupiter's radiation environment have important implications for interpretation of compositional measurements of the moon's surface and atmosphere (e.g., Hibbitts et al. 2019; Brown et al. 2022). Existing and emerging sputtering measurements and models for condensed ices (Famá et al. 2008; Raut and Baragiola 2013; Teolis et al. 2017; Meier and Loefller 2020) and for non-ice constituents (e.g., hydrated salts and acids) will improve constraints on the abundance of exospheric species (Cipriani et al. 2009). These studies can be fine-tuned after direct measurements are made by the Europa Clipper instruments, and will be used to quantify the effects of the competing processes, such as crystallization vs. radiation-induced amorphization, unfolding on Europa's surface.

7.3 Implications for Composition and Composition-Related Processes on Other Moons, Planetary Bodies and Beyond

The data to be returned by Europa Clipper will likely shed light on composition and processes on other solar system and exoplanetary bodies. Compositional constraints on Europa's formation (Sect. 6.2) have implications for the origin of the other Galilean satellites. Insights into the composition and geological histories of ocean worlds may be applicable to water-bearing objects in the main asteroid belt, such as Ceres and Pallas, D and P type asteroids, Jovian Trojans, Triton, and other ocean worlds throughout our Solar System and beyond. A detection of elevated carbon contents and ammoniated species together with some isotopic enrichments (e.g., ^{18}O, ^{15}N) through Europa Clipper investigations would indicate migration of outer Solar System materials to the Jovian system and place constraints on the large-scale dynamical evolution of the early solar system.

The composition of endogenic salts, mainly the sulfate, chloride, and carbonate content found at Europa, will provide insights into the composition and oxidation state of deep-water oceans on Ganymede and Callisto. Inferred composition of Ionian grains, ions and molecules near Europa and in surface materials will reveal new insights about Io's volcanism and its contribution to surface and atmospheric materials on Ganymede and Callisto. Likewise, data on other exogenic constituents, such as inorganic/organic species in chondritic and cometary dust, will have implications for exogenic accumulation on Galilean satellites. The Europa Clipper data on speciation of radiolytic products in surface and atmospheric materials will be indicative of radiolysis on other icy bodies in the current and early solar system, and in the universe. If plumes are found at Europa, their sampling will serve as direct insight into their source in the ice shell, ocean, or volatile rich (e.g., liquid) bodies within the crust. Comparisons with Enceladus's plumes will further constrain the differences between the Jovian and Saturnian systems. The rich, synergistic compositional dataset promised by the Europa Clipper mission will not only illuminate this icy world's formation, evolution, and habitability; its in-depth investigation will provide context for the numerous ocean worlds that exist within our Solar System and beyond.

Acknowledgements This work was supported by NASA through the Europa Clipper Project. FP acknowledges the support by a European Research Council (ERC) Consolidator Grant 724908-Habitat OASIS.

Declarations

Competing Interests This work was financially supported by NASA through the Europa Clipper project. Partial support was provided to FP by a Europa Research Council (ERC) Consolidator Grant 724908-Habitat OASIS.

Open Access This article is licensed under a Creative Commons Attribution 4.0 International License, which permits use, sharing, adaptation, distribution and reproduction in any medium or format, as long as you give appropriate credit to the original author(s) and the source, provide a link to the Creative Commons licence, and indicate if changes were made. The images or other third party material in this article are included in the article's Creative Commons licence, unless indicated otherwise in a credit line to the material. If material is not included in the article's Creative Commons licence and your intended use is not permitted by statutory regulation or exceeds the permitted use, you will need to obtain permission directly from the copyright holder. To view a copy of this licence, visit http://creativecommons.org/licenses/by/4.0/.

References

Aglyamov Y, Schroeder DM, Vance SD (2017) Bright prospects for radar detection of Europa's ocean. Icarus 281:334–337. https://doi.org/10.1016/j.icarus.2016.08.014

Alexander CMO, Cody GD, De Gregorio BT, Nittler LR, Stroud RM (2017) The nature, origin and modification of insoluble organic matter in chondrites, the major source of Earth's C and N. Chem Erde, Geochem 77:227–256. https://doi.org/10.1016/j.chemer.2017.01.007

Anderson JD, Schubert G, Jacobson RA, Lau EL, Moore WB, Sjogren WL (1998) Europa's differentiated initial structure: inferences from four Galileo encounters. Science 281:2019–2022. https://doi.org/10.1126/science.281.5385.2019

Anderson SE, Mousis O, Ronnet T (2021) Formation conditions of Titan's and Enceladus's building blocks in Saturn's circumplanetary disk. Planet Sci J 2:50. https://doi.org/10.3847/PSJ/abe0ba

Ashkenazy Y (2019) The surface temperature of Europa. Heliyon 5(6):e01908. https://doi.org/10.1016/j.heliyon.2019.e01908

Bagenal F, Dols V (2020) The space environment of Io and Europa. J Geophys Res Space Phys 125:e2019JA027485. https://doi.org/10.1029/2019JA027485

Barr AC, Showman AP (2009) Heat transfer in Europa's icy shell. In: Pappalardo RT, McKinnon WB, Khurana KK (eds) Europa. University of Arizona Press, Tucson, pp 405–430

Becker TM, Retherford KD, Roth L, Hendrix AR, McGrath MA, Saur J (2018) The Far-UV albedo of Europa from HST observations. J Geophys Res, Planets 123:1327–1342. https://doi.org/10.1029/2018JE005570

Becker TM, Trumbo SK, Molyneux PM, Retherford KD, Hendrix AR, Roth L, Raut U, Alday J, McGrath MA (2022) Mid-ultraviolet Hubble observations of Europa and the global surface distribution of SO_2. Planet Sci J 3:129. https://doi.org/10.3847/PSJ/ac69eb

Behounkova et al (2021). https://doi.org/10.1029/2020GL090077

Běhounková M, Tobie G, Choblet G, Kervazo M, Melwani Daswani M, Dumoulin C, Vance SD (2021) Tidally induced magmatic pulses on the oceanic floor of Jupiter's moon Europa. Geophys Res Lett 48:e2020GL090077. https://doi.org/10.1029/2020GL090077

Berdis JR, Gudipati MS, Murphy JR, Chanover NJ (2020) Europa's surface water ice crystallinity: discrepancy between observations and thermophysical and particle flux modeling. Icarus 341:113660. https://doi.org/10.1016/j.icarus.2020.113

Bierhaus EB, Zahnle K, Chapman CK (2009) Europa's crater distributions and surface ages. In: Pappalardo RT, McKinnon WB, Khurana KK (eds) Europa. University of Arizona Press, Tucson, p 161

Bierson CJ, Nimmo F (2020) Explaining the Galilean satellites' density gradient by hydrodynamic escape. Astrophys J Lett 897:L43. https://doi.org/10.3847/2041-8213/aba11a

Bierson CJ, Fortney JJ, Trinh KT, Kreslavsky MA (2023) Jupiter's early luminosity may have driven off Io's initial water inventory. Planet Sci J 4:122. https://doi.org/10.3847/PSJ/ace2c7

Billings and Kattenhorn (2005). https://doi.org/10.1016/j.icarus.2005.03.013

Black GJ, Campbell DB, Nicholson PD (2001) Icy Galilean satellites: modeling radar reflectivities as a coherent backscatter effect. Icarus 151:167–180. https://doi.org/10.1006/icar.2001.6616

Blackford JR (2007) Topical review: sintering and microstructure of ice: a review. J Phys D, Appl Phys 40:R355–385. https://doi.org/10.1088/0022-3727/40/21/R02

Bland MT, McKinnon WB (2013) Does folding accommodate Europa's contractional strain? The effect of surface temperature on fold formation in ice lithospheres. Geophys Res Lett 40:1–5. https://doi.org/10.1002/grl.50506

Blaney DL, Hibbitts K, Diniega S et al (2024) The Mapping Imaging Spectrometer for Europa (MISE). Space Sci Rev 220

Blankenship DD, Young DA, Moore WB, Moore JC (2009) Radar sounding of Europa's subsurface properties and processes: the view from Earth. In: Europa. University of Arizona Press, Tucson, pp 631–654

Blankenship D et al (2024) Radar for Europa Assessment and Sounding: Ocean to Near-surface (REASON). Space Sci Rev 220

Bouquet A, Glein CR, Wyrick D, Waite JH (2017) Alternative energy: production of H_2 by radiolysis of water in the rocky cores of icy bodies. Astrophys J Lett 840:L8. https://doi.org/10.1006/icar.2001.6616

Bouquet A, Mousis O, Glein CR, Danger G, Waite JH (2019) The role of clathrate formation in Europa's ocean composition. Astrophys J 885:14. https://doi.org/10.3847/1538-4357/ab40b0

Brearley AJ (2006) The action of water. In: Lauretta DS, McSween HY (eds) Meteorites and the Early Solar System II. University of Arizona Press, Tucson, pp 587–624

Brown ME (2001) Potassium in Europa's atmosphere. Icarus 151:190–195. https://doi.org/10.1006/icar.2001.6612

Brown ME, Hand KP (2013) Salts and radiation products on the surface of Europa. Astron J 145:110. https://doi.org/10.1088/0004-6256/145/4/110

Brown ME, Hill RE (1996) Discovery of an extended sodium atmosphere around Europa. Nature 380:229–231. https://doi.org/10.1038/380229a0

Brown et al (1977). https://doi.org/10.1103/PhysRevLett.40.1027

Brown WL et al (1982) Erosion and molecular formation in condensed-gas films by the electronic energyloss of fast ions. Nucl Instrum Methods, B 1:307

Brown RH, Clark RN, Buratti BJ, Cruikshank DP, Barnes JW, Mastrapa RME, Bauer J, Newman S, Momary T, Baines KH, Bellucci G, Capaccioni F, Cerroni P, Combes M, Coradini A, Drossart P, Formisano V, Jaumann R, Langevin Y, Matson DR, McCord TB, Nelson RM, Nicolson PD, Sicardy B, Sotin C (2006) Composition and physical properties of Enceladus' surface. Science 311:1425–1428. https://doi.org/10.1126/science.1121031

Brown ME, Denman WTP, Trumbo SK (2022) The mid-UV spectrum of irradiated NaCl at Europa-like conditions. Planet Sci J 3:28. https://doi.org/10.3847/PSJ/ac457f

Buffo JJ, Schmidt BE, Huber C, Walker CC (2020) Entrainment and dynamics of ocean-derived impurities within Europa's ice shell. J Geophys Res, Planets 125(10):e2020JE006394. https://doi.org/10.1029/2020JE006394

Buratti BJ, Thomas PC, Roussos E, Howett C, Seiß M, Hendrix AR, Helfenstein P, Brown RH, Clark RN, Denk T, Filacchione G, Hoffmann H, Jones GH, Khawaja N, Kollmann P, Krupp N, Lunine J, Momary TW, Paranicas C, Postberg F, Sachse M, Spahn F, Spencer J, Srama R, Albin T, Baines KH, Ciarniello

M, Economou T, Hsu H-W, Kempf S, Krimigis SM, Mitchell D, Moragas-Klostermeyer G, Nicholson PD, Porco CC, Rosenberg H, Simolka J, Soderblom LA (2019) Close Cassini flybys of Saturn's ring moons Pan, Daphnis, Atlas, Pandora, and Epimetheus. Science 364:6445. https://doi.org/10.1126/science.aat2349

Canup RM, Ward WR (2002) Formation of the Galilean satellites: conditions of accretion. Astron J 124:3404–3423. https://doi.org/10.1086/344684

Canup RM, Ward WR (2009) Origin of Europa and the Galilean satellites. In: Pappalardo RT, McKinnon WB, Khurana K (eds) Europa. University of Arizona Press, Tucson

Carlson et al (1999). https://doi.org/10.1126/science.283.5410.2062

Carlson RW, Anderson MS, Johnson RE, Smythe WD, Hendrix AR, Barth CA, Soderblom LA, Hansen GB, McCord TB, Dalton JB, Clark RN, Shirley JH, Ocampo AC, Matson DL (1999a) Hydrogen peroxide on the surface of Europa. Science 283(5410):2062–2064. https://doi.org/10.1126/science.283.5410.2062

Carlson RW, Johnson RE, Anderson MS (1999b) Sulfuric acid on Europa and the radiolytic sulfur cycle. Science 286:97–99. https://doi.org/10.1126/science.286.5437.97

Carlson R, Anderson M, Johnson R, Schulman M, Yavrouian A (2002) Sulfuric acid production on Europa: the radiolysis of sulfur in water ice. Icarus 157(2):456–463. https://doi.org/10.1006/icar.2002.6858

Carlson RW, Anderson MS, Mehlman R, Johnson RE (2005) Distribution of hydrate on Europa: further evidence for sulfuric acid hydrate. Icarus 177(2):461–471. https://doi.org/10.1016/j.icarus.2005.03.026

Carlson RW, Calvin W, Dalton JB, Hansen GB, Hudson RL, Johnson RE, McCord TB, Moore MH (2009) Europa's surface composition. In: Pappalardo RT, McKinnon WB, Khurana KK (eds) Europa, pp 283–328. https://doi.org/10.2307/j.ctt1xp3wdw.18

Carr MH, Belton MJS, Chapman CR, Davies ME, Geissler P, Greenberg R, McEwen AS, Tufts BR, Greeley R, Sullivan R, Head JW, Pappalardo RT, Klaasen KP, Johnson TV, Kaufman J, Senske D, Moore J, Neukum G, Schubert G, Burns JA, Thomas P, Veverka J (1998) Evidence for a subsurface ocean on Europa. Nature 391(6665):363–365. https://doi.org/10.1038/34857

Cassidy TA, Paranicas CP, Shirley JH, Dalton JB III, Teolis BD, Johnson RE, Kamp L, Hendrix AR (2013) Magnetospheric ion sputtering and water ice grain size at Europa. Planet Space Sci 77:64–73. https://doi.org/10.1016/j.pss.2012.07.008

Chan K, Grima C, Rutishauser A, Young DA, Culberg R, Blankenship DD (2023) Spatial characterization of near-surface structure and meltwater runoff conditions across the Devon Ice Cap from dual-frequency radar reflectivity. Cryosphere 17:1839–1852. https://doi.org/10.5194/tc-17-1839-2023

Chivers CJ, Buffo JJ, Schmidt BE (2021) Thermal and chemical evolution of small, shallow water bodies in Europa's ice shell. J Geophys Res, Planets 126:e2020JE006692. https://doi.org/10.1029/2020JE006692

Choukroun M, Kieffer SW, Lu X, Tobie G (2013) Clathrate hydrates: implications for exchange processes in the outer solar system. In: The science of solar system ices, pp 409–454

Choukroun M, Molaro JL, Hodyss R, Marteau E, Backes P, Carey EM et al (2020) Strength evolution of ice plume deposit analogs of Enceladus and Europa. Geophys Res Lett 47(15):e2020GL088953. https://doi.org/10.1029/2020gl088953

Christensen PR, Spencer JR, Mehall GL et al (2024) The Europa Thermal Emission Imaging System (E-THEMIS) Investigation for the Europa Clipper Mission. Space Sci Rev 220

Chyba CF, Phillips CB (2001) Possible ecosystems and the search for life on Europa. Proc Natl Acad Sci 98:801–804. https://doi.org/10.1073/pnas.98.3.801

Chyba CF, Phillips CB (2002) Europa as an abode of life. Orig Life Evol Biosph 32(1):47–67. https://doi.org/10.1023/A:1013958519734

Chyba et al (2021). https://doi.org/10.1016/j.icarus.2021.114360

Cipriani F, Leblanc F, Witasse O, Johnson RE (2009) Exopsheric signatures of alkali abundances in Europa's regolith. Geophys Res Lett 36(12):L122202. https://doi.org/10.1029/2009GL038636

Clark RN (1981) Water frost and ice: the near-infrared spectral reflectance of 0.625–2.5 microns. J Geophys Res 86(B4):3087–3096. https://doi.org/10.1029/JB086iB04p03087

Clark RN (1999) Rencz AN (ed) Spectroscopy of rocks and minerals, and principles of spectroscopy. In: Manual of remote sensing, Volume 3, Remote sensing for the Earth sciences. Wiley, New York, pp 3–58. Chapter 1

Clark RN, McCord TB (1980) The Galilean satellites: new near-infrared spectral reflectance measurements (0.65–2.5 μm) and a 0.325–5 μm summary. Icarus 41:323–329. https://doi.org/10.1016/0019-1035(80)90217-1

Clark and Roush (1984). https://doi.org/10.1029/JB089iB07p06329

Clark et al (1980). https://doi.org/10.1016/0019-1035(80)90033-0

Clark RN, Fanale FP, Zent AP (1983) Frost grain size metamorphism: implications for remote sensing of planetary surfaces. Icarus 56:233–245. https://doi.org/10.1016/0019-1035(83)90036-2

Clark RN, Curchin JM, Hoefen TM, Swayze GA (2009) Reflectance spectroscopy of organic compounds I: alkanes. J Geophys Res 114:E03001. https://doi.org/10.1029/2008JE003150

Clark RN, Cruikshank DP, Jaumann R, Brown RH, Stephan K, Dalle Ore CM, Livo KE, Pearson N, Curchin JM, Hoefen TM, Buratti BJ, Filacchione G, Baines KH, Nicholson PD (2012) The composition of Iapetus: mapping results from Cassini VIMS. Icarus 218:831–860. https://doi.org/10.1016/j.icarus.2012.01.008

Clark RN, Carlson R, Grundy W, Noll K (2013) Observed ices in the solar system. In: Gudipati MS, Castillo-Rogez J (eds) The science of solar system ices. Springer, Berlin, pp 3–46

Clark RN, Swayze GA, Carlson R, Grundy W, Noll K (2014) Spectroscopy from space. In: Henderson G (ed) Spectroscopic methods in mineralogy and material sciences, reviews in mineralogy & geochemistry, vol 78. Mineralogical Society of America, Chantilly, pp 399–446, Chap. 10

Clark RN, Brown RH, Cruikshank DP, Swayze GA (2019) Isotopic ratios of Saturn's rings and satellites: implications for the origin of water and Phoebe. Icarus 321:791–802. https://doi.org/10.1016/j.icarus.2018.11.029

Clay PL, Burgess R, Busemann H, Ruzié-Hamilton L, Bastian J, Day JMD, Ballentine CJ (2017) Halogens in chondritic meteorites and terrestrial accretion. Nature 551:614–618. https://doi.org/10.1038/nature24625

Cooper JF, Johnson RE, Mauk BH, Garrett HB, Gehrels N (2001) Energetic ion and electron irradiation of the icy Galilean satellites. Icarus 149(1):133–159. https://doi.org/10.1006/icar.2000.6498

Coradini A, Cerroni P, Magni G, Federico C (1989) Formation of the satellites of the outer solar system: sources of their atmospheres. In: Origin and evolution of planetary and satellite atmospheres. University of Arizona Press, Tucson, pp 723–762

Costello ES, Ghent RR, Hirabayashi M, Lucey PG (2020) Impact gardening as a constraint on the age, source, and evolution of ice on Mercury and the Moon. J Geophys Res, Planets 125(3):e2019JE006172. https://doi.org/10.1029/2019JE006172

Costello ES, Phillips CB, Lucey PG, Ghent RR (2021) Impact gardening on Europa and repercussions for possible biosignatures. Nat Astron 5(9):951–956. https://doi.org/10.1038/s41550-021-01393-1

Court RW, Sephton MA, Parnell J, Gilmour I (2006) The alteration of organic matter in response to ionising irradiation: chemical trends and implications for extraterrestrial sample analysis. Geochim Cosmochim Acta 70:1020–1039. https://doi.org/10.1016/j.gca.2005.10.017

Cruikshank DP, Moroz L, Clark RN (2020) Visible and infrared spectroscopy of ices, volatiles and organics. In: Bishop JL, Bell JF III, Moersch JE (eds) Remote compositional analysis: techniques for understanding spectroscopy, mineralogy, and geochemistry of planetary surfaces. Cambridge University Press, Cambridge, pp 102–119, Chap. 5

Cuffey KM, Paterson WSB (2010) The physics of glaciers, 4th edn. Academic Press, Amsterdam, 704 pp.

Culha C, Schroeder DM, Jordan TM, Haynes MS (2020) Assessing the detectability of Europa's eutectic zone using radar sounding. Icarus 339:113578. https://doi.org/10.1016/j.icarus.2019.113578

Dalton JB III, Pitman KM (2012a) Low temperature optical constants of some hydrated sulfates relevant to planetary surfaces. J Geophys Res 117:E09001. https://doi.org/10.1029/2011JE004036

Dalton JB III, Shirley J, Kamp L (2012b) Europa's icy bright plains and dark linea: exogenic and endogenic contributions to composition and surface properties. J Geophys Res, Planets 117:E03003. https://doi.org/10.1029/2011JE003909

Dalton JB (2003) Spectral behavior of hydrated sulfate salts: implications for Europa mission spectrometer design. Astrobiology 3:771–784. https://doi.org/10.1089/153110703322736097

Dalton JB (2007) Linear mixture modeling of Europa's non-ice material based on cryogenic laboratory spectroscopy. Geophys Res Lett 34:L21205. https://doi.org/10.1029/2007GL031497

Dalton JB, Prieto-Ballesteros O, Kargel JS, Jamieson CS, Jolivet J, Quinn R (2005) Spectral comparison of heavily hydrated salts with disrupted terrains on Europa. Icarus 177:472–490. https://doi.org/10.1016/j.icarus.2005.02.023

Dalton JB, Cassidy T, Paranicas C, Shirley JH, Prockter LM, Kamp LW (2013) Exogenic controls on sulfuric acid hydrate production at the surface of Europa. Planet Space Sci 77:45–63. https://doi.org/10.1016/j.pss.2012.05.013

Dannenmann M, Klenner F, Pavlista M, Boenigk J, Napoleoni M, Khawaja N, Hillier J, Khawaja N, Olsson-Francis K, Cable M, Malaska M, Abel B, Postberg F (2023) Toward detecting biosignatures of DNA, lipids and metabolic intermediates from bacteria in ice grains emitted by Enceladus and Europa. Astrobiology 23(1):60–75. https://doi.org/10.1089/ast.2022.0063

Daubar IJ, Hayes AG, Collins GC et al (2024) Planned geological investigations of the Europa Clipper Mission. Space Sci Rev 220:18. https://doi.org/10.1007/s11214-023-01036-z

Davis MR, Brown ME, Trumbo SK (2023) The spatial distribution of the unidentified 2.07 micon absorption feature on Europa and implications for its origin. Planet Sci J 4:148. https://doi.org/10.3847/PSJ/aced96

De Sanctis MC, Raponi A, Ammannito E et al (2016) Bright carbonate deposits as evidence of aqueous alteration on (1) Ceres. Nature 536:54–57

Denman WTP, Trumbo SK, Brown ME (2022) The influence and photobleaching on irradiated sodium chloride at Europa-like conditions. Planet Sci J 3:26. https://doi.org/10.3847/PSJ/ac4581
Desch SJ, Kalyaan A, Alexander CMO'D (2018) The effect of Jupiter's formation on the distribution of refractory elements and inclusions in meteorites. Astrophys J Suppl Ser 238(1):11. https://doi.org/10.3847/1538-4365/aad95f
Doggett T, Greeley R, Figueredo P, Tanaka K (2009) Geologic stratigraphy and evolution of Europa's surface. In: Pappalardo RT, McKinnon WB, Khurana K (eds) Europa. University of Arizona Press, Tucson
Dols V, Delamere PA, Bagenal F (2008) A multispecies chemistry model of Io's local interaction with the plasma torus. J Geophys Res 113:A09208. https://doi.org/10.1029/2007JA012805
Dols VJ, Bagenal F, Cassidy TA, Crary FJ, Delamere PA (2016) Europa's atmospheric neutral escape: importance of symmetrical O_2 charge exchange. Icarus 264:387–397. https://doi.org/10.1016/j.icarus.2015.09.026
Domingue D, Verbiscer A (1997) Re-analysis of the solar phase curves of the icy Galilean satellites. Icarus 128(1):49–74. https://doi.org/10.1006/icar.1997.5730
Dougherty et al (2006). https://doi.org/10.1126/science.1120985
Drebushchak VA, Oienko AG, Yunoschev AS (2017) Metastable eutectic melting in the NaCl-H_2O system. Thermochim Acta 647:94–100. https://doi.org/10.1016/j.tca.2016.12.004
Durham WB, Prieto-Ballesteros O, Goldsby D, Kargel J (2010) Rheological and thermal properties of icy materials. Space Sci Rev 153(1):273–298
Fagents SA (2003) Considerations for effusive cryvolcanism on Europa: the post-Galileo perspective. J Geophys Res 108(E12):5139. https://doi.org/10.1029/2003JE002128
Fagents SA, Greeley R, Sullivan RJ, Pappalardo RT, Prockter LM, Galileo SSI Team (2000) Cryomagmatic mechanisms for the formation of Rhadamanthys Linea, triple band margins, and other low-albedo features on Europa. Icarus 144:54–88. https://doi.org/10.1006/icar.1999.6254
Famá M, Shi J, Baragiola R (2008) Sputtering of ice by low-energy ions. Surf Sci 602:156–161. https://doi.org/10.1016/j.susc.2007.10.002
Fanale FP et al (1999) Galileo's multiinstrument spectral view of Europa's surface composition. Icarus 139:179–188. https://doi.org/10.1006/icar.1999.6117
Fegley B Jr, Zolotov MY (2000) Chemistry of sodium, potassium and chlorine in volcanic gases on Io. Icarus 148:193–210. https://doi.org/10.1006/icar.2000.6490
Figueredo PH, Greeley R (2004) Resurfacing history of Europa from pole-to-pole geological mapping. Icarus 167:287–312. https://doi.org/10.1016/j.icarus.2003.09.016
Fischer et al (2015). https://doi.org/10.1088/0004-6256/150/5/164
Formisano M, Federico C, Castillo-Rogez J, De Sanctis MC, Magni G (2020) Thermal convection in the crust of the dwarf planet – 1. Ceres. Mon Not R Astron Soc 484:5704–5712. https://doi.org/10.1093/mnras/staa1115
Fortes AD, Choukroun M (2010) Phase behaviour of ices and hydrates. Space Sci Rev 153:185–218. https://doi.org/10.1007/s11214-010-9633-3
Foustoukos DI, Houghton JL, Seyfried WE Jr, Sievert SM, Cody GD (2011) Kinetics of H_2-O_2 redox equilibria and formation of metastable H_2O_2 under low temperature hydrothermal conditions. Geochim Cosmochim Acta 75:1594–1607. https://doi.org/10.1016/j.gca.2010.12.020
Geissler et al (1998). https://doi.org/10.1006/icar.1998.5980
Ghormley (1967). https://doi.org/10.1063/1.1840851
Giono G, Roth L, Ivchenko N, Saur J, Retherford K, Schlegel S, Ackland M, Strobel D (2020) An analysis of the statistics and systematics of limb anomaly detections in HST/STIS transit images of Europa. Astron J 159:155. https://doi.org/10.3847/1538-3881/ab7454
Gissinger C, Petitdemange L (2019) A magnetically driven equatorial jet in Europa's ocean. Nat Astron 3:401–407. https://doi.org/10.1038/s41550-019-0713-3
Gladstone GR, Retherford KD, Egan AF, Kaufmann DE, Miles PF, Parker JW, Horvath D, Rojas PM, Versteeg MH, Davis MW, Greathouse TK, Slater DC, Mukherjee J, Steffl AJ, Feldman PD, Hurley DM, Pryor WR, Hendrix AR, Mazarico E, Stern SA (2012) Far-ultraviolet reflectance properties of the Moon's permanently shadowed regions. J Geophys Res 117:E00H04. https://doi.org/10.1029/2011JE003913
Glein CR, Waite JH (2020) The carbonate geochemistry of Enceladus' ocean. Geophys Res Lett 47:e2019GL085885. https://doi.org/10.1029/2019GL085885
Glein CR, MYu Z, Shock EL (2008) The oxidation state of hydrothermal systems on early Enceladus. Icarus 197:157–163. https://doi.org/10.1016/j.icarus.2008.03.021
Glein CR, Baross JA, Waite JH (2015) The pH of Enceladus' ocean. Geochim Cosmochim Acta 162:202–219. https://doi.org/10.1016/j.gca.2015.04.017
Glein CR, Postberg F, Vance SD (2018) The geochemistry of Enceladus: composition and controls. In: Schenk PM et al (eds) Enceladus and the icy moons of Saturn. University of Arizona Press, Tucson, pp 39–56

Glein CR, Grundy WM, Lunine JI, Wong I, Protopapa S, Pinilla-Alonso N, Stansberry JA, Holler BJ, Cook JC, Souza-Feliciano AC (2024) Moderate D/H ratios in methane ice on Eris and Makemake as evidence of hydrothermal or metamorphic processes in their interiors: geochemical analysis. Icarus 412:115999. https://doi.org/10.1016/j.icarus.2024.115999

Gomez Casajus L, Zannoni M, Modenini D, Torora P, Nimmo F, Hoolst TV, Buccino D, Oudrhiri K (2021) Updated Europa gravity field and interior structure from a reanlysis of Galileo tracking data. Icarus 358:114187. https://doi.org/10.1016/j.icarus.2020.114187

Goode W, Kempf S, Schmidt J (2021) Detecting the surface composition of geological features on Europa and Ganymede using a surface dust analyzer. Planet Space Sci 208:105343. https://doi.org/10.1016/j.pss.2021.105343

Grasset O, Dougherty MK, Coustenis A, Bunce EJ, Erd C, Titov D, Blanc M, Coates A, Drossart P, Flecter LN, Hussman H, Jaumann R, Krupp N, Lebreton J-P, Preito-Ballestrero O, Tortora P, Tosi F, Van Hoolst T (2013) Jupiter Icy moons Explorer (JUICE): an ESA mission to orbit Ganymede and to characterize the Jupiter system. Planet Space Sci 78:1–21. https://doi.org/10.1016/j.pss.2012.12.002

Grava C, Chaufray JY, Retherford KD, Gladstone GR, Greathouse TK, Hurley DM, Hodges RR, Bayless AJ, Cook JC, Stern SA (2015) Lunar exospheric argon modeling. Icarus 255:135–147. https://doi.org/10.1016/j.icarus.2014.09.029

Grava C, Hurley DM, Feldman PD, Retherford KD, Greathouse TK, Pryor WR, Gladstone GR, Halekas JS, Mandt KE, Wyrick DY, Davis MW, Egan AF, Kaufmann DE, Versteeg MH, Stern SA (2021) LRO/LAMP observations of the lunar helium exosphere: constraints on thermal accommodation and outgassing rate. Mon Not R Astron Soc 501:4438–4451. https://doi.org/10.1093/mnras/staa3884

Greeley R, Sullivan R, Klemaszewski J, Homan K, Head JW, Pappalardo RT, Veverka J, Clark BE, Johnson TV, Klaasen KP, Belton M, Moore J, Asphaug E, Carr MH, Neukum G, Denk T, Chapman CR, Pilcher CB, Geissler PE, Greenberg R, Tufts R (1998) Europa: initial Galileo geological observations. Icarus 135(1):4–23. https://doi.org/10.1006/icar.1998.5969

Greeley R, Figueredo PH, Williams DA, Chuang FC, Klemaszewski JE, Kadel SD, Prockter LM, Pappalardo RT, Head JW, Collins GC, Spaun NA, Sullivan RJ, Moore JM, Senske DA, Tufts BR, Johnson TV, Belton MJS, Tanaka KL (2000) Geologic mapping of Europa. J Geophys Res, Planets 105(E9):22559–22578. https://doi.org/10.1029/1999JE001173

Greeley R, Chyba CF, Head JW, McCord T, McKinnon WB, Pappalardo RT, Figueredo PH (2004) Geology of Europa. In: Jupiter: the planet, satellites and magnetosphere, pp 329–362

Greenberg R (2010) Transport rates of radiolytic substances into Europa's ocean: implications for the potential origin and maintenance of life. Astrobiology 10(3):275–283. https://doi.org/10.1089/ast.2009.0386

Greenberg R, Hoppa GV, Tufts BR, Geissler P, Riley J (1999) Chaos on Europa. Icarus 141:263–286. https://doi.org/10.1006/icar.1999.6187

Greenberg R, Leake MA, Hoppa GV, Tufts BR (2003) Pits and uplifts on Europa. Icarus 161(1):102–126. https://doi.org/10.1016/S0019-1035(02)00013-1

Grima (2017). www.hou.usra.edu/meetings/lpsc2017/pdf/2816.pdf

Grima C, Blankenship DD, Young DA, Schroeder DM (2014a) Surface slope control on firn density at Thwaites Glacier, West Antarctica: results from airborne radar sounding. Geophys Res Lett 41(19):6787–6794. https://doi.org/10.1002/2014GL061635

Grima C, Schroeder DM, Blankenship DD, Young DA (2014b) Planetary landing-zone reconnaissance using ice-penetrating radar data: concept validation in Antarctica. Planet Space Sci 103:191–204. https://doi.org/10.1016/j.pss.2014.07.018

Grima C, Greenbaum JS, Lopez Garcia EJ, Soderlund KM, Rosales A, Blankenship DD, Young DA (2016) Radar detection of the brine extent at McMurdo Ice Shelf, Antarctica, and its control by snow accumulation. Geophys Res Lett 43(13):7011–7018. https://doi.org/10.1002/2016GL069524

Grün E, Zook A, Baguhl M, Balogh A, Bame SJ, Fechtig H, Forsyth R, Hanner MS, Horányi M, Kissel J, Lindblad B-A, Linkert D, Linkert G, Mann I, McDonnell JAM, Morfill GE, Phillips JL, Polanskey C, Schwehm G, Siddique N, Staubach P, Svestka J, Taylor A (1993) Discovery of Jovian dust streams and interstellar grains by the Ulysses spacecraft. Nature 362:428–430. https://doi.org/10.1038/362428a0

Grundy WM, Schmitt B (1998) The temperature-dependent near-infrared absorption spectrum of hexagonal H_2O ice. J Geophys Res 103(E11):25809–25822. https://doi.org/10.1029/98JE00738

Gudipati and Allamandola (2006). https://doi.org/10.1086/498816

Gudipati MS, Henderson BL, Bateman FB (2021) Laboratory predictions for the night-side surface ice glow of Europa. Nat Astron 5:276–282. https://doi.org/10.1038/s41550-020-01248-1

Hall DT, Strobel DF, Feldman PD, McGrath MA, Weaver HA (1995) Detection of an oxygen atmosphere on Jupiter's moon Europa. Nature 373:677–679. https://doi.org/10.1038/373677a0

Hall et al (1998). https://doi.org/10.1086/305604

Hand KP, Brown ME (2013) Keck II observations of hemispherical differences in H_2O_2 on Europa. Astrophys J Lett 766:L21. https://doi.org/10.1088/2041-8205/766/2/L21
Hand and Carlson (2011). https://doi.org/10.1016/j.icarus.2011.06.031
Hand KP, Carlson RW (2015) Europa's surface color suggests an ocean rich with sodium chloride. Geophys Res Lett 42:3174–3178. https://doi.org/10.1002/2015GL063559
Hand KP, Chyba CF, Carlson RW, Cooper JF (2006) Clathrate hydrates of oxidants in the ice shell of Europa. Astrobiology 6(3):463–482. https://doi.org/10.1089/ast.2006.6.463
Hand KP, Carlson RW, Chyba CF (2007) Energy, chemical disequilibrium, and geological constraints on Europa. Astrobiology 7:1006–1022. https://doi.org/10.1088/2041-8205/766/2/L21
Hand KP et al (2022) Science goals and mission architecture of the Europa Lander mission concept. Planet Sci J 3:22. https://doi.org/10.3847/PSJ/ac4493
Hanley J, Dalton JB III, Chevrier VF, Jamieson CS, Barrows RS (2014) Reflectance spectra of hydrated chlorine salts: the effect of temperature with implications for Europa. J Geophys Res 119:2370–2377. https://doi.org/10.1002/2013JE004565
Hansen GB, McCord TB (2004) Amorphous and crystalline ice on the Galilean satellites: a balance between thermal and radiolytic processes. J Geophys Res, Planets 109:E01012. https://doi.org/10.1029/2003JE002149
Hansen GB, McCord TB (2008) Widespread CO_2 and other non-ice compounds on the anti-Jovian and trailing sides of Europa from Galileo/NIMS observations. Geophys Res Lett 35:L01202. https://doi.org/10.1029/2007GL031748
Hansen CJ, Shemansky DE, Hendrix AR (2005) Cassini UVIS observations of Europa's oxygen atmosphere and torus. Icarus 176(2):305–315. https://doi.org/10.1016/j.icarus.2005.02.007
Hansen CJ, Esposito LW, Hendrix AR (2019) Ultraviolet observation of Enceladus' plume in transit across Saturn, compared to Europa. Icarus 330:256–260. https://doi.org/10.1016/j.icarus.2019.04.031
Hansen CJ, Esposito LW, Colwell JE, Hendrix AR, Portyankina G, Stewart AIF, West RA (2020) The composition and structure of Enceladus' plume from the complete set of Cassini UVIS occultation observations. Icarus 344:113461. https://doi.org/10.1016/j.icarus.2019.113461
Hao J, Glein CR, Huang F et al (2022) Abundant phosphorus expected for possible life in Enceladus's ocean. Proc Natl Acad Sci USA 119:e2201388119
Hapke B (1986) Bidirectional reflectance spectroscopy 4. The extinction coefficient and the opposition effect. Icarus 67(2):264–280. https://doi.org/10.1016/0019-1035(86)90108-9
Hapke (2012). https://doi.org/10.1016/j.icarus.2012.10.022
Heggy E, Scabbia G, Bruzzone L, Pappalardo RT (2017) Radar probing of Jovian icy moons: understanding subsurface water and structure detectability in the JUICE and Europa missions. Icarus 285:237–251. https://doi.org/10.1016/j.icarus.2016.11.039
Heller RH, Marleau G-D, Pudritz RE (2015) The formation of the Galilean moons and Titan in the Grand Tack scenario. Astron Astrophys 579:L4. https://doi.org/10.1051/0004-6361/201526348
Hendrix AR, Barth CA, Stewart AIF, Hord CW, Lane AL (1999) Hydrogen peroxide on the icy Galilean satellites. Lunar and planetary science XXX. LPI contribution, vol 964. Lunar and Planetary Institute, Houston (CD-ROM). Abstract # 2043
Hendrix AR, Domingue DL, King K (2005) The icy Galilean satellites: ultraviolet phase curve analysis. Icarus 173(1):29–49. https://doi.org/10.1016/j.icarus.2004.06.017
Hendrix AR, Hansen CJ, Holsclaw GM (2010) The ultraviolet reflectance of Enceladus: implications for surface composition. Icarus 206:608–617. https://doi.org/10.1016/j.icarus.2009.11.007
Hendrix AR, Cassidy TA, Johnson RE, Paranicas C, Carlson RW (2011) Europa's disk-resolved ultraviolet spectra: relationships with plasma flux and surface terrains. Icarus 212:736–743. https://doi.org/10.1016/j.icarus.2011.01.023
Hibbitts CA, Stockstill-Cahill K, Wing B, Paranicas C (2019) Color centers in salts – evidence for the presence of sulfates on Europa. Icarus 326:37–47. https://doi.org/10.1016/j.icarus.2019.02.022
Hillier JK, Schmidt J, Hsu H-W, Postberg F (2018) Dust emission by active moons. Space Sci Rev 213:131. https://doi.org/10.1007/s11214-018-0539-9
Horányi M, Juhasz A (2022) Dust delivery from Io to the icy Galilean moons of Jupiter. 44th COSPAR Scientific Assembly, B5.2-0006-22
Horányi M, Morfill GE, Grün E (1993) Mechanism for the acceleration and ejection of dust grains from Jupiter's magnetosphere. Nature 363:144–146. https://doi.org/10.1029/93JA02588
Howell SM (2021) The likely thickness of Europa's icy shell. Planet Sci J 2:129. https://doi.org/10.3847/PSJ/abfe10
Howell SM, Pappalardo RT (2018) Band formation and ocean-surface interaction on Europa and Ganymede. Geophys Res Lett 45(10):4701–4709. https://doi.org/10.1029/2018GL077594
Howell SM, Pappalardo RT (2019) Can Earth-like plate tectonics occur in ocean world ice shells? Icarus 322:69–79. https://doi.org/10.1016/j.icarus.2019.01.011

Howett CJA, Spencer J, Pearl J, Segura M (2010) Thermal inertia and bolometric bond albedo values for Mimas, Enceladus, Tethys, Dione, Rhea and Iapetus as derived from Cassini/CIRS measurements. Icarus 206:573–593. https://doi.org/10.1016/j.icarus.2009.07.016

Hsu HW, Krüger H, Postberg F (2012) Dynamics, composition, and origin of Jovian and saturnian dust-stream particles. In: Mann I, Meyer-Vernet N, Czechowski A (eds) Nanodust in the solar system: discoveries and interpretations. Astrophysics and space science library, vol 385. Springer, Berlin. https://doi.org/10.1007/978-3-642-27543-2_5

Hsu H-W, Postberg F, Yasuhito S, Shibuya T, Kempf S, Horány M, Juhász A, Altobelli N, Suzuki K, Masaki Y, Kuwatani T, Tachibana S, Sirono S-I, Moragas-Klostmermeyer G, Drama R (2015) Ongoing hydrothermal activities within Enceladus. Nature 519:207–210. https://doi.org/10.1038/nature14262

Hudson and Donn (1991). https://doi.org/10.1016/0019-1035(91)90231-H

Hudson RL, Moore MH (2001) Radiation chemical alterations in solar system ices: an overview. J Geophys Res 106(E12):33275–33284. https://doi.org/10.1088/0022-3727/40/21/R02

Hurley DM, Lawrence DJ, Bussey BJ, Vondrak RR, Elphic RC, Gladstone GR (2012) Two-dimensional distribution of volatiles in the lunar regolith from space weathering simulations. Geophys Res Lett 39:L09203. https://doi.org/10.1029/2012GL051105

Hussmann H, Spohn T (2004) Thermal-orbital evolution of Io and Europa. Icarus 171:391–410. https://doi.org/10.1016/j.icarus.2004.05.020

Ingersoll AP, Svitek T, Murray BC (1992) Stability of polar frosts in spherical bowl-shaped craters on the Moon, Mercury, and Mars. Icarus 100:40–47. https://doi.org/10.1016/0019-1035(92)90016-Z

Intriligator DS, Miller WD (1982) First evidence for a Europa plasma torus. J Geophys Res 87(A10):8081–8090. https://doi.org/10.1029/JA087iA10p08081

Intriligator DS, Miller WD (1982) First evidence for a Europa plasma torus. J Geophys Res 87(A10):8081–8090. https://doi.org/10.1029/JA087iA10p08081

Ireland TR, Avila J, Greenwood RC, Hicks LJ, Bridges JC (2020) Oxygen isotopes and sampling of the solar system. Space Sci Rev 216(2):25. https://doi.org/10.1007/s11214-020-0645-3

Jaramillo-Botero A, Cable ML, Hofmann AE, Malaska M, Hodyss R, Lunine J (2021) Understanding hypervelocity sampling of biosignatures in space missions. Astrobiology 21(4):421–442. https://doi.org/10.1089/ast.2020.2301

Jenniskens P, Blake D (1996) Crystallization of amorphous water ice in the solar system. Astrophys J 473(2):1104. https://doi.org/10.1086/178220

Jia X, Kivelson MG, Khurana KK, Kurth WS (2018) Evidence of a plume on Europa from Galileo magnetic and plasma wave signatures. Nat Astron 2:459–464. https://doi.org/10.1038/s41550-018-0450-z

Johnson TV (1970) Galilean satellites: narrowband photometry 0.30 to 1.10 microns. Icarus 14:94–111. https://doi.org/10.1016/0019-1035(71)90104-7

Johnson RE (1996) Sputtering of ices in the outer solar system. Rev Mod Phys 68(1):305–312. https://doi.org/10.1103/RevModPhys.68.305

Johnson TV, McCord TB (1971) Spectral geometric albedo of the Galilean satellites, 0.3 to 2.5 microns. Astrophys J 169:589–594. https://articles.adsabs.harvard.edu/pdf/1971ApJ...169..589J

Johnson RE, Sundqvist BUR (2018) Sputtering and detection of large organic molecules from Europa. Icarus 309:338–344. https://doi.org/10.1016/j.icarus.2018.01.027

Johnson et al (1981). https://doi.org/10.1126/science.212.4498.1027

Johnson JW, Oelkers EH, Helgeson HC (1992) SUPCRT92: a software package for calculating the standard molal thermodynamic properties of minerals, gases, aqueous species, and reactions from 1 to 5000 bar and 0 to 1000 °C. Comput Geosci 18:899–947. https://doi.org/10.1016/0098-3004(92)90029-Q

Johnson RE, Carlson RW, Cooper JF, Paranicas C, Moore MH, Wong MC (2004) Radiation effects on the surfaces of the Galilean satellites. In: Bagenal F, Downling T, McKinnon W (eds) Jupiter – the planet, satellites, and magnetosphere. Cambridge Planetary Science, Cambridge

Johnson BC, Sheppard RY, Pascuzzo AC, Fisher EA, Wiggins SE (2017) Porosity and salt content determine if subduction can occur in Europa's ice shell: subduction in Europa's ice shell. J Geophys Res, Planets 122(12):2765–2778. https://doi.org/10.1002/2017JE005370

Johnson PV, Hodyss R, Vu TH, Choukroun M (2019) Insights into Europa's ocean composition derived from its surface expression. Icarus 321:857–865. https://doi.org/10.1016/j.icarus.2018.12.009

Journaux B, Pakhomova A, Collings IE, Petitgirard S, Ballaran TB et al (2023) On the identification of hyperhydrated sodium chloride hydrates, stable at icy moon conditions. Proc Natl Acad Sci USA 120:e2217125120. https://doi.org/10.1073/pnas.2217125120

Kalousová K, Souček O, Tobie G, Choblet G, Čadek O (2016) Water generation and transport below Europa's strike-slip faults: water generation below Europa's faults. J Geophys Res, Planets 121:2444–2462. https://doi.org/10.1002/2016JE005188

Kalousová K, Schroeder DM, Soderlund KM (2017) Radar attenuation in Europa's ice shell: obstacles and opportunities for constraining the shell thickness and its thermal structure. J Geophys Res, Planets 122:524–545. https://doi.org/10.1002/2016JE005110

Kamata S, Nimmo F, Sekine Y, Kuramoto K, Noguchi N, Kimura J, Tani A (2019) Pluto's ocean is capped and insulated by gas hydrates. Nat Geosci 12:407–410. https://doi.org/10.1038/s41561-019-0369-8

Kargel JS, Kaye JZ, Head JW, Marion GM, Sassen R et al (2000) Europa's crust and ocean: origin, composition, and prospects for life. Icarus 148:226–265. https://doi.org/10.1006/icar.2000.6471

Kattenhorn (2002). https://doi.org/10.1006/icar.2002.6825

Kattenhorn SA, Prockter LM (2014) Evidence for subduction in the ice shell of Europa. Nat Geosci 7:762–767. https://doi.org/10.1038/ngeo2245

Kempe and Kazmierczak (1997). https://doi.org/10.1016/S0032-0633(97)00116-5

Kempf S, Beckmann U, Schmidt J (2010) How the Enceladus dust plume feeds Saturn's E ring. Icarus 206(2):446–457. https://doi.org/10.1016/j.icarus.2009.09.016

Kempf S, Srama R, Grün E, Mocker A, Postberg F et al (2012) Linear high resolution dust mass spectrometer for a mission to the Galilean satellites. Planet Space Sci 65(1):10–20. https://doi.org/10.1016/j.pss.2011.12.019

Kempf S, Tucker S, Altobelli N et al (2024) SUDA: A SUrface Dust Analyser for compositional mapping of the Galilean moon Europa. Space Sci Rev 220

Khawaja N, Postberg F, Hillier J, Klenner F, Kempf S et al (2019) Low-mass nitrogen-, oxygen-bearing, and aromatic compounds in Enceladean ice grains. Mon Not R Astron Soc 489:5231–5243. https://doi.org/10.1093/mnras/stz2280

Kivelson MG, Khurana KK, Russel CT, Volwek M, Walker RJ, Zimmer C (2000) Galileo magnetometer measurements: a stronger case for a subsurface ocean and Europa. Science 289:1340–1343. https://doi.org/10.1126/science.289.5483.1340

Kivelson MG, Jia X, Lee KA et al (2023) The Europa Clipper Magnetometer. Space Sci Rev 219:48. https://doi.org/10.1007/s11214-023-00989-5

Klenner F, Postberg F, Hillier J, Khawaja N, Cable ML et al (2020a) Discriminating abiotic and biotic fingerprints of amino acids and fatty acids in ice grains relevant to ocean worlds. Astrobiology 20(10):1168–1184. https://doi.org/10.1089/ast.2019.2188

Klenner F, Postberg F, Hillier J, Khawaja N, Reviol R et al (2020b) Analog experiments for the identification of trace biosignatures in ice grains from extraterrestrial ocean worlds. Astrobiology 20(2):179–189. https://doi.org/10.1089/ast.2019.2065

Kliore AJ, Hinson DP, Flasar FM, Nagy AF, Cravens TE (1997) The ionosphere of Europa from Galileo radio occultations. Science 277:355–358. https://doi.org/10.1126/science.277.5324.355

Kokaly RF, Clark RN, Swayze GA, Livo KE, Hoefen TM et al (2017) USGS Spectral Library Version 7 Data: U.S. Geological Survey data release. https://doi.org/10.5066/F7RR1WDJ

Kollman P, Clark G, Paranicas C, Mauk B, Haggerty D, Rymer A, Allegrini F (2022) Ganymede's radiation cavity and radiation belts. Geophys Res Lett 49(23):e2022GL098474. https://doi.org/10.1029/2022GL098474

Kouchi and Sirono (2001). https://doi.org/10.1029/2000GL011350

Krivov AV, Krüger H, Grün E, Thiessenhusen K-U, Hamilton DP (2002) A tenuous dust ring of Jupiter formed by escaping ejecta from the Galilean satellites. J Geophys Res, Planets 107(E1):5002. https://doi.org/10.1029/2000JE001434

Krivov AV, Sremčević M, Spahn F, Dikarev VV, Kholshevnikov KV (2003) Impact-generated dust clouds around planetary satellites: spherically symmetric case. Planet Space Sci 51(3):251–269. https://doi.org/10.1016/S0032-0633(02)00147-2

Krüger H, Geissler P, Horanyi M, Graps AL, Kempf S et al (2003a) Jovian dust streams: a monitor of Io's volcanic plume activity. Geophys Res Lett 30(21):2101. https://doi.org/10.1029/2003GL017827

Krüger H, Krivov AV, Sremčević M, Grün E (2003b) Impact-generated dust clouds surrounding the Galilean moons. Icarus 164:170–187. https://doi.org/10.1016/S0019-1035(03)00127-1

Kuskov OL, Kronrod VA (2005) Internal structure of Europa and Callisto. Icarus 177:550–569. https://doi.org/10.1016/j.icarus.2005.04.014

Lagg A, Krupp N, Woch J, Williams DJ (2003) In-situ observations of a neutral gas torus at Europa. Geophys Res Lett 30:1556. https://doi.org/10.1029/2003GL017214

Lane AL, Nelson RM, Matson DL (1981) Evidence for sulphur implantation in Europa's UV absorption band. Nature 292:38–39. https://doi.org/10.1038/292038a0

Leblanc F, Potter AE, Killen RM, Johnson RE (2005) Origins of Europa Na cloud and torus. Icarus 178:367–385. https://doi.org/10.1016/j.icarus.2005.03.027

Lee S, Pappalardo RT, Makris NC (2005) Mechanics of tidally driven fractures in Europa's ice shell. Icarus 177:367–379. https://doi.org/10.1016/j.icarus.2005.07.003

Leonard EJ, Pappalardo RT, Yin A (2018) Analysis of very-high-resolution Galileo images and implications for resurfacing mechanisms on Europa. Icarus 312:100–120. https://doi.org/10.1016/j.icarus.2018.04.016

Leonard EJ, Yin A, Pappalardo RT (2020) Ridged plains on Europa reveal a compressive past. Icarus 343:113709. https://doi.org/10.1016/j.icarus.2020.113709
Leong JM, Shock EL (2020) Thermodynamic constraints on the geochemistry of low-temperature, continental, serpentinization-generated fluids. Am J Sci 320:185–235. https://doi.org/10.2475/03.2020.01
Lesage E, Massol H, Schmidt F (2020) Cryomagma ascent on Europa. Icarus 335:113369. https://doi.org/10.1016/j.icarus.2019.07.003
Lesage E, Schmidt F, Andrieu F, Massol H (2021) Constraints on effusive cryovolcanic eruptions on Europa using topography obtained from Galileo images. Icarus 361:114373. https://doi.org/10.1016/j.icarus.2021.114373
Leto G, Baratta G (2003) Ly-α photon induced amorphization of ice water ice at 16 Kelvin-effects and quantitative comparison with ion irradiation. Astron Astrophys 397(1):7–13. https://doi.org/10.1051/0004-6361:20021473
Li et al (2020). https://doi.org/10.1016/j.icarus.2020.113999
Ligier N, Poulet F, Carter J, Brunetto R, Gourgeot F (2016) VLT/SINFONI observations of Europa: new insights into the surface composition. Astron J 151(6):163. https://doi.org/10.3847/0004-6256/151/6/163
Lignell and Gudipati (2015). https://doi.org/10.1021/jp509513s
Litwin KL, Zygielbaum BR, Polito PJ, Sklar LS, Collins GC (2012) Influence of temperature, composition, and grain size of the tensile failure of water ice: implications for erosion on Titan. J Geophys Res, Planets 117:E08013. https://doi.org/10.1029/2012JE004101
Liu X, Sachse M, Spahn F, Schmidt J (2016) Dynamics and distribution of Jovian dust ejected from the Galilean satellites. J Geophys Res, Planets 121:1141–1173. https://doi.org/10.1002/2016JE004999
Lodders (2021). https://doi.org/10.1007/s11214-021-00825-8
Lodders and Fegley (2023). https://doi.org/10.1016/j.chemer.2023.125957
Loeffler M, Raut U, Vidal R, Baragiola R, Carlson R (2006) Synthesis of hydrogen peroxide in water ice by ion irradiation. Icarus 180:265–273. https://doi.org/10.1016/j.icarus.2005.08.001
Lowell RP, DuBose M (2005) Hydrothermal systems on Europa. Geophys Res Lett 32:L05202. https://doi.org/10.1029/2005GL022375
Lunine JI, Stevenson DJ (1982) Formation of the Galilean satellites in a gaseous nebula. Icarus 52:14–39. https://doi.org/10.1016/0019-1035(82)90166-X
Lyons TW, Reinhard CT, Planavsky NJ (2014) The rise of oxygen in Earth's early ocean and atmosphere. Nature 506:307–315. https://doi.org/10.1038/nature13068
Magee BA, Waite JH (2017) Neutral gas composition of Enceladus' plume – model parameter insights from Cassini-INMS. Lunar Planet Sci 58:2974. https://www.hou.usra.edu/meetings/lpsc2017/pdf/2974.pdf
Mandt KE, Mousis O, Lunine J, Gautier D (2014) Protosolar ammonia as the unique source of Titan's nitrogen. Astrophys J Lett 788(2):L24. https://doi.org/10.1088/2041-8205/788/2/L24
Manga M, Michaut C (2017) Formation of lenticulae on Europa by saucer-shaped sills. Icarus 286:261–269. https://doi.org/10.1016/j.icarus.2016.10.009
Marion GM, Kargel JS, Catling DC, Jakubowski SD (2005) Effects of pressure on aqueous chemical equilibria at subzero temperatures with applications to Europa. Geochim Cosmochim Acta 69:259–274. https://doi.org/10.1016/j.gca.2004.06.024
Marion G, Kargel J, Catling D, Lunine J (2012) Modeling ammonia–ammonium aqueous chemistries in the solar system's icy bodies. Icarus 220:932–946. https://doi.org/10.1016/j.icarus.2012.06.016
Marty B (2012) The origins and concentrations of water, carbon, nitrogen and noble gases on Earth. Earth Planet Sci Lett 313(314):56–66. https://doi.org/10.1016/j.epsl.2011.10.040
Mastrapa RM (2004) Water ice and radiation in the Solar System. University of Arizona, DAI-B 65/04, p 1909
Mastrapa RM, Brown RH (2006) Ion irradiation of crystalline H_2O–ice: effect on the 1.65-μm band. Icarus 183:207–214. https://doi.org/10.1016/j.icarus.2006.02.006
Mastrapa RM, Bernstein MP, Sandford SA, Roush TL, Cruikshank DP, Dalle Ore CM (2008) Optical constants of amorphous and crystalline H_2O-ice in the near infrared from 1.1 to 2.6 μm. Icarus 197:307–320. https://doi.org/10.1016/j.icarus.2008.04.008
Mauk BH, Mitchell DG, Krimigis SM, Roelof EC, Paranicas CP (2003) Energetic neutral atoms from a trans-Europa gas torus at Jupiter. Nature 421:920–922. https://doi.org/10.1038/nature01431
Mazarico E, Buccino D, Castillo-Rogez J et al (2023) The Europa Clipper gravity and radio science investigation. Space Sci Rev 219:30. https://doi.org/10.1007/s11214-023-00972-0
McCarthy C, Cooper RF, Goldsby DL, Durham WB, Kirby SH (2011) Transient and steady state creep response of ice I and magnesium sulfate hydrate eutectic aggregates. J Geophys Res, Planets 116:E04007. https://doi.org/10.1029/2010JE003689
McCollom TM (2016) Abiotic methane formation during experimental serpentinization of olivine. Proc Natl Acad Sci 113:13965–13970. https://doi.org/10.1073/pnas.1611843113

McCollom TM, Seewald JS (2007) Abiotic synthesis of organic compounds in deep-sea hydrothermal environments. Chem Rev 107:382–401. https://doi.org/10.1021/cr0503660
McCord TB, Hansen GB, Fanale FP, Carlson RW, Matson DL et al (1998) Salts on Europa's surface detected by Galileo's Near Infrared Mapping Spectrometer. Science 280:1242–1245. https://doi.org/10.1126/science.280.5367.1242
McCord TB, Hansen GB, Matson DL, Jonhson TV, Crowley JK et al (1999) Hydrated salt minerals on Europa's surface from the Galileo near-infrared mapping spectrometer (NIMS) investigation. J Geophys Res 104:11827–11852. https://doi.org/10.1029/1999JE900005
McCord TB, Teeter G, Hansen GB, Sieger MT, Orlando TM (2002) Brines exposed to Europa surface conditions. J Geophys Res, Planets 107:4-1. https://doi.org/10.1029/2000JE001453
McFadden LA, Bell JF, McCord TB (1980) Visible spectral reflectance measurements (0.33-1.1 um) of the Galilean satellites at many orbital phase angles. Icarus 44:410–430. https://doi.org/10.1016/0019-1035(80)90034-2
McGrath and Sparks (2017). https://doi.org/10.3847/2515-5172/aa988e
McGrath MA, Lellouch E, Strobel DF, Feldman PD, Johnson RE (2004) Satellite atmospheres. In: Bagenal F, Downling T, McKinnon W (eds) Jupiter – the planet, satellites, and magnetosphere. Cambridge Planetary Science, Cambridge
McGrath MA, Hansen CJ, Hendrix AR (2009) Observations of Europa's tenuous atmosphere. In: Pappalardo RT, McKinnon WB, Khurana KK (eds) Europa. University of Arizona Press, Tucson
McGrath MA, Sparks WB, Spencer JR (2015) Search for trace species in Europa's exosphere. American Geophysical Union, Fall Meeting 2015, Abstract #P11C-2111
McKinnon WB (1998) Geodynamics of icy satellites. In: Schmitt B, de Bergh C, Festou M (eds) Solar system ices. Kluwer Academic, Dordrecht, pp 525–550
McKinnon WB (1999) Convective instability in Europa's floating ice shell. Geophys Res Lett 26:951–954. https://doi.org/10.1029/1999GL900125
McKinnon WB, Zolensky ME (2003) Sulfate content of Europa's ocean and shell: evolutionary considerations and some geological and astrobiological implications. Astrobiology 3:879–897. https://doi.org/10.1029/1999GL900125
Meier and Loeffler (2020). https://doi.org/10.1016/j.susc.2019.121509
Meitzler R, Jun I, Blase R et al (2023) Investigating Europa's radiation environment with the Europa Clipper Radiation Monitor. Space Sci Rev 219:61. https://doi.org/10.1007/s11214-023-01003-8
Melwani Daswani M, Vance SD, Mayne MJ, Glein CR (2021) A metamorphic origin for Europa's ocean. Geophys Res Lett 48(18):e94143. https://doi.org/10.1029/2021GL094143
Mével L, Mercier E (2005) Resorption processes in Astypalaea Linea extensive region (Europa). Planet Space Sci 53(7):772–779. https://doi.org/10.1016/j.pss.2004.12.005
Michaut C, Manga M (2014) Domes, pits, and small chaos on Europa produced by water sills. J Geophys Res, Planets 119(3):550–573. https://doi.org/10.1002/2013JE004558
Miles G, Howett C, Spencer J, Schenk P (2020) Modeling cold traps on Rhea. Bull Am Astron Soc 52:109
Milesi V, Shock E, Ely T, Lubetkin M, Sylva SP et al (2021) Geochemical modeling as a guiding tool during exploration of the Sea Cliff hydrothermal field, Gorda Ridge. Planet Space Sci 197:105151. https://doi.org/10.1016/j.pss.2020.105151
Miller KE, Glein CR, Waite JH (2019) Contributions from organic nitrogen to Titan's N2 atmosphere: new insights from cometary and chondritic data. Astrophys J 871:59. http//doi.org/10.3847/1538-4357/aaf561
Molaro JL, Choukroun M, Phillips CB, Phelps ES, Hodyss R, Mitchell KL, Lora JM, Meirion-Griffith G (2019) The microstructural evolution of water ice in the solar system through sintering. J Geophys Res, Planets 124:243–276. https://doi.org/10.1029/2018JE005773
Molyneux PM, Nichols JD, Becker TM, Raut U, Retherford KD (2020) Ganymede's far-ultraviolet reflectance: constraining impurities in the surface ice. J Geophys Res, Planets 125:e2020JE006476. https://doi.org/10.1029/2020JE006476
Molyneux et al (2022) 2022AGUFM.P36B..06M. https://agu.confex.com/agu/fm22/meetingapp.cgi/Paper/1184688
Moore JC (2000) Models of radar absorption in Europan ice. Icarus 147:292–300. https://doi.org/10.1006/icar.2000.6425
Mosqueira I, Estrada PR (2003a) Formation of the regular satellites of giant planets in an extended gaseous nebula. I. Subnebula model and accretion of satellites. Icarus 163:198–231. https://doi.org/10.1016/S0019-1035(03)00076-9
Mosqueira I, Estrada PR (2003b) Formation of the regular satellites of giant planets in an extended gaseous nebula. II. Satellite migration and survival. Icarus 163:232–255. https://doi.org/10.1016/S0019-1035(03)00077-0
Mouginot J, Kofman W, Safaeinili A, Grima C, Herique A, Plaut JJ (2009) MARSIS surface reflectivity of the south residual cap of Mars. Icarus 201:454–459. https://doi.org/10.1016/j.icarus.2009.01.009

Mousis O, Gautier D (2004) Constraints on the presence of volatiles in Ganymede and Callisto from an evolutionary turbulent model of the Jovian subnebula. Planet Space Sci 52:361–370. https://doi.org/10.1016/j.pss.2003.06.004

Mousis O, Gautier D, Coustenis A (2002) The D/H ratio in methane in Titan: origin and history. Icarus 159:156–165. https://doi.org/10.1006/icar.2002.6930

Mousis O, Lunine JI, Thomas C, Pasek M, Marboeuf U et al (2009a) Clathration of volatiles in the solar nebula and implications for the origin of Titan's atmosphere. Astrophys J 691:1780–1786. https://doi.org/10.1088/0004-637X/691/2/1780

Mousis O, Lunine JI, Waite JH, Magee B, Lewis WS et al (2009b) Formation conditions of Enceladus and origin of its methane reservoir. Astrophys J 701:L39–L42. https://doi.org/10.1088/0004-637X/701/1/L39

Mousis O, Lunine J, Luspay-Kuti A, Guillot T, Marty B et al (2016) A protosolar nebula origin for the ices agglomerated by comet 67P/Churyumov–Gerasimenko. Astrophys J Lett 819(2):L33. https://doi.org/10.3847/2041-8205/819/2/L33

Muñoz-Iglesias V, Bonales LJ, Prieto-Ballesteros O (2013) pH and salinity evolution of Europa's brines: Raman spectroscopy study of fractional precipitation at 1 and 300 bar. Astrobiology 13(8):693–702. https://doi.org/10.1089/ast.2012.0900

Muñoz-Iglesias V, Prieto-Ballesteros O, Bonales LJ (2014) Conspicuous assemblages of hydrated minerals from the H_2O-$MgSO_4$-CO_2 system on Jupiter's Europa satellite. Geochim Cosmochim Acta 125:446–475. https://doi.org/10.1016/j.gca.2013.10.033

Muñoz-Iglesias V, Prieto-Ballesteros O, López I (2019) Experimental petrology to understand Europa's crust. J Geophys Res, Planets 124:2660–2678. https://doi.org/10.1029/2019JE005984

Nakamura T, Matsumoto M, Amano K, Enokido Y, Zolensky ME et al (2022) Formation and evolution of carbonaceous asteroid Ryugu: direct evidence from returned samples. Science 379:eabn8671. https://doi.org/10.1126/science.abn8671

Napoleoni M, Klenner F, Khawaja N, Hillier JK, Postberg F (2023a) Mass spectrometric fingerprints of organic compounds in NaCl-rich ice grains from Europa and Enceladus. ACS Earth Space Chem 7:735–752. https://doi.org/10.1021/acsearthspacechem.2c00342

Napoleoni M, Klenner F, Sánchez LH et al (2023b) Mass spectrometric fingerprints of organic compounds in sulfate-rich ice grains: Implications for Europa Clipper. ACS Earth Space Chem 7:1675–1693. https://doi.org/10.1021/acsearthspacechem.3c00098

Napoleoni et al (2024). https://doi.org/10.3847/PSJ/ad2462

Nelson RM, Lane AL, Matson DL, Veeder GJ, Buratti BJ, Tedesco EF (1987) Spectral geometric albedos of the Galilean satellites from 0.24 to 0.34 micrometers: observations with the International Ultraviolet Explorer. Icarus 72:358–380. https://doi.org/10.1016/0019-1035(87)90180-1

Néri A, Guyot F, Reynard B, Sotin C (2020) A carbonaceous chondrite and cometary origin for icy moons of Jupiter and Saturn. Earth Planet Sci Lett 530:115920. https://doi.org/10.1016/j.epsl.2019.115920

Nimmo F, Manga M (2009) Geodynamics of Europa's ice shell. In: Pappalardo RT, McKinnon WB, Khurana KK (eds) Europa. University of Arizona Press, Tucson. https://doi.org/10.2307/j.ctt1xp3wdw

Nimmo F, Pappalardo RT, Giese B (2003) On the origins of band topography, Europa. Icarus 166:21–32. https://doi.org/10.1016/j.icarus.2003.08.002

Noll KS, Weaver HA, Gonnella AM (1995) The albedo spectrum of Europa from 2200 Å to 3300 Å. J Geophys Res, Planets 100(E9):19057–19059. https://doi.org/10.1029/94JE03294

Nordheim T, Hand K, Paranicas C (2018) Preservation of potential biosignatures in the shallow subsurface of Europa. Nat Astron 2(8):673–679. https://doi.org/10.1038/s41550-018-0499-8

Nulsen S, Kraft R, Germain G, Dunn W, Tremblay G et al (2020) X-ray emission from Jupiter's Galilean moons: a tool for determining their surface composition and particle environment. Astrophys J 895:79. https://doi.org/10.3847/1538-4357/ab8cbc

Ockman N (1958) The infrared and Raman spectra of ice. Adv Phys 7:199–220. https://doi.org/10.1080/00018735800101227

Ohmoto H, Lasaga AL (1982) Kinetics of reactions between aqueous sulfates and sulfides in hydrothermal systems. Geochim Cosmochim Acta 46:1727–1745. https://doi.org/10.1016/0016-7037(82)90113-2

Orlando et al (2005). https://doi.org/10.1016/j.icarus.2005.05.009

Paganini L, Villanueva GL, Roth L, Mandell AM, Hurford TA et al (2020) A measurement of water vapour amid a largely quiescent environment on Europa. Nat Astron 4:266–272. https://doi.org/10.1038/s41550-019-0933-6

Paige DA, Siegler MA, Harmon JK, Neumann GA, Mazarico EM et al (2013) Thermal stability of volatiles in the North polar region of Mercury. Science 339:300–303. https://doi.org/10.1126/science.1231106

Pappalardo RT, Barr AC (2004) The origin of domes on Europa: the role of thermally induced compositional diapirism. Geophys Res Lett 31(1):L01701. https://doi.org/10.1029/2003GL019202

Pappalardo RT, Head JW, Greeley R, Sullivan RJ, Pilcher C et al (1998) Geological evidence for solid-state convection in Europa's ice shell. Nature 391:365–368. https://doi.org/10.1038/34862
Pappalardo RT, Belton MJS, Breneman HH, Carr MH, Chapman CR et al (1999) Does Europa have a subsurface ocean? Evaluation of the geological evidence. J Geophys Res, Planets 104(E10):24015–24055. https://doi.org/10.1029/1998JE000628
Pappalardo RT, McKinnon WB, Khurana KK (eds) (2009) Europa University of Arizona Press, Tucson
Pappalardo RT, Buratti BJ, Korth H et al (2024) Science overview of the Europa Clipper Mission. Space Sci Rev 220
Pasek MA, Greenberg R (2012) Acidification of Europa's subsurface ocean as a consequence of oxidant delivery. Astrobiology 12:151–159. https://doi.org/10.1089/ast.2011.066
Petrenko VF, Whitworth RW (1999) Physics of ice. ISBN-10:0198518951
Pettinelli E, Cosciotti B, Di Paolo F, Lauro SE, Mattei E, Orosei R, Vannaroni G (2015) Dielectric properties of Jovian satellite ice analogs for subsurface radar exploration: a review. Rev Geophys 53(3):593–641. https://doi.org/10.1002/2014RG000463
Pettinelli E, Lauro SE, Cosciotti B, Mattei E, Di Paolo F, Vannaroni G (2016) Dielectric characterization of ice/$MgSO_4 \cdot 11H_2O$ mixtures as Jovian icy moon crust analogues. Earth Planet Sci Lett 439:11–17. https://doi.org/10.1016/j.epsl.2016.01.021
Phillips CB (2000) Voyager and Galileo SSI views of volcanic resurfacing on Io and the search for geologic activity on Europa. The University of Arizona, PhD Thesis 9965918; p 1284
Phillips CB, Chyba CF (2001) Impact gardening rates on Europa: comparison with sputtering. Proc Lunar Planet Sci Conf 32:2111. https://www.lpi.usra.edu/meetings/lpsc2001/pdf/2111.pdf
Phillips CB, Scully J, Cameron ME, Craft K, Persuad DMM et al (2023) A reconnaissance strategy for landing on Europa, based on Europa Clipper data. In preparation
Pierazzo E, Chyba CF (2002) Cometary delivery of biogenic elements to Europa. Icarus 157(1):120–127. https://doi.org/10.1006/icar.2001.6812
Plainaki C, Cassidy TA, Shematovich VI, Milillo A, Wurz P et al (2018) Towards a global unified model of Europa's tenuous atmosphere. Space Sci Rev 214:40. https://doi.org/10.1007/s11214-018-0469-6
Platz T, Nathues A, Schorghofer N, Preusker F, Mazarico E et al (2016) Surface water-ice deposits in the northern shadowed regions of Ceres. Nat Astron 1:0007. https://doi.org/10.1038/s41550-016-0007
Pollack et al (1978). https://doi.org/10.1016/0019-1035(78)90110-0
Porco CC, Helfenstein P, Thomas PC, Ingersoll AP, Wisdom J et al (2006) Cassini observes the active south pole of Enceladus. Science 311:1393–1401. https://doi.org/10.1126/science.1123013
Postberg FK, Kempf S, Srama R, Green SF, Hillier JK, McBride N, Grün E (2006) Composition of Jovian stream particles. Icarus 183:122–134. https://doi.org/10.1016/j.icarus.2006.02.001
Postberg F, Kempf S, Hillier JK, Srama R, Green SF, McBride N, Grün E (2008) The E-ring in the vicinity of Enceladus: II. Probing the moon's interior—the composition of E-ring particles. Icarus 193(2):438–454. https://doi.org/10.1016/j.icarus.2007.09.001
Postberg F, Kempf S, Schmidt J, Brilliantov N, Beinsen A, Abel B, Buck U, Srama R (2009) Sodium salts in E-ring ice grains from an ocean below the surface of Enceladus. Nature 459:1098–1101. https://doi.org/10.1038/nature08046
Postberg F, Grün E, Horanyi M, Kempf S, Krüger H, Schmidt J, Spahn F, Srama R, Sternovsky Z, Trieloff M (2011b) Compositional mapping of planetary moons by mass spectrometry of dust ejecta. Planet Space Sci 59(14):1815–1825. https://doi.org/10.1016/j.pss.2011.05.001
Postberg F, Schmidt J, Hillier JK, Kempf S, Srama R (2011a) A salt-water reservoir as the source of a compositionally stratified plume on Enceladus. Nature 474(7353):620–622. https://doi.org/10.1038/nature10175
Postberg F, Clark RN, Hansen CJ, Coates AJ, Dalle Ore CM, Scipioni F, Hedman MM, Waite JH (2018a) Plume and surface composition of Enceladus. In: Schenk PM, Clark RN, Howett CJA, Verbiscer AJ, Waite JH (eds) Enceladus and the Icy Moons of Saturn. University of Arizona Press, Tucson, pp 129–162
Postberg F, Khawaja N, Abel B, Choblet G, Glein CR, Gudipati MS, Henderson BL, Hsu H-W, Kempf S, Klenner F, Moragas-Klostermeyer G, Magee B, Nöelle L, Perry M, Reviol R, Schmidt J, Srama R, Stolz F, Gabriel T, Trieloff M, Waite JH (2018b) Macromolecular organic compounds from the depths of Enceladus. Nature 558(7711):564–568. https://doi.org/10.1038/s41586-018-0246-4
Postberg F, Sekine Y, Klenner F et al (2023) Detection of phosphates originating from Enceladus's ocean. Nature 618:489–493. https://doi.org/10.1038/s41586-023-05987-9
Poston MJ, Carlson RW, Hand KP (2017) Spectral behavior of irradiated sodium chloride crystals under Europa-like conditions. J Geophys Res, Planets 122(12):2644–2654. https://doi.org/10.1002/2017JE005429
Price LC, DeWitt E (2001) Evidence and characteristics of hydrolytic disproportionation of organic matter during metasomatic processes. Geochim Cosmochim Acta 65:3791–3826. https://doi.org/10.1016/S0016-7037(01)00762-1

Prieto-Ballesteros O, Kargel JS (2005) Thermal state and complex geology of a heterogeneous salty crust of Jupiter's satellite, Europa. Icarus 173(1):212–221. https://doi.org/10.1016/j.icarus.2004.07.019

Prieto-Ballesteros O, Kargel JS, Fernández-Sampedro M, Selsis F, Martínez ES, Hogenboom DL (2005) Evaluation of the possible presence of clathrate hydrates in Europa's icy shell or seafloor. Icarus 177(2):491–505. https://doi.org/10.1016/j.icarus.2005.02.021

Prinn RG, Fegley B (1981) Kinetic inhibition of CO and N_2 reduction in circumplanetary nebulae – implications for satellite composition. Astrophys J 249:308–317. https://doi.org/10.1086/159289

Prinn RGP, Fegley B (1989) Solar nebula chemistry: origins of planetary, satellite and cometary volatiles. In: Origin and evolution of planetary and satellite atmospheres. University of Arizona Press, Tucson, pp 78–136

Prockter LM, Head JW, Pappalardo RT, Sullivan RJ, Clifton AE, Giese B, Wagner R, Neukum G (2002) Morphology of Europan bands at high resolution: a mid-ocean ridge-type rift mechanism. J Geophys Res, Planets 107(E5):4-1. https://doi.org/10.1029/2000JE001458

Prockter LM, Shirley JH, Dalton JB, Kamp L (2017) Surface composition of pull-apart bands in Argadnel Regio, Europa: evidence of localized cryovolcanic resurfacing during basin formation. Icarus 285:27–42. https://doi.org/10.1016/j.icarus.2016.11.024

Quick LC, Hedman MM (2021) Corrigendum to: characterizing deposits emplaced by cryovolcanic plumes on Europa. Icarus 357:113952. https://doi.org/10.1016/j.icarus.2020.113952

Quick LC, Barnouin OS, Prockter LM, Patterson GW (2013) Constraints on the detection of cryovolcanic plumes on Europa. Planet Space Sci 86:1–9. https://doi.org/10.1016/j.pss.2013.06.028

Quick LC, Glaze LS, Baloga SM (2017) Cryovolcanic emplacement of domes on Europa. Icarus 284:477–488. https://doi.org/10.1016/j.icarus.2016.06.029

Quick LC, Fagents SA, Núñez KA, Wilk KA, Beyer RA, Beddingfield CB, Martin ES, Prockter LM, Hurford TA (2022) Cryolava Dome growth resulting from active eruptions on Jupiter's moon Europa. Icarus 287:115185. https://doi.org/10.1016/j.icarus.2022.115185

Raut U, Baragiola RA (2013) Sputtering and molecular synthesis induced by 100 keV protons in condensed CO_2 and relevance to the outer solar system. Astrophys J 772:53. https://doi.org/10.1088/0004-637X/772/1/53

Raut U, Karne PL, Retherford KD, Davis MW, Liu Y, Gladstone GR, Patrick EL, Greathouse TK, Hendrix AR, Mokashi P (2018) Faru-ultraviolet photometric response of Apollo soil 10084. J Geophys Res, Planets 123:5. https://doi.org/10.1029/2018JE005567

Raut U, Teolis BD, Mamo BD, Tucker OJ, Becker TM, Molyneux PM, Retherford KD, Greathouse TK, Gladstone GR (2023) Radiation Darkening of Europa's Cryoplume Fallouts. LPI contribution No. 2806, id 2299

Ray C, Glein CR, Waite JR, Teolos B, Hoehler T, Huber JA, Lunine J, Postberg F (2021) Oxidation processes diversify the metabolic menu on Enceladus. Icarus 364:114248. https://doi.org/10.1016/j.icarus.2020.114248

Retherford KD, Becker TM, Gladstone GR et al (2024) Europa Ultraviolet Spectrograph (Europa-UVS). Space Sci Rev 220

Roberts JH, McKinnon WB, Elder CM et al (2023) Exploring the interior of Europa with the Europa Clipper. Space Sci Rev 219:46. https://doi.org/10.1007/s11214-023-00990-y

Ronnet T, Mousis O, Vernazza P (2017) Pebble accretion at the origin of water in Europa. Astrophys J 845:92. https://doi.org/10.3847/1538-4357/aa80e6

Roth L (2021) A stable H_2O atmosphere on Europa's trailing hemisphere from HST images. Geophys Res Lett 48:e2021GL094289. https://doi.org/10.1029/2021GL094289

Roth L, Retherford KD, Saur J, Strobel DF, Feldman PD, McGrath MA, Nimmo F (2014a) Orbital apocenter is not a sufficient condition for HST/STIS detection of Europa's water vapor aurora. Proc Natl Acad Sci 111(48):E5123–E5132. https://doi.org/10.1073/pnas.1416671111

Roth L, Saur J, Retherford KD, Strobel DF, Feldman PD, McGrath MA, Nimmo F (2014b) Transient water vapor at Europa's south pole. Science 343(6167):171–174. https://doi.org/10.1126/science.1247051

Roth L, Saur J, Retherford KD, Strobel DF, Feldman PD, McGrath MA, Spencer JR, Blöcker A, Ivchenko N (2016) Europa's far ultraviolet oxygen aurora from a comprehensive set of HST observations. J Geophys Res Space Phys 121(3):2143–2170. https://doi.org/10.1002/2015JA022073

Roth L, Retherford K, Ivchenko N, Schlatter N, Strobel DF, Becker TM, Grava C (2017) Detection of a hydrogen corona in HST Lyα images of Europa in transit of Jupiter. Astron J 153:67. https://doi.org/10.3847/1538-3881/153/2/67

Rovira-Navarro M, Rieutord M, Gerkema T, Maas LRM, van der Wal W, Vermeersen B (2019) Do tidally-generated inertial waves heat the subsurface oceans of Europa and Enceladus? Icarus 321:126–140. https://doi.org/10.1016/j.icarus.2018.11.010

Rubey WW (1951) Geological history of sea water. Bull Geol Soc Am 62:1111–1148

Rutishauser A, Grima C, Sharp M, Blankenship DD, Young DA, Cawkwell F, Dowdeswell JA (2016) Characterizing near-surface firn using the scattered signal component of the glacier surface return from airborne radio-echo sounding. Geophys Res Lett 43:12502–12510. https://doi.org/10.1002/2016GL071230

Sarid AR, Greenberg R, Hoppa GV, Hurford TA, Tufts BR, Geissler P (2002) Polar wander and surface convergence of Europa's ice shell: evidence from a survey of strike-slip displacement. Icarus 158(1):24–41. https://doi.org/10.1006/icar.2002.6873

Scanlan (2019). https://doi.org/10.1016/j.pss.2019.07.010

Scanlan KM, Young DA, Blankenship DD (2022) Non-linear radar response to the radial structure of Europa plume fallout deposits. Icarus 378:114935. https://doi.org/10.1016/j.icarus.2022.114935

Schaible MJ, Johnson RE, Zhigilei LV, Piqueux S (2017) High energy electron sintering of icy regoliths: formation of the PacMan thermal anomalies on the icy Saturnian moons. Icarus 285:211–223. https://doi.org/10.1016/j.icarus.2016.08.033

Schmidt BE, Blankenship DD, Patterson GW, Schenk PM (2011) Active formation of 'chaos terrain' over shallow subsurface water on Europa. Nature 479(7374):502–505. https://doi.org/10.1038/nature10608

Schreier R, Eviatar A, Vasyliunas VM, Richardson JD (1993) Modeling the Europa plasma torus. J Geophys Res 98(A12):21231–21244. https://doi.org/10.1029/93JA02585

Seewald JS, Zolotov MY, McCollom T (2006) Experimental investigation of single carbon compounds under hydrothermal conditions. Geochim Cosmochim Acta 70:446–460. https://doi.org/10.1016/j.gca.2005.09.002

Seinen J, Weerkamp JRW, Groote JC, Den Hartog HW (1994) Radiation damage in NaCl. III. Melting phenomena of sodium colloids. Phys Rev B 50(14):9793

Senske DA, Leonard EJ, Patthoff DA (2019) Geologic mapping of Europa at global and regional scales: providing comprehensive insight into crustal history and evolution. In: 50th lunar and planetary science conference, Woodlands, TX

Sephton MA (2014) Organic geochemistry of meteorites. In: Treatise on geochemistry, 2nd edn., vol 12, pp 1–31. https://doi.org/10.1016/B978-0-08-095975-7.01002-0

Sephton MA, Waite JH, Brockwell TG (2018) How to detect life on Icy Moons. Astrobiology 18(7):843–855. https://doi.org/10.1089/ast.2017.1656

Shematovich VI, Johnson RE, Cooper JF, Wong MC (2005) Surface-bounded atmosphere of Europa. Icarus 173:480–498. https://doi.org/10.1016/j.icarus.2004.08.013

Shirley JH, Dalton JB, Prockter LM, Kamp LW (2010) Europa's ridged plains and smooth low albedo plains: distinctive compositions and compositional gradients at the leading side–trailing side boundary. Icarus 210:358–384. https://doi.org/10.1016/j.icarus.2010.06.018

Shirley et al (2016). https://doi.org/10.1002/2015EA000149

Shock EL, Canovas P, Yang Z, Boyer G, Johnson K, Robinson K, Fecteau K, Wingman T, Cox A (2013) Thermodynamics of organic transformations in hydrothermal fluids. Rev Mineral Geochem 76:311–350. https://doi.org/10.2138/RMG.2013.76.9

Shock E, Bockisch C, Estrada C, Fecteau K, Gould I, Hartnett H, Johnson K, Robinson K, Shipp J, Williams L (2019) Earth as organic chemist. In: Orcutt B, Daniel I, Dasgupta R (eds) Deep carbon, past to present. Cambridge University Press, Cambridge, pp 415–446

Singer KN, McKinnon WB, Schenk PM (2021) Pits, uplifts and small chaos features on Europa: morphologic and morphometric evidence for intrusive upwelling and lower limits to ice shell thickness. Icarus 364:114465. https://doi.org/10.1016/j.icarus.2021.114465

Sloan ED Jr, Koh CA, Koh CA (2007) Clathrate hydrates of natural gases, 3rd edn. CRC Press, Boca Raton. https://doi.org/10.1201/9781420008494

Smith HT, Mitchell DG, Johnson RE, Mauk BH, Smith JE (2019) Europa neutral torus confirmation and characterization based on observations and modeling. Astrophys J 871(1):69. https://doi.org/10.3847/1538-4357/aaed38

Smyth WH, Marconi ML (2006) Europa's atmosphere, gas tori, and magnetospheric implications. Icarus 181:510–526. https://doi.org/10.1016/j.icarus.2005.10.019

Smythe WD, Carlson RW, Ocampo A, Matson D, Johnson TV, McCord TB, Hansen GE, Soderblom LA, Clark RN (1998) Absorption bands in the spectrum of Europa detected by the Galileo NIMS instrument. In: Lunar and planetary science conference, vol 1532, p 1532

Sohl F, Choukroun M, Kargel J, Kimura J, Pappalardo R, Vance S, Zolotov M (2010) Subsurface water oceans on icy satellites: chemical composition and exchange processes. Space Sci Rev 153(1–4):485–510. https://doi.org/10.1007/s11214-010-9646-y

Sparks WB, Hand KP, McGrath MA, Bergeron E, Cracraft M, Deustua SE (2016) Probing for evidence of plumes on Europa with HST/STIS. Astrophys J 829:121. https://doi.org/10.3847/0004-637X/829/2/121

Sparks WB, Schmidt BE, McGrath MA, Hand KP, Spencer JR, Cracraft M, Deustua SE (2017) Active cryovolcanism on Europa? Astrophys J 839:L18. https://doi.org/10.3847/2041-8213/aa67f8

Sparks WB, Richter M, deWitt C, Montiel E, Dello Russo N, Grunsfeld JM, McGrath MA, Weaver H, Hand KP, Bergeron E, Reach W (2019) A search for water vapor plumes on Europa using SOFIA. Astrophys J 871:L5. https://doi.org/10.3847/2041-8213/aafb0a

Spaun NA, Head JW (2001) A model of Europa's crustal structure: recent Galileo results and implications for an ocean. J Geophys Res 106:7567–7576. https://doi.org/10.1029/2000JE001270

Spencer JR (1987) Thermal segregation of water ice on the Galilean satellites. Icarus 69:297–313. https://doi.org/10.1016/0019-1035(87)90107-2

Spencer JR, Calvin WM (2002) Condensed O_2 on Europa and Callisto. Astron J 124:3400–3403. https://doi.org/10.1086/344307

Spencer JR, Calvin WM, Person MJ (1995) Charge-coupled device spectra of the Galilean satellites: molecular oxygen on Ganymede. J Geophys Res, Planets 100(E9):19049–19056. https://doi.org/10.1029/95JE01503

Spencer JR, Tamppari LK, Martin TZ, Travis LD (1999) Temperatures on Europa from Galileo PPR: nighttime thermal anomalies. Science 284:1514–1516. https://doi.org/10.1126/science.284.5419.1514

Spiers EM, Schmidt BE (2021) Water activity of Europa's ocean: temporal variability and implications. In: 52nd lunar and planetary science conference, 15–19 Mar 2021, vol 2548, id. 2643

Sremčević M, Krivov AV, Spahn F (2003) Impact-generated dust clouds around planetary satellites: asymmetry effects. Planet Space Sci 51(7–8):455–471. https://doi.org/10.1016/S0032-0633(03)00050-3

Sremčević M, Krivov AV, Krüger H, Spahn F (2005) Impact-generated dust clouds around planetary satellites: model versus Galileo data. Planet Space Sci 53:625–641. https://doi.org/10.1016/j.pss.2004.10.001

Szalay JR, Smith HT, Zirnstein EJ, McComas DJ, Belgey LJ, Bagenal F, Delamere PA, Wilson RJ, Valek PW, Poppe AR, Nénon Q, Allegrini F, Ebert RW, Bolton SJ (2022) Water-group pickup ions from Europa-genic neutrals orbiting Jupiter. Geophys Res Lett 49:e2022GL098111. https://doi.org/10.1029/2022GL098111

Szulagyi J, Masset F, Lega E, Crida A, Morbidelli A, Guillot T (2016) Circumplanetary disc or circumplanetary envelope? Mon Not R Astron Soc 460:2853–2861. https://doi.org/10.1093/mnras/stw1160

Teolis BD, Waite JH (2016) Dione and Rhea seasonal exospheres revealed by Cassini CAPS and INMS. Icarus 272:277. https://doi.org/10.1016/j.icarus.2016.02.031

Teolis BD, Plainaki C, Cassidy TA, Raut U (2017b) Water ice radiolytic O_2, H_2, and H_2O_2 yields for any projectile species, energy, or temperature: a model for icy astrophysical bodies. J Geophys Res, Planets 122:1996–2012. https://doi.org/10.1002/2017JE005285

Teolis BD, Wyrick DY, Bouquet A, Magee BA, Waite JH (2017) Plume and surface feature structure and compositional effects on Europa's global exosphere: preliminary Europa mission predictions. Icarus 284:18. https://doi.org/10.1016/j.icarus.2016.10.027

Thomas EC, Hodyss R, Vu TH, Johnson PV, Choukroun M (2017) Composition and evolution of frozen chloride brines under the surface conditions of Europa. ACS Earth Space Chem 1:14–23. https://doi.org/10.1021/acsearthspacechem.6b00003

Toner J, Catling DC (2020) A carbonate-rich lake solution to the phosphate problem of the origin of life. Proc Natl Acad Sci USA 117:883–888. https://doi.org/10.1073/pnas.1916109117

Tosca NJ, Macdonald FA, Strauss JV, Johnston DT, Knoll AH (2011) Sedimentary talc in Neoproterozoic carbonate successions. Earth Planet Sci Lett 306:11–22. https://doi.org/10.1016/j.epsl.2011.03.041

Travis BJ, Palguta J, Schubert G (2012) A whole-moon thermal history model of Europa: impact of hydrothermal circulation and salt transport. Icarus 218:1006–1019. https://doi.org/10.1016/j.icarus.2012.02.008

Trinh KT, Bierson CJ, O'Rourke JG (2023) Slow evolution of Europa's interior: metamorphic ocean origin, delayed metallic core formation, and limited seafloor volcanism. Sci Adv 9:eadf3955. https://doi.org/10.1126/sciadv.adf3955

Trumbo SK, Brown ME (2023) The distribution of CO_2 on Europa indicates an internal source of carbon. Science 381:1308–1311. https://doi.org/10.1126/science.adg4155

Trumbo SK, Brown ME, Fischer PD, Hand KP (2017) A new spectral feature on the trailing hemisphere of Europa at 3.78 μm. Astron J 153:250. https://doi.org/10.3847/1538-3881/aa6d80

Trumbo SK, Brown ME, Hand KP (2019a) Sodium chloride on the surface of Europa. Sci Adv 5:eaaw7123. https://doi.org/10.1126/sciadv.aaw7123

Trumbo SK, Brown ME, Hand KP (2019b) H_2O_2 within chaos terrain on Europa's leading hemisphere. Astron J 158:127. https://doi.org/10.3847/1538-3881/ab380c

Trumbo et al (2020). https://doi.org/10.3847/1538-3881/abc34c

Trumbo SK, Becker TM, Brown ME, Denman WTP, Molyneux PM, Hendrix AD, Retherford KD, Roth L, Alday J (2022) A new UV spectral feature on Europa: confirmation of NaCl in lead-hemisphere chaos terrain. Planet Sci J 3:27. https://doi.org/10.3847/PSJ/ac4580

Tse JS, White MA (1988) Origin of glassy crystalline behavior in the thermal properties of clathrate hydrates: a thermal conductivity study of tetrahydrofuran hydrate. J Phys Chem 92:5006–5011

Turtle E et al (2024) Europa Imaging System (EIS). Space Sci Rev 220
Ulibarri Z, Munsat T, Voss M, Fontanese J, Horányi M, Kempf S, Sternovsky Z (2023) Detection of the amino acid histidine and its breakup products in hypervelocity impact ice spectra. Icarus 391:115319. https://doi.org/10.1016/j.icarus.2022.115319
Vance S, Harnmeijer J, Kimra J, Hussmann H, Demartin B, Brown JM (2007) Hydrothermal systems in small ocean planets. Astrobiology 7:987–1005. https://doi.org/10.1002/2016GL068547
Vance SD, Hand KP, Pappalardo RT (2016) Geophysical controls of chemical disequilibria in Europa. Geophys Res Lett 43:4871–4879. https://doi.org/10.1002/2016GL068547
Vance SD, Panning MP, Stähler S, Cammarano F, Bills BG, Tobie G et al (2018) Geophysical investigations of habitability in ice-covered ocean worlds. J Geophys Res, Planets 123:180–205. https://doi.org/10.1002/2017JE005341
Vance SD, Craft KL, Shock E et al (2023) Investigating Europa's habitability with the Europa Clipper. Space Sci Rev 219:81. https://doi.org/10.1007/s11214-023-01025-2
Vasavada AR, Paige DA, Wood SE (1999) Near-surface temperatures on Mercury and the Moon and the stability of polar ice deposits. Icarus 141:179–193. https://doi.org/10.1006/icar.1999.6175
Velbel MA, Zolensky ME (2021) Thermal metamorphism of CM chondrites: a dehydroxylation-based peak-temperature thermometer and implications for sample return from asteroids Ryuguand Bennu. Meteorit Planet Sci 56:546–585. https://doi.org/10.1111/maps.1363
Villanueva GL, Hammel HB, Milam SN, Faggi S, Kofman V (2023) Endogenous CO_2 ice mixture on the surface of Europa and no detection of plume activity. Science 381:1305–1308. https://doi.org/10.1126/science.adg4270
Volwerk M, Kivelson MG, Khurana KK (2001) Wave activity in Europa's wake: implications for ion pickup. J Geophys Res 106:26033–26048. https://doi.org/10.1029/2000JA000347
Vu TH, Hodyss R, Choukroun M, Johnson PV (2016) Chemistry of frozen sodium–magnesium–sulfate–chloride brines: implications for surface expression of Europa's ocean composition. Astrophys J Lett 816(2):L26. https://doi.org/10.3847/2041-8205/816/2/L26
Waite JH, Lewis WS, Magee BA, Lunine JI, McKinnon WB, Glein CR, Mousis O, Young DT, Brockwell T, Westlake J, Nguyen M-J (2009) Liquid water on Enceladus from observations of ammonia and ^{40}Ar in the plume. Nature 460:487–490. https://doi.org/10.1038/nature08153
Waite JH, Glein C, Perryman RS, Teolis BD, Magee BA, Miller G, Grimes J, Perry ME, Miller KE, Bouquet A, Lunine JI, Brockwell T, Bolton SJ (2017) Cassini finds molecular hydrogen in the Enceladus plume: evidence for hydrothermal processes. Science 356:155–159. https://doi.org/10.1126/science.aai8703
Waite JH, Burch JL, Brockwell TG et al (2024) MASPEX-Europa: The Europa Clipper neutral gas mass spectrometer investigation. Space Sci Rev 220:30. https://doi.org/10.1007/s11214-024-01061-6
Walsh KJ, Morbidelli A (2011) The effect of an early planetesimal-driven migration of the giant planets on terrestrial planet formation. Astron Astrophys 526:A126. https://doi.org/10.1051/0004-6361/201015277
Wamsteker W (1972) Narrow-band photometry of the Galilean satellites. Commun Lunar Planet Lab 9(3):171–177
Warren SG, Brandt RE (2008) Optical constants of ice from the ultraviolet to the microwave: a revised compilation. J Geophys Res 113(D14220):1–10. https://doi.org/10.1029/2007JD009744
Watson K, Murray B, Brown H (1961) On the possible presence of ice on the Moon. J Geophys Res 66:1598–1600. https://doi.org/10.1029/JZ066i005p01598
Westlake JH, McNutt RL, Grey M et al (2023) The Plasma Instrument for Magnetic Sounding (PIMS) on the Europa Clipper Mission. Space Sci Rev 219:62. https://doi.org/10.1007/s11214-023-01002-9
Widman T, Shock E (2008) A web-based interactive version of SUPCRT92. Geochim Cosmochim Acta 72(12):A1027
Wilson JK, Schneider NM (1999) Io's sodium directional feature: evidence for ionospheric escape. J Geophys Res 104:16567–16583. https://doi.org/10.1029/1999JE900017
Wolfenbarger N, Buffo J, Soderlund K, Blankenship D (2022a) Ice shell structure and composition of ocean worlds: insights from accreted ice on Earth. Astrobiology 22:937–961. https://doi.org/10.1089/ast.2021.0044
Wolfenbarger NS, Fox-Powell MG, Buffo JJ, Soderlund KM, Blankenship DD (2022b) Compositional controls on the distribution of brine in Europa's ice shell. J Geophys Res, Planets 127:e2022JE007305. https://doi.org/10.1029/2022JE007305
Wolfenbarger NS et al (2024). Radar characterization of salt layers in Europa's ice shell as a window into critical ice-ocean exchange processes. Submitted to Geophys Res Lett
Yung YL, McElroy MB (1977) Stability of an oxygen atmosphere on Ganymede. Icarus 30:97–103. https://doi.org/10.1016/0019-1035(77)90124-5
Zahnle K, Dones L, Levison HF (1998) Cratering rates on the Galilean satellites. Icarus 136:202–222. https://doi.org/10.1006/icar.1998.6015

Zhang JA, Paige DA (2009) Cold-trapped organic compounds at the poles of the Moon and Mercury: Implications for origins. Geophys Res Lett 36:L16203. https://doi.org/10.1029/2009GL038614
Zolensky et al (2017). https://doi.org/10.1098/rsta.2015.0386
Zolotov MY (2012) Aqueous fluid composition in CI chondritic materials: chemical equilibrium assessments in closed systems. Icarus 220:713–729. https://doi.org/10.1016/j.icarus.2012.05.036
Zolotov MY (2016) Formation of sulfates on parent bodies of carbonaceous chondrites, Ceres, Europa, and other icy bodies. Lunar Planet Sci 47:1778. https://www.hou.usra.edu/meetings/lpsc2016/pdf/1778.pdf
Zolotov MY (2020) The composition and structure of Ceres' interior. Icarus 335:113404. https://doi.org/10.1016/j.icarus.2019.113404
Zolotov and Fegley (1999). https://doi.org/10.1006/icar.1999.6164
Zolotov MY, Kargel JS (2009) On the chemical composition of Europa's icy shell, ocean, and underlying rocks. In: Pappalardo RT, McKinnon WB, Khurana KK (eds) Europa. University of Arizona Press, Tucson, pp 431–457. https://doi.org/10.2307/j.ctt1xp3wdw
Zolotov MY, Mironenko MV (2015) Metasomatism on early Ceres: a global rock alteration and fluid transfer. Lunar Planet Sci 46:1466. https://www.hou.usra.edu/meetings/lpsc2015/pdf/1466.pdf
Zolotov MY, Shock EL (2001) Composition and stability of salts on the surface of Europa and their oceanic origin. J Geophys Res 106:32815–32827. https://doi.org/10.1029/2000JE001413
Zolotov MY, Shock EL (2004) A model for low-temperature biogeochemistry of sulfur, carbon, and iron on Europa. J Geophys Res 109:E06003. https://doi.org/10.1029/2003JE002194
Zolotov MY, Shock EL, Barr AC, Pappalardo RT (2004) Brine pockets in the icy crust of Europa: distribution, chemistry, and habitability. In: Workshop on Europa's icy shell: past, present, and future. LPI contribution, vol 1195. Lunar and Planetary Institute, Houston, pp 100–101. https://www.lpi.usra.edu/meetings/europa2004/pdf/7028.pdf

Publisher's Note Springer Nature remains neutral with regard to jurisdictional claims in published maps and institutional affiliations.

Authors and Affiliations

T.M. Becker[1,2] · M.Y. Zolotov[3] · M.S. Gudipati[4] · J.M. Soderblom[5] · M.A. McGrath[6] · B.L. Henderson[4] · M.M. Hedman[7] · M. Choukroun[4] · R.N. Clark[8] · C. Chivers[9] · N.S. Wolfenbarger[10] · C.R. Glein[1] · J.C. Castillo-Rogez[4] · O. Mousis[11] · K.M. Scanlan[10] · S. Diniega[4] · F.P. Seelos[12] · W. Goode[13] · F. Postberg[14] · C. Grima[10] · H.-W. Hsu[13] · L. Roth[15] · S.K. Trumbo[16] · K.E. Miller[1] · K. Chan[10] · C. Paranicas[12] · S.M. Brooks[4] · K.M. Soderlund[10] · W.B. McKinnon[17] · C.A. Hibbitts[12] · H.T. Smith[12] · P.M. Molyneux[1] · G.R. Gladstone[1,2] · M.L. Cable[4] · Z.E. Ulibarri[13] · B.D. Teolis[1] · M. Horanyi[13] · X. Jia[18] · E.J. Leonard[4] · K.P. Hand[4] · S.D. Vance[4] · S.M. Howell[4] · L.C. Quick[19] · I. Mishra[16] · A.M. Rymer[12] · C. Briois[20] · D.L. Blaney[4] · U. Raut[1,2] · J.H. Waite[1] · K.D. Retherford[1,2] · E. Shock[3] · P. Withers[21] · J.H. Westlake[12] · I. Jun[4] · K.E. Mandt[19] · B.J. Buratti[4] · H. Korth[12] · R.T. Pappalardo[4] · the Europa Clipper Composition Working Group

✉ T.M. Becker
tracy.becker@swri.org

1 Southwest Research Institute, San Antonio, TX, USA

2 University of Texas at San Antonio, San Antonio, TX, USA

3 Arizona State University, Tempe, AZ, USA

4 Jet Propulsion Laboratory, Pasadena, CA, USA

5 Massachusetts Institute of Technology, Cambridge, MA, USA

6 NASA Marshall Space Flight Center, Huntsville, AL, USA

7 University of Idaho, Moscow, ID, USA

8 Planetary Science Institute, Tucson, AZ, USA

9 Georgia Institute of Technology, Atlanta, GA, USA

10 University of Texas, Austin, TX, USA

11 Aix-Marseille Université, CNRS, CNES, LAM, Marseille, France

12 Johns Hopkins University Applied Physics Laboratory, Laurel, MD, USA

13 University of Colorado, Boulder, CO, USA

14 Freie Universität, Berlin, Germany

15 KTH Royal Institute of Technology, Stockholm, Sweden

16 Cornell University, Ithaca, NY, USA

17 Washington University, St. Louis, MO, USA

18 University of Michigan, Ann Arbor, MI, USA

19 NASA Goddard Space Flight Center, Greenbelt, MD, USA

20 Laboratoire de Physique et Chimie de l'Environnement et de l'Espace (LPC2E), Orléans, France

21 Boston University, Boston, MA, USA